

**To Alpha Centauri in a box and beyond:
motion in Relativistic Quantum
Information**

David Edward Bruschi

Thesis submitted to The University of Nottingham
for the degree of Doctor of Philosophy

April 2012

Abstract

In this work we mainly focus on two main aspects of interest within the field of Relativistic Quantum Information. We first expand on the current knowledge of the effects of relativity on entanglement between global field modes. Within this aspect, we focus on two topics: we address and revise the single mode approximation commonly used in the literature. We study the nonlocal correlations of charged bosonic field modes and the degradation of entanglement initially present in maximally entangled states as a function of acceleration, when one observer is accelerated. In the second part of this work we introduce, develop and exploit a method for confining quantum fields within one (or two) cavities and analyzing the effects of motion of one cavity on the entanglement initially present between cavity field modes. One cavity is always allowed to undergo arbitrary trajectories composed of segments of inertial motion and uniform acceleration. We investigate how entanglement is degraded, conserved and created as a function of the parameters describing the motion and we provide the analytical tools to understand how these effects occur. We conclude this work by analyzing the effects of the change of spatial topology on the nonlocal correlations present in the Hawking-Unruh radiation in the topological geon analogue of black hole spacetimes.

Contents

1	Introduction and overview	4
1.1	Author's declaration	8
2	Technical tools	9
2.1	Introduction to the technical tools	10
2.2	Quantum Field Theory	10
2.2.1	Quantum fields	11
2.2.2	Lagrangian formulation in Quantum Field Theory	11
2.2.3	Tools and notation for spacetime structure in Quantum Field Theory	12
2.2.4	The uncharged scalar field	13
2.2.5	Klein Gordon equation in Minkowski coordinates	14
2.2.6	Klein Gordon equation in Rindler coordinates	16
2.2.7	Bogoliubov transformations	19
2.3	Quantum Information	23
2.3.1	Separability and Entanglement	24
2.3.2	Purity and mixedness	25
2.3.3	Partial tracing and partial transposition	25
2.3.4	Measures of entanglement	26
2.4	Outline - Part I	28
2.4.1	Beyond the Single Mode Approximation	28
2.4.2	Entanglement redistribution between charged bosonic field modes in relativistic settings	29
2.5	Outline - Part II	29

2.5.1	Entanglement degradation of cavity modes due to motion	29
2.5.2	Kinematic entanglement degradation of fermionic cavity modes	30
2.5.3	Generation of entanglement within a moving cavity	31
2.5.4	Entanglement resonances within a moving cavity	31
2.6	Outline - Part III	32
2.6.1	Effects of topology on the nonlocal correlations within the Hawking-Unruh radiation	32
3	Beyond the Single Mode Approximation	34
3.1	Global Minkowski, Unruh and Rindler modes revised	35
3.2	Entanglement revised beyond the single mode approximation	38
3.3	Wave packets: recovering the single mode approximation	40
3.3.1	Example: logarithmic Gaussian wave packet	42
3.3.2	Example: non Gaussian wave packet	44
3.4	Conclusions	44
4	Entanglement redistribution between charged bosonic field modes in relativistic settings	45
4.1	Charged bosonic field states for uniformly accelerated observers	47
4.1.1	Quantization of charged scalar fields	47
4.1.2	States of charged bosonic field modes	48
4.2	Particle and Anti-particle entanglement in non-inertial frames	49
4.2.1	Entanglement in states $ \Psi_+\rangle$ and $ \Psi_-\rangle$	51
4.2.2	Entanglement in state $ \Psi_1\rangle$	54
4.3	Conclusions	58
5	Entanglement degradation of cavity modes due to motion	60
5.1	Cavity prototype configuration	62
5.1.1	Field quantization inside a Dirichlet box	62
5.1.2	Basic Building Block	63
5.1.3	Bogoliubov transformations	65

5.1.4	$h \ll 1$ perturbative expansion	66
5.1.5	Pre-trip preparation	68
5.1.6	Travel techniques	68
5.2	Massless field.	71
5.2.1	Basic Building Block travel scenario	71
5.2.2	One way trip travel scenario	72
5.2.3	Return trip travel scenario	74
5.2.4	Validity of the perturbation regime $\mathbf{h} \ll \mathbf{1}$	76
5.3	Massive field	76
5.4	(3 + 1) dimensions.	77
5.5	Conclusions	79
6	Kinematic entanglement degradation of fermionic cavity modes	80
6.1	Quantization of fermions within an inertial cavity	82
6.2	Uniformly accelerated cavity	84
6.3	Quantization and BVT	85
6.3.1	Pre-trip to post-trip Bogoliubov transformations	87
6.3.2	Relations between operators and vacua	88
6.4	Evolution of entangled states	89
6.4.1	Rob’s cavity: vacuum and single-particle states	90
6.4.2	Entangled two-mode states	91
6.4.3	States with entanglement between opposite charges	92
6.5	Entanglement degradation and nonlocality	93
6.5.1	Entanglement of two-mode states	93
6.5.2	Entanglement between opposite charges	96
6.6	One-way journey	96
6.7	Conclusions	98
7	Generation of entanglement within a moving cavity	100
7.1	Bosons	101

7.1.1	Cavity configuration	101
7.1.2	Pre-trip preparation	102
7.1.3	Initial state: $ 0\rangle$	102
7.1.4	Initial state: $ 1_k\rangle$	103
7.2	Conclusions	104
8	Entanglement resonances within a moving cavity	107
8.1	Setup and development of the Two Mode Truncation technique	109
8.2	Techniques for Gaussian states	111
8.2.1	Continuous variables	111
8.2.2	Evolution of the initial state	113
8.3	Resonance condition	115
8.4	Position of the resonance	117
8.5	General description of the increase of entanglement	119
8.6	Travel example: Casimir-like scenario	120
8.6.1	Casimir-type scenario: same acceleration/deceleration	120
8.6.2	Casimir-type scenario: different acceleration/deceleration	121
8.7	Bogoiubov operations	123
8.8	Conclusions	123
9	Effects of topology on the nonlocal correlations within the Hawking-Unruh radiation	125
9.1	Introduction to geons	126
9.1.1	Geons in brief	128
9.2	Scalar field coupled to a $\mathbb{Z}_2 \times U(1)$ Maxwell field	129
9.2.1	Constant background magnetic field: preliminaries	131
9.2.2	Constant background magnetic field - Classical case	132
9.2.3	Constant background magnetic field - Quantum case: \mathcal{M}_0	134
9.2.4	Constant background magnetic field - Quantum case: \mathcal{M}_-	137
9.2.5	Constant background magnetic field - Quantum case: \mathcal{M}_+	139
9.2.6	Particle correlations and the meaning of charge	140

CONTENTS

9.3	Electrically charged Reissner Nordtrøm spacetime	140
9.3.1	Normalisation	142
9.3.2	Low frequencies: $\omega < m$	142
9.3.3	Electrically charged Reissner Nordtrøm spacetime - Quantum Case	143
9.3.4	High frequencies: $\Omega > m$	146
9.4	Conclusions	149
10	Work in progress and future work	151
10.1	Work in progress and future work	152
	References	156

Notation and conventions

Symbols and abbreviations which might be used:

RQI Relativistic Quantum Information

QI Quantum Information

QFT Quantum Field Theory

GR General Relativity

BVT Bogoliubov Transformations

RRW Right Rindler wedge.

LRW,FRW,PRW for Left/Future/Past Rindler wedge (or R,L,F,P when no misunderstanding is possible)

KG Klein Gordon

DE Dirac Equation

SMA Single Mode Approximation

LO Local Operations

LOCC Local Operations and Classical Communications

Throughout this work we assume $\hbar = c = 1$ unless explicitly specified.

$\mathcal{O}(x)$ is defined as follows: $\mathcal{O}(x)/x$ is bounded for $x \rightarrow 0$.

Spacetime signature is $(-, +, +, +)$ in $3 + 1$ dimensions (or $(-, +)$ in $1 + 1$). Full coordinates are denoted by x^μ , while roman index x^i denotes coordinates on some space like foliation .

Alice and Bob stand for inertial observers, Rob for an observer which undergoes non-inertial motion.

We will use Einstein's convention throughout the work, namely $\sum_{\mu=0}^3 a_\mu b^\mu \equiv a_\mu b^\mu$ and $\sum_{i=1}^3 a_i b^i \equiv a_i b^i$

CONTENTS

The Universe is talking to Us

Foreword

“ The Way that can be told of is not an unchanging way;
The names that can be named are not unchanging names.
It was from the Nameless that Heaven and Earth sprang;
The named is but the mother that rears the ten thousand creatures,
each after its kind.”

Tao Te Ching

The most beautiful thing about the Universe is the identity between Atman and Brahman. Our perception of the world is misleading, we see ourselves as separated entities from the rest which interact with other entities. We are not able to connect ourselves to our inner selves, the true Us which guides from within. Everyone is a Buddha but we have forgot it and don't believe it. Once we are able to crush the ignorance we finally realize that there is no such thing as Us and the rest. We are one with the Universe.

Physics does not escape this Unity, neither do the human ways of thinking. It has always excited and amused scientists that new and fresh insight about any phenomena can be achieved by simply changing point of view. This, of course, does not pertain only to the realm of Physics but also to Heaven and the Ten Thousand Things. When a scientist studies a discipline, there are standard references he or she will learn from. Experts in this or that field will have great understanding and piercing insight into those phenomena that can be explained, at least to some degree of accuracy, by the intuition and mathematical skills they have developed, trained and perfected. Still, somebody from a completely different area might address, maybe moved by simple curiosity, some difficult problem yet unsolved and, almost by magic, provide a simple and elegant solution.

The Universe does work by mysterious ways.

Acknowledgements

The time for acknowledgements has come. Although I might be crazy, lots of people have nevertheless walked along with me. They say that “Chi va con lo zoppo impara a zoppicare”. We shall see.

I would like to thank Jorma for his supervision during these years, for his suggestions, and especially for his (almost infinite) patience towards my (many many) mistakes of all sorts, kinds, shapes and forms.

Thanks to my mother and father for their continuous love and support. They have always encouraged me to follow my own way, which is the only Way.

Thanks to my brother who I know is always there for me regardless the spacelike or timelike distance.

Thanks to Ivette for support, help, discussions and helping me in the School of Mathematics as well as the School of Life. I have found to have lots in common with you, regardless it is the love for Physics, the happiness within or the attraction towards the mysterious mysteries of Life. I still believe, though, that italian beaches are the best!

Thanks to Ant and Nico for not finding a way to permanently dispose of me regardless of how annoying (on purpose) I have been to them. They have helped me for a long time now and have become good friends. Along with them, I would like to thank Jack Bauer and Chuck Norris for (unknowingly) being part of our student lives.

Thanks to Dayana for all the time she has dedicated to me, her unconditional support, help and patience towards my craziness. She has seen almost all of the results presented in this work grow and has always backed me up.

Thanks to Francesco. I will always see him when the time is ripe. Our building of the ten meters-tall stone tower continues.

Thanks to Andrzej for the help he gave during his stay in Nottingham and for introducing us to amazing new songs.

Thanks to Gerardo for his help and support (and Samanta for bringing a small portion of italian cuisine to this strange island).

Thanks to the Flat 4 crew: Mirentxu, Mila, Hon, Tanisha, Sasha! I love you guys.

Thanks to the Karate Dojo for walking with me along the Way: Hanshi, Nanna,

CONTENTS

Kumi, Yaei, Sonny, Pasq, David, Tony, Pino, Rosie, Carol, Simon, Guy, Mike, Paul, Marcus, Susumu, Tom, and all the rest of the gang. Ossaaaaaaaah! Thanks also to my hometown Karate Dojo: Giuseppe Righi, Giovanni Tedeschi, Luigi Schianchi, Andrea Bertorelli.

Thanks to the Pete for our chats and for teaching me a lot about plants.

Thanks to Davide back in Italy. Together with Francesco we have played some many games of Ciapanò. We acknowledge the “asso di bastoni” for making our rounds of Ciapanò (as well as our lives) more thrilling.

Thanks to my friends in Parma. We have known each others for soooo long.

Thanks to Annalaura Manghi and Elena Portinaro for their outstanding friendship.

I would like to thank the staff of the School of Mathematics, Andrea Blackburn, Helen Cunliffe, Cathie Shipley, Judi Walker, Krystyna Glowczewska, Lorraine Hammond, Jill Hutchinson, Hilary Lonsdale, Jane Mason, Eve Mulligan, Claire Parnell, Mark Eatherington, Dave Parkin, Daniel Rhodes, for their help with all sorts of administrative and IT tasks I had to deal with in the past years

I would like to thank the RQI “family” for interesting discussions, exchanges of ideas and drinking sessions. Among my collaborators, colleagues and friends I would like to thank Daniele Faccio, Silke Weinfurtner, Marcus Huber (I see you), Eduardo Martin Martinez, Achim Kempf, Juan Leon, (uniformly accelerated) Rob Mann, Danny Terno, Peter Kok, Chris Binns, Sergio Cacciatori, Iacopo Carusotto, Tim Ralph, Barry Sanders, Adrian Kent, Bodhidharma , Ian Jones, Carsten Gundlach, Andreas Winter, Sandu Popescu, Marcin Pawlowski, Paolo Volloresi, Tlaloc, John Barrett, Kirill Krasnov, Alberto Camara, Gianluca Delfino, Eleni Verikouki, Sara Sala, Luca Visinelli, Stefano Evangelisti, Giovanna Venturi, Emilio Ciuffoli, Giovanna Pintori, Cesare Stocchi, Fabio Cavatorta. Apologies if names are missing.

I cannot list everybody. So thank you. You, yes *you* know how much you have or have not contributed to my life.

My studies have been fully funded by a *University Research Studentship Award*. I would like to acknowledge the *University of Nottingham Travel Prize* for support for attending the “First NASA Quantum Future Technologies” conference which took place in January 2012 at NASA Ames Research Center in Mountain View, California, USA. I would also like to acknowledge the Institute of Mathematics and its Applications for the *Small Research Grant* awarded to attend the “RQI 2012 - N” meeting which took place in June 2012 at the Perimeter Institute, Waterloo, Canada

Last, I thank the Universe. Floating on the river and looking at the stars, one feels the water and *that* is the world. A drop is the sea itself. The Universe is indeed a wonderful place.

CHAPTER 1

Introduction and overview

The young field of Relativistic Quantum Information represents, in its own dimension, the expression of the unity between Universe and its parts. For a long time, scientists have investigated separately the main areas of Quantum Field Theory and Quantum Information. Little was known about the overlap between the two and the few results that might have been found within this overlap were not investigated further. Recently, scientists have begun to understand that the well-developed results from Quantum Information must take into account effects which are predicted by relativity. The underlying motivation is strikingly simple: if the Universe is one, why should phenomena described by the language of Quantum Information not be affected by the language of Quantum Field Theory? In other words, if the aim is to understand Nature, should some effects be ignored by hand?

The field of Relativistic Quantum Information aims to understand how relativity affects quantum information tasks. Any quantum information protocol requires the use of a resource, which typically consists of non-classical correlations, also known as entanglement (i.e. see [1]). Although Quantum Information predictions have been successfully verified experimentally (for example see [2]) and are now also implemented commercially, only recently there has been growing attention towards the analysis of the effects of relativity on entanglement (for example see [3, 4]). In particular, questions such as is entanglement an observer independent quantity have been thoroughly analyzed within the community.

Pioneering work in RQI investigated such questions and it was found that indeed entanglement is not an observer independent quantity. Although inertial observers will agree regarding the amount of entanglement present between, say, modes of a quantum field, given an initially maximally entangled state of global fields, which is analyzed by two inertial observers, the amount of entanglement present in the *same* state when one of the two observers is uniformly accelerated changes. It was shown that the greater the acceleration, the more entanglement was lost; for bosonic fields, in the limit of infinite acceleration none survived (for a selection see [5, 6]). Similar analysis was performed for fermionic fields and it was found that entanglement was still degraded with acceleration but did not vanish in the limit of infinite acceleration [7, 60]. The main reason behind this exciting discovery lies in the Unruh effect [8], which is a prediction of QFT solely. Intuitively, different observers will not (in general) agree on the particle content of a state. For example, the vacuum state for an inertial observer is a “highly” populated state for an accelerated observer [9, 10]. An alternative and equivalent way of understanding this phenomenon is that there is in general no unique and natural definition of particles in QFT. These preliminary works addressed theoretical questions, which involved the

analysis of global fields, that are relativistic quantum fields with non compact support. It is not clear how to experimentally prepare and access such fields and therefore the question remained of how to analyze the effects of relativity on entanglement in more physical scenarios.

Quantum protocols involve manipulation and transmission of information and it is of vital interest to provide efficient and effective ways of storing it. A simple way to store information is to employ localized physical systems (for example, in the classical case, the memory of a computer): it is fundamental to be able to store information in order to retrieve and use it when necessary at a later stage. It is therefore natural to ask if relativity will affect stored information and perhaps if it can be used to improve the ability to store it in the first place. The most natural system, which “localizes” fields is a cavity, modeled by a quantum field with compact support and boundary conditions at the cavity walls. Preliminary investigation in this direction showed that given two cavities, one at rest and one in uniform acceleration, the ability to entangle the cavity modes when the cavities come close, decreases with increasing acceleration [11]. Another attempt to address effects of relativity on entanglement in localized systems showed that, once entanglement between modes within two different cavities has been created, it is “shielded” by the cavity walls and no degradation effects are observed [11]. These works did not address directly how relativistic motion affects the entanglement.

In this work we focus on two main topics and we conclude with an extensions of the first topic in the third part:

PART I - The first part addresses questions, which involve global fields, as previously done in literature. Although it is accepted that physical and experimental settings require localized fields, understanding how entanglement between global modes is affected by the state of motion of the observer or the topology of the spacetime can provide insight on the mechanisms that are involved in the process.

Chapter 3 - We start by addressing the validity of the Single Mode Approximation extensively used in literature (for a selection see [5–7, 60] and references therein), which allowed for simplifications of transformations of the fields as described by different observers. This approximation was used incorrectly and we revise and extend it. We expand on the concept of Unruh particle and show that new degrees of freedom arise. Finally, we construct Minkowski wave packets and Unruh wave packets and show in which sense one can justify and recover the Single Mode Approximation.

Chapter 4 - As a second step we analyze entanglement degradation between modes of charged bosonic fields. Untill present, only uncharged bosonic fields and Grassman fermionic fields were employed in the analysis and it was found that striking differences between the two types of fields occurred. Part of these might be attributed to the presence of both particles and antiparticles in fermionic fields and the question remained to understand the behavior of entanglement when charged bosonic fields were considered.

PART II [Chapters 5,6,7,8] - The second topic is centered around the idea that in order to access, manipulate, store and process information resources one must employ localized physical systems. In a realistic situation, relativity will affect these systems. Institutes and space agencies such as IQC and CSA (Canada) and NASA (U.S.A.) have recently shown growing interest in understanding how relativity affects entanglement.

In this part of the work we introduce relativistic quantum fields in localized systems (cavities) where the field has compact support and satisfies some boundary conditions. We study how entanglement between field modes in one cavity or two cavities is affected by motion of one of the cavities. We introduce a perturbative regime, that allows one to analyze any (arbitrary) trajectory of rigid cavities, which is obtained by composing segments of uniform motion with segments of uniform acceleration in an arbitrary yet controlled way. Times of acceleration and inertial coasting can be arbitrary and provide the natural variables of the problem, together with the accelerations. We are interested in understanding how entanglement is degraded or can be created in any travel scenario when one cavity concludes its voyage. Such understanding could be of great use in space based experiments, which aim to investigate Quantum Key Distribution and multiparty satellite quantum communication.

In addition, from a completely different perspective, the Casimir community has been awaiting experimental verification of the so called “Dynamical Casimir effect” (see [12] and references therein). Such effect occurs when a (perhaps small) cavity with conducting walls has one of the boundaries free to move. Rapid and periodic oscillations induce the electromagnetic field to spontaneously emit pairs of correlated particles even if the initial state of the field is the vacuum. The oscillations of the boundary have to occur with a mean speed which is a significant fraction of the speed of light. Although this imposes severe limitations to the experiments, such experiment was undertaken recently with superconducting circuits instead of a mechanical resonator, therefore allowing for the speeds required [13]. The application of the techniques developed in this part of the work might bring new

insight into this field of research and possibly lead to the development of concrete experimental proposals.

PART III [Chapter 9] - At last, we address how non-trivial spacetime topologies affect the nonlocal correlations present in the Unruh effect. It is of great interest for research in the field of Quantum Gravity to be able to describe the topology of the spacetime and explain if and how it is nontrivial. Although a full understanding might be possible only once a viable theory of Quantum Gravity becomes available, indications in any direction might be of great help in guiding research. In addition, from the perspective of Relativistic Quantum Information, finding a signature of the topology in the Hawking-Unruh particle correlations could provide a theoretical basis for proposing new ways of measuring the parameters of spacetime. Work in this direction was already attempted in [14].

In Chapter 2 we introduce the technical tools that will be used throughout the work. In particular, we introduce techniques from Quantum Field Theory and techniques from Quantum Information. In Chapter 10 I briefly summarize part of my current and future projects, which are related to work done in this thesis.

1.1 Author's declaration

I declare that the results presented in this thesis are the result of my own work, together with my collaborators, which I have produced during my PhD studies. Chapters 3 to 8 present the results of work I have majorly contributed to and which have appeared as eprints or have been published in journals. In Chapter 6 I have majorly contributed by supervising the use of the techniques and analyzing results and equations. In Chapter 3 I have developed the bosonic part of the work. The fermionic analysis, which is not included in the thesis, can be found in [15] and has been developed by collaborators. In Chapter 7 I have again contributed by analyzing the bosonic field modes while collaborators have worked on the fermionic counterpart. The main idea behind Chapter 9 was suggested to me by my supervisor Dr. Jorma Louko and constitutes work done in the first year of the PhD. Figures in Chapter 9 have been drawn by Jorma Louko (at the School of Mathematical Sciences, University of Nottingham) and were used in [16]. Figures in Chapters 4, 5 and 3 were totally or partially redrawn by Antony Lee (at the School of Mathematical Sciences, University of Nottingham).

CHAPTER 2

Technical tools

2.1 Introduction to the technical tools

Relativistic Quantum Information is a field that requires the use of techniques from two different areas: Quantum Field Theory and Quantum Information. It is a trademark of this framework to merge concepts such as transformation of quantum states under a change of coordinate with those that involve resources for quantum protocols and measures of entanglement. Both theories are well established and have been corroborated each to its own degree. While QI uses the formalism of standard Quantum Mechanics, QFT introduces special relativity and (background) curved spacetimes in the game. One of the main differences lies in the following observation: a state in standard Quantum Mechanics can be described at any time by any observer regardless of his state of motion and all observers will “see” the same state.

This is not the case in QFT. Two different observers need not agree on the particle content of a state. For example, the vacuum as described by an inertial observer will be a state populated by particles when described by, say, an accelerated observer [10, 17]. In order to address questions that take into account these effects, one needs to develop a systematic way of using techniques from QI and from QFT. In this chapter we introduce to some detail such techniques as required when addressing questions in RQI.

2.2 Quantum Field Theory

Quantum Field Theory and its most powerful application, the Standard Model, aim to comprehensively explain all phenomena with the exception of gravity. The main objects under study are the quantum field and its kinematics, together with the mutual interactions with other fields (dynamics). Fields pertain to two categories depending on their spin taking integer or half-integer values: the former are called bosons and the latter fermions. The main improvement with respect to standard QM is that relativity is explicitly introduced in the theory from the beginning [18]. Einstein equations are *not* solved within this framework but a fixed background spacetime is assumed from the start; the spacetime where the fields live is a solution to Einstein’s equations, for example Minkowski spacetime is a solution of Einstein’s equations in the vacuum or Schwarzschild spacetime is a solution of Einstein’s equations in the presence of a massive objects [19]. In this sense, the relativistic properties of the spacetime are built in the theory as fixed, non-dynamical background elements.

2.2.1 Quantum fields

Quantum fields are operator-valued functions defined on points of the spacetime. The algebra where these functions take values depends on the nature of field. Fermionic fields are represented by spinors, while spin 0 fields are represented by (operator valued) complex distributions. QFT is extremely vast and we will not try to give an introduction here. A standard reference is [18]. For the purposes of this work, we will need to deal with uncharged or charged bosonic fields and only partly with fermions. We therefore briefly present the necessary tools to describe uncharged scalar fields. When relevant, we will give a brief account of fermionic and charged bosonic fields.

The standard textbook presentation of QFT starts by explaining how classic field theory develops and then introduces quantization techniques for the classical fields. We will not follow this approach but instead discuss the quantum version from the start. Scientists that investigate complicated physical settings such as interacting fields of the same nature or possibly even different nature use the *path integral* formulation that allows for (often already difficult in this language) computable results to be obtained. For our purposes, such formulation is not necessary.

2.2.2 Lagrangian formulation in Quantum Field Theory

A physical setting in QFT consists of (operator valued) fields $\Phi(x^\mu)$ defined over a manifold \mathcal{M} , where $x^\mu \in \mathcal{M}$, and that take values in an appropriate algebra. Starting from the fields, one builds the Lagrangian density

$$\mathcal{L} = \mathcal{L}(\Phi, \partial_\mu \Phi), \quad (2.2.1)$$

which must obey some basic constraints, for example must be Hermitian and might satisfy some particular gauge invariance. Given the action

$$I := \int d^4x \mathcal{L}, \quad (2.2.2)$$

one invokes the *least action principle* that leads to Euler-Lagrange type equations

$$\frac{\partial}{\partial^\mu} \frac{\partial \mathcal{L}}{\partial(\partial_\mu \Phi)} - \frac{\partial \mathcal{L}}{\partial \Phi} = 0. \quad (2.2.3)$$

Given (2.2.3), one can find the *field equations* or equations of motion that describe the kinematics of the (free) fields. In general, the Lagrangian might contain a potential term that accounts for interactions; however, in this work we will focus on non-interacting free fields and therefore the field equations will describe the kinematics of the fields themselves. In chapter 3 we introduce the interaction of the field with a classical background gauge field. Relevant techniques will be addressed therein.

2.2.3 Tools and notation for spacetime structure in Quantum Field Theory

We briefly introduce objects from differential geometry that are necessary in order to understand relativity and QFT to the extent used in this work. Standard references are [19, 20].

A *spacetime* is a d -dimensional manifold \mathcal{M} equipped with a symmetric tensor \mathbf{g} with components $g_{\mu\nu}(x^\alpha)$ called *metric* (we employ signature $(-, +, +, +)$). The determinant of the metric is $g = \det(g_{\mu\nu})$, the metric is nonsingular ($\det(g_{\mu\nu}) \neq 0$) and the line element associated with the metric is

$$ds^2 = g_{\mu\nu} dx^\mu dx^\nu. \quad (2.2.4)$$

A *set of coordinates* is a map

$$x^\alpha : \mathcal{X} \subset \mathcal{M} \rightarrow \mathcal{U} \subset \mathbb{R}^d, \quad (2.2.5)$$

where \mathcal{X}, \mathcal{U} are open sets. In general, a set of coordinates will not cover the entire manifold. A collection of sets of coordinates that covers the manifold is called *coordinate chart*.

Given two sets of coordinates $x^\alpha \in \mathcal{X} \subset \mathcal{M}$, $y^\alpha \in \mathcal{Y} \subset \mathcal{M}$ where $\mathcal{X} \cap \mathcal{Y} \neq \emptyset$, a *change of coordinates* or *coordinate transformation* is C^∞ (smooth) invertible map

$$y^\beta = y^\beta(x^\alpha) \quad (2.2.6)$$

defined on $\mathcal{X} \cap \mathcal{Y}$.

A *path* $\Gamma \subset \mathcal{M}$ is a curve

$$\Gamma : \lambda \mapsto \Gamma(\lambda) \quad (2.2.7)$$

parametrized by $\lambda \in \mathbb{R}$. When a set of coordinates $\{x^\mu\}$ is introduced, a path takes the form

$$\Gamma : \lambda \mapsto x^\mu(\lambda). \quad (2.2.8)$$

A *vector* \bar{v} is an element of the tangent space T_P defined at each point $P \in \mathcal{M}$. A *vector field* $\bar{v} = \partial_\lambda$ is a collection of vectors along a congruence of curves Γ parametrized by λ and is defined by its action on functions $f : \mathcal{M} \rightarrow \mathbb{R}$ as

$$\bar{v}(f) \equiv \frac{\partial f(P(\lambda))}{\partial \lambda}. \quad (2.2.9)$$

The metric \mathbf{g} is a tensor that takes as input two vectors and gives as output a real number. The invariant (under change of coordinates) length $\mathbf{g}(\bar{v}, \bar{v})$ of a vector field $\bar{v} = v^\mu \bar{e}_\mu$, where $\{\bar{e}_\mu\}$ is a basis for the tangent space, is

$$\mathbf{g}(\bar{v}, \bar{v}) = g_{\mu\nu} v^\mu v^\nu = v^\nu v_\nu \quad (2.2.10)$$

and vectors are divided in three categories depending on the sign of $g(\bar{v}, \bar{v})$ (signs are reversed for a different choice of the metric signature):

$$\begin{aligned}\bar{v} \text{ is } \underline{\text{timelike}} \text{ if } \mathbf{g}(\bar{v}, \bar{v}) < 0 \\ \bar{v} \text{ is } \underline{\text{null}} \text{ if } \mathbf{g}(\bar{v}, \bar{v}) = 0 \\ \bar{v} \text{ is } \underline{\text{spacelike}} \text{ if } \mathbf{g}(\bar{v}, \bar{v}) > 0.\end{aligned}\tag{2.2.11}$$

A path is timelike if the tangent vectors to it are always timelike. Analogously for spacelike and null paths.

If there exists a vector field $\bar{\Xi} = \partial_\lambda$ such that

$$\mathcal{L}_{\bar{\Xi}}\mathbf{g} = 0,\tag{2.2.12}$$

where $\mathcal{L}_{\bar{\Xi}}$ is the *Lie derivative* with respect to $\bar{\Xi}$, then $\bar{\Xi}$ is called a *Killing vector*. An example is the vector $\bar{\Xi} = \partial_t$ in Minkowski spacetime. In the specific case of Minkowski spacetime, given a spacetime foliation in hyper surfaces labeled by $t = \text{const}$, the metric $g_{\mu\nu}$ naturally reduces to the spatial metric g_{ij} , which does not change by changing the hypersurface.

A spacetime is *globally hyperbolic* if there exists a Cauchy surface Σ , which is a spacelike hyper surface that enjoys the following property: any inextendible causal path intersects the hyper surface exactly once. Solutions to hyperbolic differential equations, such as the field equations, uniquely determine the field at any point on \mathcal{M} once initial conditions are specified on Σ . In Minkowski spacetime, any hyper surface $t = \text{const}$. is an equivalent choice of Cauchy surface.

The proper time associated to a point-like inertial observer that follows a timelike path $x^\mu(\lambda)$ parametrized by λ is

$$\tau = \frac{1}{c} \int ds = \frac{1}{c} \int \frac{ds}{d\lambda} d\lambda,\tag{2.2.13}$$

which can be computed once a trajectory for the observer is specified. τ is normally chosen to increase towards the future.

2.2.4 The uncharged scalar field

The *uncharged massive scalar field* is a map

$$\Phi : x^\mu \rightarrow \Phi(x^\nu),\tag{2.2.14}$$

where $\Phi(x^\nu) = \Phi^\dagger(x^\nu)$ is an operator valued distribution. The standard free Lagrangian takes the form

$$\mathcal{L} = \partial_\nu \Phi \partial^\nu \Phi - \frac{1}{2} \mu^2 \Phi^2.\tag{2.2.15}$$

Invoking the least action principle one uses (2.2.3) and finds the field equations that determine the kinematics of Φ

$$(\square - \mu^2)\Phi = 0, \quad (2.2.16)$$

where

$$\square = (\sqrt{-g})^{-1} \partial_\nu \sqrt{-g} \partial^\nu \quad (2.2.17)$$

and $\mu > 0$ is the mass of the field. Equation (2.2.16) is commonly known as the *Klein Gordon equation* (KG). The conjugate momentum to Φ is defined as

$$\Pi := \frac{\partial \Phi}{\partial x^0} \quad (2.2.18)$$

and one imposes the algebra relations

$$[\Phi(x^0, \mathbf{x}), \Pi(x^0, \mathbf{y})] = i\delta^3(\mathbf{x} - \mathbf{y}). \quad (2.2.19)$$

2.2.5 Klein Gordon equation in Minkowski coordinates

In this section we solve (2.2.16) using Minkowski coordinates.

Given a flat metric on a 3 + 1 dimensional manifold \mathcal{M} , the *Minkowski coordinates*

$$(t, x, y, z) \equiv (x^0, x^i) \quad (2.2.20)$$

have the line element

$$ds^2 = -dt^2 + dx^2 + dy^2 + dz^2 \quad (c = 1), \quad (2.2.21)$$

where the line element takes the form $ds^2 = -dt^2 + dx^2$ in 1+1 dimensions. The vector field ∂_t is a global timelike Killing vector. The manifold \mathcal{M} is a globally hyperbolic spacetime, where it is sufficient to specify initial conditions on the $t = 0$ Cauchy surface. In addition, such spacetime enjoys the property of being invariant under *Lorentz transformations*, which are composed by (spatial) rotations, boosts and translations. We will call such spacetime *Minkowski spacetime*.

Let us focus on 1 + 1 dimensions. To add 2 extra dimensions will be straightforward. One can expand the field Φ in Fourier basis as

$$\Phi = \int d^2k a(k_\mu) e^{ik_\mu x^\mu}, \quad (2.2.22)$$

where $a(k_\mu)$ are (operator valued) Fourier coefficients and substitute this in (2.2.16). The derivation of the mode solutions is standard and can be found in every QFT textbook

[18]. We just give the result. The positive frequency modes with respect to ∂_t of a massless scalar field with $\mu = 0$ are

$$u_{\omega,M}(t,x) = \frac{1}{\sqrt{4\pi\omega}} \exp[-i\omega(t - \epsilon x)], \quad (2.2.23)$$

where $\omega > 0$ is the Minkowski frequency and $\epsilon = \pm$ stands for right or left movers (we note that these decouple only in the 1 + 1 massless case).

Therefore, Φ takes the form

$$\Phi = \sum_{\epsilon=\pm 1} \int_{\mathbb{R}^+} dk [a(k_\mu) e^{ik_\mu x^\mu} + a^\dagger(k_\mu) e^{-ik_\mu x^\mu}] \quad (2.2.24)$$

If $\mu \neq 0$ one must replace

$$\omega \rightarrow \omega = \sqrt{k^2 + \mu^2}, \quad (2.2.25)$$

where $k \in \mathbb{R}$ is the momentum and labels the solutions, and also replace

$$\exp[-i\omega(t - \epsilon x)] \rightarrow \exp[-i\omega t + kx]. \quad (2.2.26)$$

In 3 + 1 dimensions one needs to replace k by \mathbf{k} and therefore

$$k^2 \rightarrow \mathbf{k} \cdot \mathbf{k} = |\mathbf{k}|^2. \quad (2.2.27)$$

Orthonormalisation of mode solutions in QFT is achieved by using the *inner product*. It is a sesquilinear functional of two fields and does not need to be positive. Such a functional is defined on a given hypersurface. We will show later that it also captures the relation between different particle contents as described by different observers. As a technical point, we stress that modes with sharp frequencies out of a continuum are not, strictly speaking, orthonormal in the sense of Kröneckers delta, but rather in the sense of Dirac delta.

We define the inner product (\cdot, \cdot) as

$$(\phi_1, \phi_2) = i \int_{\Sigma} \phi_1^* \overleftrightarrow{\partial}_a \phi_2 n^a d\Sigma, \quad (2.2.28)$$

where n^a is a normal vector to Σ pointing to the future, Σ is an arbitrary space like hyper surface and the operator $\overleftrightarrow{\partial}_a$ is defined through

$$f \overleftrightarrow{\partial}_a g := f \partial_a g - (\partial_a f) g. \quad (2.2.29)$$

If ϕ_1, ϕ_2 satisfy the field equation then the inner product (2.2.28) is conserved.

Specializing to Minkowski coordinates and choosing $\Sigma : t = 0$, one finds that the solutions to the 1 + 1 massless version of (2.2.16) are delta-normalised by

$$\begin{aligned} (u_{\omega,M}, u_{\omega',M}) &= \delta_{\epsilon,\epsilon'} \delta(\omega - \omega'), \\ (u_{\omega,M}^*, u_{\omega',M}^*) &= -\delta_{\epsilon,\epsilon'} \delta(\omega - \omega'), \\ (u_{\omega,M}^*, u_{\omega',M}) &= 0. \end{aligned} \quad (2.2.30)$$

In the 3 + 1 massive or massless case one has

$$\begin{aligned}
 (u_{\mathbf{k},M}, u_{\mathbf{k}',M}) &= \delta(\mathbf{k} - \mathbf{k}'), \\
 (u_{\mathbf{k},M}^*, u_{\mathbf{k}',M}^*) &= -\delta(\mathbf{k} - \mathbf{k}'), \\
 (u_{\mathbf{k},M}^*, u_{\mathbf{k}',M}) &= 0
 \end{aligned} \tag{2.2.31}$$

and to obtain the 1+1 massive relations it is sufficient to replace the frequency $\omega > 0$ with the momenta $k \in \mathbb{R}$ and remove the $\delta_{\epsilon,\epsilon'}$ pre factors since right and left movers no longer decouple. Given such normalization, bosonic modes with a positive delta-normalization are called positive energy modes while those with negative delta-normalisation are called negative energy modes. We note that given a complete orthonormal (in the sense of delta normalization) set of modes which are solutions to the KG equation (2.2.16), it is always possible to choose a subset which has positive norm and a subset which has negative norm. In this sense, we define as particle excitations those that are carried by positive frequency modes. In case of charged fields, we shall see that antiparticles are carried by negative frequency modes.

2.2.6 Klein Gordon equation in Rindler coordinates

Given 3 + 1 Minkowski spacetime with coordinates (t, x, y, z) , it is possible to divide it into four regions, which, if covered by suitable coordinates, are globally hyperbolic spacetimes on their own right. To do this one needs to explicitly break Poincaré invariance by choosing an origin for the Minkowski coordinates and dividing the spacetime in the following parts:

$$\left\{ \begin{array}{l} \text{RRW: } |t| < x, 0 < x \\ \text{LRW: } |t| < |x|, x < 0 \end{array} \right. \tag{2.2.32}$$

$$\left\{ \begin{array}{l} \text{FRW: } |x| < t, 0 < t \\ \text{PRW: } |x| < |t|, t < 0. \end{array} \right. \tag{2.2.33}$$

For each region, one can introduce appropriate *Rindler coordinates* [10], which are designed to cover only the relevant part. One can see a schematic representation in Fig. 2.1 For the sake of simplicity we describe the coordinates on the RRW first.

One starts from the transformation from Minkowski coordinates (t, x, y, z) to Rindler coordinates (η, χ, y', z')

$$\begin{aligned}
 t &= \chi \sinh \eta \\
 x &= \chi \cosh \eta,
 \end{aligned} \tag{2.2.34}$$

while $y' = y, z' = z$). The coordinate $\eta \in \mathbb{R}$ is the dimensionless Rindler time and $\chi > 0$ is the dimension length spatial coordinate in the RRW.

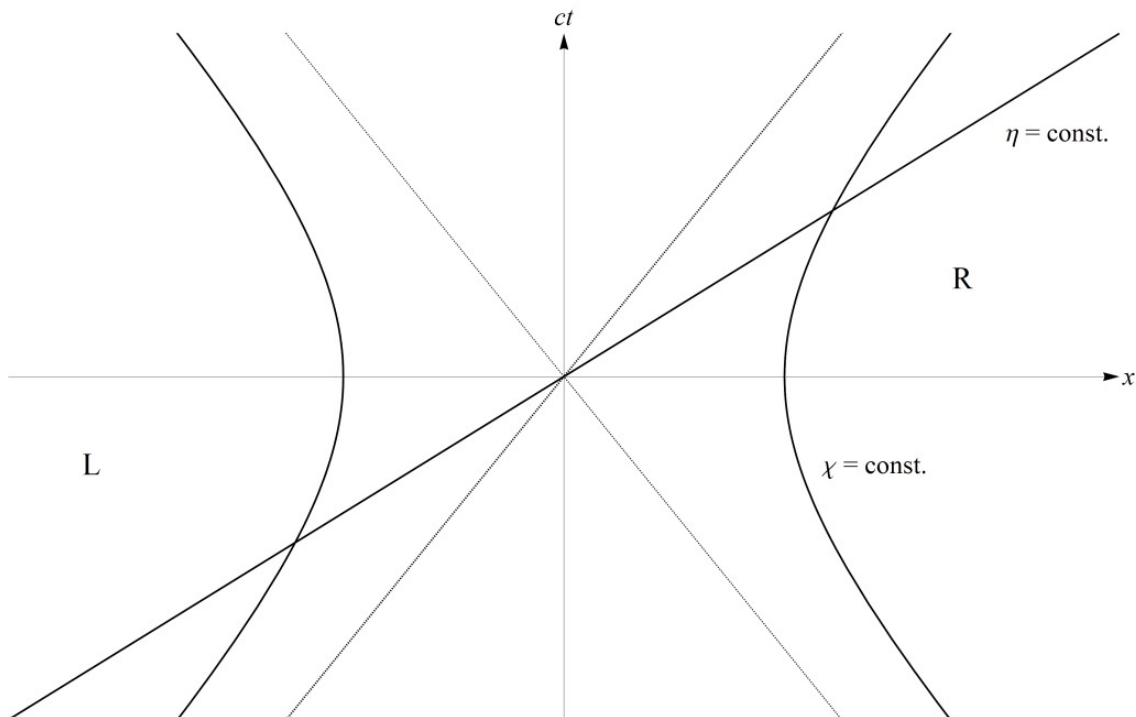


Figure 2.1: Minkowski spacetime and the four Rindler wedges: the 45° lines are “causal horizons” for observers moving on Rindler trajectories $\chi = \text{const.}$. Hypersurfaces of constant Rindler time η are straight lines through the origin.

The dimensionless time coordinate η is defined as the parameter that determines the global (in the RRW) timelike Killing vector field ∂_η defined in terms of Minkowski coordinates as

$$\partial_\eta := t\partial_x + x\partial_t \quad (2.2.35)$$

and which represents a boost in the (t, x) plane and η increases towards the future. We refer to (2.2.36) when recalling the Rindler transformations and we ignore the trivial action on the y, z components. In the figure 2.1 hyper surfaces $\eta = \text{const}$ are straight lines through the origin and world lines $\chi = \text{const}$ are hyperbolae.

In a similar fashion, we introduce Rindler coordinates in the LRW. One starts from the transformation

$$\begin{aligned} t &= \chi \sinh \eta \\ x &= -\chi \cosh \eta, \end{aligned} \quad (2.2.36)$$

where the dimensionless Rindler time $\eta \in \mathbb{R}$ increases towards the past. The coordinate $\chi > 0$ has dimension length.

The 3 + 1 line element in such coordinates reads

$$ds^2 = -\chi^2 d\eta^2 + d\chi^2 + dy^2 + dz^2, \quad (2.2.37)$$

while in 1 + 1 it reads $ds^2 = -\chi^2 d\eta^2 + d\chi^2$. From this, one can verify that a point like observer that follows a trajectory $\chi = \text{const.}$ perceives a proper acceleration

$$A = \frac{1}{\chi} \quad (2.2.38)$$

and measures proper time τ along his trajectory as

$$\tau := \frac{c\eta}{A}. \quad (2.2.39)$$

Such an observer travels along an hyperbola as seen in Fig. 2.1 and will measure physical frequencies with respect to the proper time τ .

Given a bosonic field in 1 + 1 dimensions with $\mu = 0$, one can compute the solutions to (2.2.16) in Rindler coordinates; one starts from

$$\square = (\sqrt{-g})^{-1} \partial_\mu \sqrt{-g} \partial^\mu, \quad (2.2.40)$$

where the determinant of the metric takes the expression $g = \det(g_{\mu\nu})$ and the matrix representing the metric takes the form

$$g_{\mu\nu} = \text{diag}(-\chi^2, 1). \quad (2.2.41)$$

One then makes the ansatz

$$\Phi(\eta, \chi) = \int d\Omega e^{-i\Omega\eta} \Psi(\chi), \quad (2.2.42)$$

which implies that the Rindler positive and negative frequency modes with respect to the timelike killing vector field ∂_η are respectively

$$u_{\Omega,I}(t, x) = \frac{1}{\sqrt{4\pi\Omega}} \left(\frac{x - \epsilon t}{l_\Omega} \right)^{\mp i\epsilon\Omega}. \quad (2.2.43)$$

We can express (2.2.43) as functions of Minkowski or Rindler coordinates by using (2.2.36). For completeness, we provide also the positive frequency solutions in the LRW

$$u_{\Omega,II}(t, x) = \frac{1}{\sqrt{4\pi\Omega}} \left(\frac{\epsilon t - x}{l_\Omega} \right)^{-i\epsilon\Omega} = \frac{1}{\sqrt{4\pi\Omega}} e^{-i\Omega\eta} e^{i\Omega \ln(\frac{x}{l_\Omega})}, \quad (2.2.44)$$

where I and II label the RRW and LRW wedges, respectively. The quantity $\Omega > 0$ is the (dimensionless) Rindler frequency and again $\epsilon = 1$ corresponds to right-movers and $\epsilon = -1$ to left-movers. One needs to introduce l_Ω , which is a constant of dimension length,

freely choosable and may depend on ϵ and Ω . Such choice needs to be made since the argument of

$$\ln\left(\frac{\chi}{l\Omega}\right) \quad (2.2.45)$$

must be dimensionless. A convenient choice will be made when appropriate within the chapters where it appears. In these formulas one can substitute for η, χ by using (2.2.36).

To compute the normalization, it is convenient to choose $t = 0 = \eta$ as hyper surface. By (2.2.28) one finds that $u_{\Omega,I}, u_{\Omega,II}$ are (delta) normalized in the same fashion as their Minkowski counterparts

$$\begin{aligned} (u_{\Omega,I}, u_{\Omega',I}) &= \delta_{\epsilon,\epsilon'} \delta(\Omega - \Omega'), \\ (u_{\Omega,I}^*, u_{\Omega',I}^*) &= -\delta_{\epsilon,\epsilon'} \delta(\Omega - \Omega'), \\ (u_{\Omega,I}^*, u_{\Omega',I}) &= 0. \end{aligned} \quad (2.2.46)$$

Analogous relations occur when I is replaced by II . Mixed products vanish. Negative frequency solutions in the RRW and LRW are obtained by taking the complex conjugates of (2.2.43) and (2.2.44).

The computations become more involved when $m \neq 0$ (and/or one considers extra dimensions): in this case right and left movers *do not* decouple and one obtains a different set of solutions to (2.2.16)

$$\phi_{\Omega}^R(\tau, \chi) = \frac{1}{\sqrt{\Omega\pi}} \left(\frac{l\mu}{2}\right)^{i\Omega} \frac{1}{\Gamma(i\Omega)} K_{i\Omega}(m\chi) e^{-i\Omega\eta} \quad (2.2.47)$$

where $K_{i\Omega}(m\chi)$ is a modified Bessel function of the second kind [21], l is a dimensional arbitrary constant.

2.2.7 Bogoliubov transformations

The choice of a complete basis for the solutions of (2.2.16) (or the fermionic counterpart) is not unique. A transformation between one basis and another is known as *Bogoliubov transformations* (BVT). Furthermore, suppose there are two regions of spacetime where there are observers that naturally describe fields with two different set of coordinates and suppose the definitions of particles are not equivalent in such coordinates. Also in this case, one can introduce BVT that relate modes in one region covered by one coordinate chart to modes in the other. Such transformations carry deep physical meaning: given the BVT between two sets of solutions to some field equations, there is a straightforward relation between the coefficients of these transformations and the particle content in a quantum state as seen by different observers [9, 10]. In general, a

positive frequency excitation as described by one observer will be a superposition of *both* positive and negative frequencies as described by a different observer. This mathematical observation is, for example, at the very basis of the Hawking-Unruh effect [8, 22]. Such effect can be easily understood as follows: when there is a mismatch between vacua associated to different particle annihilation operators, one observer will describe the vacuum of the other observer as a state highly populated by particles. The consequences of these mathematical techniques are vast: they imply that in QFT there is no such thing as a universal notion of particle [10]. This conclusion is striking, though predictions based on it have been awaiting decades for verification (i.e. dynamical Casimir effect, where the vacuum state of the quantized electromagnetic field confined in a cavity becomes a state populated by particles when one wall of the cavity rapidly oscillates).

Solutions to any field equation are usually expanded in terms of Fourier modes. Let

$$\begin{aligned}\Phi &= \sum_i a_i \phi_i = a \cdot \phi \\ \Phi &= \sum_j a'_j \phi'_j = a' \cdot \phi'\end{aligned}\tag{2.2.48}$$

be two different decompositions of the quantum field Φ where we assume the spectrum to be discrete for simplicity. One can then write the change of basis as

$$\phi' = \mathcal{A} \cdot \phi,\tag{2.2.49}$$

where \mathcal{A} is a matrix that represents the change of basis and encodes all the properties of the BVT. Notice that \mathcal{A} will be fundamental throughout Part II of this work. The (trivial) matrix relation

$$\mathcal{A}^{-1} \mathcal{A} = 1\tag{2.2.50}$$

encodes the Bogoliubov identities, which, in the simple case of an uncharged scalar field, assume the well known expressions that can be found in [10]. Such relations have to hold in order for the field expansion to be invariant under a change of basis.

Given a global Killing vector ∂_τ , one can pick a preferred basis $\{\phi_i\}$ of solutions to the field equations that can naturally be split in two subsets

$$\{\phi_i^+\} \cup \{\phi_i^-\} = \{\phi_i\}\tag{2.2.51}$$

such that

$$i\partial_\tau \phi_i^\pm = \pm \omega_i \phi_i^\pm\tag{2.2.52}$$

and ω_i is the corresponding eigenvalue to ϕ_i . We define ϕ_i^\pm as *positive* and *negative* energy modes respectively; they enjoy the property that

$$(\phi_i^\pm, \phi_j^\pm) = \pm \delta_{ij}\tag{2.2.53}$$

if they are properly normalized bosonic fields or

$$(\phi_i^\pm, \phi_j^\pm) = \delta_{ij} \quad (2.2.54)$$

if they are properly normalized fermionic fields. (\cdot, \cdot) is understood to be the appropriate inner product for bosonic and fermionic fields respectively and mixed inner products always vanish.

We are in a position to establish the connection between the inner product and the BVT. We consider bosons for simplicity and use (2.2.49) and (2.2.53). (2.2.49) can be written in components as

$$\phi_{i'} = \sum_j \mathcal{A}_{i'j} \phi_j^+ + \sum_{j'} \mathcal{A}_{i'j'} \phi_{j'}^- = \sum_j [A_{i'j} \phi_j^+ + B_{i'j} \phi_j^-], \quad (2.2.55)$$

where we choose the upper case notation A, B for the standard generic alpha and beta coefficients (α and β , see [10]) for bosons. We will see in the second part of the work that such choice allows to consider BVT in different travel regimes. We now compute

$$\begin{aligned} (\phi_i^+, \phi_{i'}) &= (\phi_i^+, \sum_j \mathcal{A}_{i'j} \phi_j) = (\phi_i^+, \sum_j [A_{i'j} \phi_j^+ + B_{i'j} \phi_j^-]) = \\ &= \sum_j A_{i'j} (\phi_i^+, \phi_j^+) + \sum_j B_{i'j} (\phi_i^+, \phi_j^-) = A_{i'i}, \end{aligned} \quad (2.2.56)$$

where we have used (2.2.53) in the last line. Therefore,

$$(\phi_i^+, \phi_{i'}) = A_{i'i} \quad (2.2.57)$$

which shows that the elements of \mathcal{A} are uniquely determined by the inner product between the different sets of modes.

As a technical point, we notice that if the spectrum is continuous, say

$$\Phi = \int d\omega a_\omega \phi_\omega, \quad (2.2.58)$$

then the Krönecker deltas will be replaced by Dirac deltas and the relation

$$\mathcal{A}^{-1} \mathcal{A} = 1 \rightarrow (\mathcal{A}^{-1} \mathcal{A})_{\omega\omega'} = \delta(\omega - \omega') \quad (2.2.59)$$

is modified accordingly. In such case, the definition of matrix inverses and the normalization of the field modes is in general ill defined. One can solve such issues by appropriately building normalized wave packets. We will not deal with such constructions in this work [18].

The operators a_i, a'_j transform accordingly to (2.2.49) as

$$a' = (\mathcal{A}^{-1})^T \cdot a \quad (2.2.60)$$

where a', a are two arrays of operators corresponding to the modes ϕ', ϕ . Therefore

$$\Phi = a' \cdot \phi' = a \cdot \mathcal{A}^{-1} \mathcal{A} \cdot \phi = a \cdot \phi \quad (2.2.61)$$

which shows that the field is independent of the choice of basis as expected.

Specifying the type of field and its properties allows to obtain more information about the elements and the structure of \mathcal{A} .

Composition of Bogoliubov transformations

We wish to understand how to compose BVT in this formalism. We start from three sets $\Gamma, \Gamma', \Gamma''$, for example three sets of mode solutions to some field equations.

Given a BVT \mathcal{A}_1 between Γ and Γ' , and a BVT \mathcal{A}_2 between Γ' and Γ'' , this matrix formalism allows us to immediately obtain the BVT \mathcal{A}_3 between Γ and Γ'' : it reads

$$\mathcal{A}_3 = \mathcal{A}_2 \mathcal{A}_1. \quad (2.2.62)$$

Schematically

$$\begin{array}{c} \mathcal{A}_3 = \mathcal{A}_2 \mathcal{A}_1 \\ \Gamma \xrightarrow{\mathcal{A}_1} \Gamma' \xrightarrow{\mathcal{A}_2} \Gamma'' \end{array}$$

This formalism allows for an easy extension to any arbitrary composition of BVT. Note that in order to compose BVT, it is necessary that the codomain of \mathcal{A}_1 must coincide with the domain of \mathcal{A}_2 . Physically, this means that the notion of particles is the same in both domains.

Bogoliubov transformations for uncharged bosons

Given a scalar uncharged bosonic field, we can find an explicit form for \mathcal{A} in terms of standard notation such as [10]. We split the solutions to (2.2.16) in positive and negative frequencies that obey

$$(\phi_i^\pm, \phi_j^\pm) = \pm \delta_{ij}. \quad (2.2.63)$$

A change of basis then takes the form

$$\mathcal{A} = \begin{pmatrix} \alpha & \beta \\ \beta^* & \alpha^* \end{pmatrix} \quad (2.2.64)$$

where α, β are defined in [10] and we use a compact matrix form. It is worth noticing that the elements $\mathcal{A}_{n,m}$ are labeled by $n, m > 0$.

In Part II of this work we will extensively employ the following notation and conventions: for any (bosonic) BVT between inertial and uniformly accelerated frames we will use lower case α and β for the different Bogoliubov coefficients. For any *composite* BVT, for example inertial-to-uniformly accelerated-to-inertial, we will employ A and B instead of the standard α and β .

we use A, B as a notation for the general travel scenario alphas and betas and use ${}_o\alpha, {}_o\beta$ for the inertial to accelerated α, β .

Fermions

For fermionic fields one can proceed in a conceptually similar way to uncharged bosons, but keep in mind that there are both particles and antiparticles for these anti-commuting fields. One again defines a transformation as (2.2.49) and the elements \mathcal{A}_{pq} are now labeled by $p, q \in \mathbb{Z}$ where $p, q > 0$ mixes positive frequencies only, $p, q < 0$ negative frequencies only and the other two cases mix positive and negative frequencies.

The matrix \mathcal{A} will be specialized in the following chapters when required.

2.3 Quantum Information

Information can be manipulated, crated, stored, processed and transmitted by classical or quantum devices. Classical physics has served the purpose very well in the last century but towards its end scientists have become aware that quantum physics can play a fundamental role in this area. One of the first astounding results [23] showed that the problem of prime factorization can be solved much more efficiently by using a quantum computer (or protocol) instead of a classical computer. Other results, such as teleportation [1] lay at the very core of QI.

One of the main aims of QI is to devise and describe protocols that can perform a certain task more efficiently than the classical counterpart. More importantly, it is desirable that such improvements *cannot* be obtained in any way by classical means. A protocol, for example, takes an input quantum state, uses a resource and some operations and produces as an output a quantum state. The main resource that is used in QI are the nonlocal correlations that can be present between any two (or more) sets of degrees of freedom in quantum systems. Such nonlocal correlations are called *entanglement*. Entanglement has sparked debate since the beginning of the past century [24, 25]. It has been understood that nonlocal correlations alone cannot be used to transmit information. If this was not the case, it would be possible to signal superluminally, and therefore

violate causality.

In the following we proceed to give a brief introduction to the techniques that will be used throughout this work.

2.3.1 Separability and Entanglement

Let's consider a state $|\Psi\rangle \in \mathcal{H}$ where \mathcal{H} is the Hilbert space of the system. The state might describe some system that contains, say, two subsets of degrees of freedom A, B whose (quantum) correlations we wish to analyze. There is no restriction on the type of partition one might choose: the subsystems A and B can be arbitrary. When such a bi-partition is chosen, the state is then called *bipartite* and we denote it by $|\Psi\rangle_{AB}$. A state might contain three (or more) subsystems and if one wishes to choose such a partition the state it is then called *multipartite*. For the purpose of this work we will analyze only correlations between two subsystems. While bipartite correlations are very well understood, multipartite correlations have so far not been completely characterized and understood.

Given a bipartite system described by $|\Psi\rangle_{AB}$, the Hilbert space \mathcal{H} is the tensor product of the individual Hilbert spaces \mathcal{H}_A and \mathcal{H}_B describing the degrees of freedom of these subsystems; the Hilbert spaces satisfy the relation

$$\mathcal{H} = \mathcal{H}_A \otimes \mathcal{H}_B, \quad (2.3.1)$$

and the dimensions of the Hilbert spaces obey

$$\dim(\mathcal{H}) = \dim(\mathcal{H}_A) \cdot \dim(\mathcal{H}_B). \quad (2.3.2)$$

It might seem natural that a similar product decomposition to (2.3.1) occurs for states $|\Phi\rangle_{AB} \in \mathcal{H}$ but in general there exist states $|\Phi'\rangle_{AB} \in \mathcal{H}$ such that

$$|\Phi'\rangle_{AB} \neq |\Phi\rangle_A \otimes |\Phi\rangle_B \quad (2.3.3)$$

for any $|\Phi\rangle_A, |\Phi\rangle_B$. We can now give a more formal definition of bipartite state. Let $\{|\phi_i\rangle_A\}$ and $\{|\phi_j\rangle_B\}$ be a basis of \mathcal{H}_A and \mathcal{H}_B respectively. Then $|\Phi\rangle_{AB}$ is bipartite if it has the form

$$|\Phi\rangle_{AB} = \sum_{i,j} C_{ij} |\phi_i\rangle_A \otimes |\phi_j\rangle_B \quad (2.3.4)$$

and

$$\sum_{i,j} |C_{ij}|^2 = 1. \quad (2.3.5)$$

The density matrix formed from $|\Phi\rangle_{AB}$ is

$$\rho_{AB} = |\Psi\rangle\langle\Psi|_{AB} \quad (2.3.6)$$

We say that a state ρ_{AB} is *separable* (with respect to such a bipartition) iff

$$\rho_{AB} = \sum_i p_i \rho_A^i \otimes \rho_B^i \quad (2.3.7)$$

where $\sum_i p_i = 1$. If this is not the case, then ρ_{AB} is *entangled* in the (sets of) degrees of freedom A and B . Notice that in the particular case of a pure state, there exists only *one* weight $p_k = 1$ while all others vanish. Therefore

$$\rho_{AB} = \rho_A^k \otimes \rho_B^k. \quad (2.3.8)$$

An important property of entanglement is that it does not increase under LOCC (Local Operations and Classical Communications) and is invariant under local unitary operations (for example an operation of the form $U_A \otimes U_B$ where U_A, U_B are unitary operations).

For the purposes of this work, we make the following observation: BVTs are global unitary maps of the Fock space to itself, which, in general, are not LO. In this sense, they *create* entanglement between different degrees of freedom, in particular between the mode number degrees of freedom.

2.3.2 Purity and mixedness

A state ρ is said to be *pure* iff $\rho^2 = \rho$. This means that there exists some vector $|\Psi\rangle$ such that

$$\rho = |\Psi\rangle\langle\Psi|. \quad (2.3.9)$$

Otherwise the state ρ is said to be *mixed*. Equivalently, a state is pure iff

$$\text{Tr}(\rho^2) = 1. \quad (2.3.10)$$

One can define the *mixedness* as

$$M[\rho] = 1 - \text{Tr}(\rho^2), \quad (2.3.11)$$

where $M[\rho] = 0$ for pure states and $M[\rho] > 0$ for mixed states.

For our purposes, the difference between pure and mixed states becomes important, for example, when one wishes to compute measures of entanglement for the state. In our work we will always start with pure states.

2.3.3 Partial tracing and partial transposition

The quantum state contains the information of the system that is being studied. Let us consider a bipartite system described by $|\Phi\rangle_{AB}$ for simplicity. It often happens that

one ignores or cannot access some part B of the system and can only obtain information about the complementary subsystem A . To describe such ignorance one employs the mathematical operation called *partial trace*. Given a bipartite state ρ_{AB} , we define the partial trace $Tr_B(\rho_{AB})$ over B as the trace over all degrees of freedom contained in B . Formally, let $\{|\phi_i\rangle_B\}$ be a basis for \mathcal{H}_B . Then

$$Tr_B(\rho_{AB}) = \sum_i \langle \phi_i | \rho_{AB} | \phi_i \rangle_B. \quad (2.3.12)$$

It is trivial to check that

$$Tr_B(\rho_{AB}) = \rho_A \Leftrightarrow \rho_{AB} = \rho_A \otimes \rho_B. \quad (2.3.13)$$

This is equivalent to the statement that A and B are not entangled since by tracing over B one still has all the information about A (which is contained in ρ_A). In general, the partial trace of a pure state ρ_{AB} over some subsystem B will leave a mixed state and we understand that information about A has been lost.

We define now an operation that will be useful when studying measures of entanglement for different states.

Let $\{|\phi_i\rangle_A\}$ and $\{|\psi_j\rangle_B\}$ be bases for \mathcal{H}_A and \mathcal{H}_B respectively. Let ρ_{AB} be a bipartite state and let its decomposition on these bases be

$$\rho_{AB} = \sum_{i,j,k,l} C_{i,j;k,l} |i,j\rangle \langle k,l| \quad (2.3.14)$$

where

$$|i,j\rangle = |\phi_i\rangle_A \otimes |\psi_j\rangle_B. \quad (2.3.15)$$

The *partial transpose* of ρ_{AB} is defined as follows [26]:

$$\rho_{AB}^{PT} := \sum_{i,j,k,l} C_{i,l;k,j} |i,j\rangle \langle k,l|. \quad (2.3.16)$$

2.3.4 Measures of entanglement

Entanglement is *not* a physical observable on its own. It is a property of a state. Entanglement can be created or degraded, it can be exchanged between subsystems but cannot be directly observed or measured. One needs to produce a *measure* of entanglement that provides an operationally well defined way to quantify such correlations. A great number of measures have been proposed. No measure is a priori preferable among others although it turns out that most measures are very difficult to compute explicitly. For the purpose of this work, we will be interested only in measures for bipartite pure or mixed states.

In general, a measure of entanglement $E[\rho]$ is a non-negative real function of a state ρ that must

- i vanish for separable states: ρ is separable $\implies E[\rho] = 0$;
- ii not increase under LOCC;
- iii is invariant under local unitaries;

(for a thorough discussion see [27]).

Given a pure bipartite state described by ρ_{AB} , the *Von Neumann Entropy* S is the standard measure for entanglement and is defined as

$$S(\rho_B) = -\text{Tr}(\rho_B \log_2(\rho_B)) = -\sum_i \lambda_i \log_2(\lambda_i), \quad (2.3.17)$$

where $\{\lambda_i\}$ are the eigenvalues of ρ_B . It is possible to show that

$$S(\rho_B) = S(\rho_A). \quad (2.3.18)$$

Measures of entanglement for a mixed bipartite state ρ_{AB} are usually not easy to compute explicitly. In this case, the entanglement can be quantified using the Peres partial-transpose criterion. Since the partial transpose of a separable state has always positive eigenvalues, then a state is non-separable (and therefore, entangled) if the partial transposed density matrix has, at least, one negative eigenvalue. However, this is a sufficient and necessary condition only for 2×2 and 2×3 dimensional systems. In higher dimensions, the criterion is only sufficient. The Peres criterion is at the core of the (only) measure that, in general, can be of practical and computational use for mixed states. Such measure is called *negativity* $\mathcal{N}[\rho]$ and is an entanglement monotone that quantifies how strongly the partial transpose of a density operator ρ fails to be positive

$$\mathcal{N}[\rho] := \sum_{\lambda < 0} |\lambda|, \quad (2.3.19)$$

where $\{\lambda_i\}$ are the eigenvalues of the partial transpose of ρ . The maximum value of the negativity \mathcal{N}_{AB}^{\max} (reached for maximally entangled states) depends on the dimension of the maximally entangled state. Specifically, for qubits

$$\mathcal{N}_{AB}^{\max} = \frac{1}{2}. \quad (2.3.20)$$

The negativity is a useful measure because all the entangled states that it fails to detect are necessarily bound entangled, that is, these states cannot be distilled [28].

\mathcal{N} has the advantage of being easy to compute for bipartite systems of arbitrary dimension [29]. The closely-related *logarithmic negativity*,

$$E_{\mathcal{N}} := \ln(1 + \mathcal{N}) \tag{2.3.21}$$

is an upper bound on the distillable entanglement E_D and is operationally interpreted as the entanglement cost E_C under operations preserving the positivity of partial transpose [30]. In this respect, the entanglement quantification based on negativity nicely interpolates between the two canonical (yet generically difficult to compute) extremal entanglement measures E_D and E_C [31].

2.4 Outline - Part I

In this first part of the work we concentrate on the effects of relativity on entanglement between global quantum fields in flat spacetime. The results in chapter 3 and 4 have appeared in [15] and [32] respectively.

2.4.1 Beyond the Single Mode Approximation

In Chapter 3 we address and revise the “single mode approximation” that is extensively used in literature. The single mode approximation assumes that the Bogoliubov transformations between Minkowski modes and the Rindler modes map one mode to one mode. We revise such transformations and show that these transformations are not injective in the frequency degree of freedom. We exploit the Unruh solutions to the field equations in Minkowski coordinates to generalize the concept of Unruh particle. Positive frequency Unruh modes come in pairs, unlike Minkowski modes. We show that when such pairs are used to define Unruh particles, new degrees of freedom naturally arise. We investigate to what extent such degrees of freedom influence the entanglement present in initially maximally entangled states of bosonic Unruh modes as described by two inertial observers when one of the two observers accelerate. We find that entanglement is degraded with increasing acceleration and vanishes with infinite acceleration.

We describe for which choice of the new degrees of freedom one can recover the single mode approximation. We show that it is possible to construct a peaked Minkowski wave packet that is mapped to a peaked Unruh wave packet by the Bogoliubov transformations. If the peaking on one side is increased, it is reduced on the other. In the sense of wave packets just presented, we argue that the single mode approximation can be recovered for suitable choice of the new degrees of freedom. We show that mass does not change qualitatively the results. In this work we will present only the analysis performed

for uncharged scalar fields.

2.4.2 Entanglement redistribution between charged bosonic field modes in relativistic settings

In chapter 4 we introduce charged bosonic field modes in the analysis of the behavior of entanglement as described by different observers. Two inertial observers Alice and Bob study three different families of maximally entangled states of charged bosonic field modes. An accelerated observer Rob analyzes Bob's modes and describes the entanglement as a function of his acceleration. It is well known that entanglement between fermionic field modes and bosonic field modes behaves differently in the infinite acceleration limit. Our aim is to analyze the same states and bipartitions considered for fermionic fields in [60] and compare the results. One bipartition occurs when Rob cannot distinguish Unruh particles and antiparticles. The second and third bipartitions occur where he can make this distinction. In particular, we wish to understand if entanglement can be redistributed between these bipartitions in the same fashion as in the fermionic case. We find that regardless of the presence of antiparticles, entanglement is still degraded and vanishes in the infinite acceleration limit. While in the literature it was found that bosonic entanglement is almost always monotonically decreasing with increasing acceleration, we also find rare cases where this does not happen.

2.5 Outline - Part II

In this part of the work we develop the techniques required to study the effects of cavity motion on mode entanglement. The chapters are arranged chronologically following the work developed during the PhD. All chapters follow logically one from another. The general techniques are developed in chapter 5 and lay the basis for the following chapters.

2.5.1 Entanglement degradation of cavity modes due to motion

In chapter 5 we start by introducing the techniques for quantizing a $1 + 1$ or $3 + 1$ massive or massless scalar field with Dirichlet boundary conditions and compact support. The spectrum of the field is discrete due to the boundary conditions. We assume that the walls of the cavity can undergo different linear accelerations such that the length of the cavity as measured by a comoving observer does not change. In this sense, the box is accelerated as a whole and we use the proper acceleration of the centre of the cavity in

the following. We can compute how the mode solutions to the field equations before any travel of the cavity (pre-trip) are related to the mode solutions of the field equations after the trip (post-trip). The BVT between the pre-trip modes and the post-trip modes can be computed analytically in a perturbative regime where the parameter is the product of the acceleration of the centre of the cavity and its proper length. Therefore large cavities with small accelerations or small cavities with large accelerations can be treated with our techniques.

We entangle one mode of the field contained in an inertial cavity held by Alice with one mode of the field contained in a cavity that travels and is held by Rob. The initial state is assumed to be maximally entangled. We compute the entanglement between the mode in Alice's cavity and the mode in Rob's cavity after the latter's travel in the following scenarios: the inertial-accelerated-inertial, the one way trip scenario and the return trip scenario.

We find that in the $1 + 1$ massless case there is degradation of entanglement and it occurs as a second order correction to the initial value. The correction appears as a function of the details of the travel scenario. Given that in this case there is exact periodicity, Alice and Rob can plan Rob's one way trip such that there will be no degradation. We verify that for reasonable values of accelerations and lengths of cavities this correction is negligible.

We notice that the extra dimensions just contribute as an effective mass. We find that the correction to the initial value of the entanglement is greatly enhanced when mass and/or transverse dimensions are present. To take advantage of this, one needs to prepare states of photons in Rob's cavity which have momenta which are highly transverse to the direction of travel.

2.5.2 Kinematic entanglement degradation of fermionic cavity modes

In chapter 6 we analyze the setting of chapter 5 using fermionic fields. Quantization of massless $1 + 1$ fermions is obtained using the Dirac equation with boundary conditions. Dirichlet boundary conditions cannot be employed for fermionic fields; for our setting we therefore require the current to vanish at the walls of the cavity. This introduces the presence of a zero mode in the spectrum, which we are able to treat by introducing a regularizing phase shift of the wave function at each wall. We then investigate the effects on entanglement of one cavity's motion. As for bosons, we find that entanglement is degraded in a fashion that depends on the type of scenario chosen. The correction to the initial value of the negativity occurs again at second order in the perturbation parameter. We also find that when the regularizing phase shift is removed, all corrections

to the entanglement are well behaved. The fermionic Hilbert space is finite dimensional. This allows us to investigate the violation of other Bell-type inequalities such as CHSH. We find that the violation is diminished when one cavity travels. Last, due to the presence of antiparticles, we also analyze entanglement degradation due to motion when there is particle-antiparticle entanglement.

2.5.3 Generation of entanglement within a moving cavity

In chapter 7 we analyze bosonic and fermionic quantum fields contained within one cavity. The initial state of the fields is separable in the mode number degree of freedom. After the cavity travels, the modes will all mix due to Bogoliubov transformations. We use the negativity to quantify the entanglement created between any two modes of the spectrum. Surprisingly, when modes are oddly separated we find that the amount of entanglement created is at first order in the perturbation parameter for both bosons and fermions. If the modes are evenly separated, the amount of entanglement created is only at second order. In addition, we find that the behavior of entanglement as a function of the time spent accelerating is different for fermions and bosons, therefore indicating that this might be of interest for practical purposes. A striking difference appears between uncharged bosons and fermions: excitations of only one type in the initial state suppress the fermionic generation of entanglement. This phenomenon arises for fermions as a direct consequence of the particle-antiparticle coherence generated by the BVT, rather than particle particle or antiparticle-antiparticle coherence.

2.5.4 Entanglement resonances within a moving cavity

In chapter 8 we look for a mechanism to enhance the entanglement generation within cavity scenarios. We notice that it is possible to select two arbitrary oddly separated modes and perform the Two Mode Truncation that allows to effectively reduce the full BVT to Bogoliubov Transformations between the two modes solely. Such reduced transformations satisfy Bogoliubov identities to second order in the perturbation parameter. We then consider initial Gaussian states, for example the vacuum or coherent states. Since the reduced BVT are Gaussian operations, we employ Continuous Variables techniques to obtain the entanglement of the two modes when the cavity undergoes some travel scenario that we call building block. When the travel scenario consists of repeating the building block an arbitrary number of times, these techniques allow us to find analytical conditions for the final entanglement to grow linearly with the number of repetitions. We find that, in general, the total time of the building block is inversely proportional to

the sum of the frequencies of the two modes. This condition is only necessary but not sufficient and one needs to analyze case by case to find extra constraints. As an example we analyze a scenario which is analogous to standard dynamical Casimir setups [12].

The work done in this chapter has been further developed and generalized at a later stage. An updated version of the results can be found in the latest version of [33].

2.6 Outline - Part III

In this last part of the work we concentrate on the effects of relativity on entanglement between global quantum fields in curved spacetime where the topology of the spatial hyper surfaces is not trivial. The results have been presented in [34].

2.6.1 Effects of topology on the nonlocal correlations within the Hawking-Unruh radiation

In chapter 9 we go beyond flat spacetimes typically considered in literature and aim at understanding how nonlocal correlations present in the Hawking-Unruh radiation in black hole spacetimes are affected by the change in spatial topology.

While typically solutions to Einstein's equations have spatial topology equivalent to \mathbb{R}^3 , there are solutions where this must not be the case. From the perspective of Quantum Gravity, it is of great interest to understand if the topology of spacetime can change. We introduce charged bosonic fields in two different spacetimes: Minkowski with a background magnetic field and electrically charged Reissner-Nordström spacetime. The quantum field is coupled to the classical background gauge field. We introduce different Geon versions of the spacetimes and show that among all there are cases where one needs to enlarge the gauge group in order to perform the Geon quotients. The next step is to investigate the particle-particle correlations in the Hawking-Unruh radiation in the Geon versions of Schwarzschild and Reissner-Nordström spacetime. We find that when there is need for enlarging the gauge group, the correlations in the radiation are modified. More specifically, instead of finding particle-antiparticle correlations we find particle-particle correlations. We emphasize that our prediction is a signature of the topology.

Part I

CHAPTER 3

Beyond the Single Mode Approximation

The first works in the field of RQI employed global quantum fields defined on the entire spacetime. These works were aimed at showing that relativity does affect entanglement. It was assumed that two inertial parties, Alice and Bob, which employed inertial coordinates to describe fields, would at first analyze nonlocal correlations present between initially entangled global relativistic quantum field modes (see [4, 5, 35] for a sample). As a second step, a third party, uniformly accelerated Rob, would describe Bob's part of the system using Rindler coordinates; the transformations between the modes in the different coordinate charts were therefore crucial. The "single mode approximation" (SMA) was employed in order to express the relations between mode solutions to relativistic wave equations in different coordinates, namely Minkowski modes in Minkowski coordinates and Rindler modes in Rindler coordinates. The main idea behind this approximation is that solutions to field equations in Rindler coordinates are peaked around some particular frequency when expressed as a combinations of Minkowski modes, and viceversa.

In this chapter we discuss the validity of this assumption and show that in general it does not hold. The BVT that relate modes in Minkowski and Rindler coordinates are non trivial and not peaked. We introduce Unruh modes in the analysis and the corresponding particle creation and annihilation operators. We are able to show that, starting from entangled states where Bob analyzes a wave packet of Unruh modes (sharply) peaked around some Unruh frequency, it is possible to recover the SMA approximation for a suitable choice of parameters. We also generalize the definition of Unruh particle which introduces additional degrees of freedom that can be used to further understand the effects of the state of motion of the observer on entanglement.

3.1 Global Minkowski, Unruh and Rindler modes revised

We start by analyzing in more detail the relations between the Minkowski, Unruh and Rindler set of solutions to the field equations.

Consider a real scalar field Φ in $(1+1)$ dimensional Minkowski spacetime. We restrict ourselves to a massless field in one spatial dimension: the results of this chapter can be generalized for massive fields or fields in $(3+1)$ Minkowski space-time without qualitative changes.

The field equations and the general (delta) normalized solutions written in Minkowski or Rindler coordinates can be found in section 2.2.6.

An "intermediate" basis for the solutions of the field equations is given in terms of

Unruh modes which are defined as follows

$$\begin{aligned}\phi_{\Omega,R} &= \cosh(r_\Omega)\phi_{\Omega,I} + \sinh(r_\Omega)\phi_{\Omega,II}^* \\ \phi_{\Omega,L} &= \cosh(r_\Omega)\phi_{\Omega,II} + \sinh(r_\Omega)\phi_{\Omega,I}^*,\end{aligned}\tag{3.1.1}$$

where

$$\tanh r_\Omega = e^{-\pi\Omega},\tag{3.1.2}$$

the parameter Ω is a dimensionless frequency and I, II refer to RRW and LRW respectively. The Right and Left Unruh modes $\phi_{\Omega,R}, \phi_{\Omega,L}$ are both linear combinations of positive Minkowski frequency modes. Negative frequency Right and Left Unruh modes can be obtained by complex conjugation. Notice that, while R, L are a short notation for Right and Left, the Unruh modes are defined on the *entire* spacetime. For Unruh modes, R, L has the following meaning: modes with greater support on the RRW or LRW respectively. To obtain the Unruh basis one starts from the Minkowski basis and performs a change of basis which does not mix positive and negative Minkowski frequencies. In addition, each Unruh mode labeled by Ω is in one to one correspondence with a corresponding Rindler mode in the RRW and in the LRW, both labeled by the same Ω .

As explained in Chapter 2, different solutions to the field equation are related by BVT. To find these transformations we consider the field expansion in the Minkowski, Unruh and Rindler bases respectively

$$\begin{aligned}\Phi &= \int_0^\infty \left(a_{\omega,M} \phi_{\omega,M} + a_{\omega,M}^\dagger \phi_{\omega,M}^* \right) d\omega = \\ &= \int_0^\infty \left(A_{\Omega,R} \phi_{\Omega,R} + A_{\Omega,R}^\dagger \phi_{\Omega,R}^* + A_{\Omega,L} \phi_{\Omega,L} + A_{\Omega,L}^\dagger \phi_{\Omega,L}^* \right) d\Omega \\ &= \int_0^\infty \left(a_{\Omega,I} \phi_{\Omega,I} + a_{\Omega,I}^\dagger \phi_{\Omega,I}^* + a_{\Omega,II} \phi_{\Omega,II} + a_{\Omega,II}^\dagger \phi_{\Omega,II}^* \right) d\Omega,\end{aligned}\tag{3.1.3}$$

where $a_{\omega,M}$, $A_{\Omega,R}$, $A_{\Omega,L}$, and $a_{\Omega,I}$, $a_{\Omega,II}$ are Minkowski, Unruh and Rindler annihilation operators, respectively. Usual bosonic commutation relations hold

$$\begin{aligned}[a_{\omega,M}, a_{\omega',M}^\dagger] &= \delta(\omega - \omega'), \\ [A_{\Omega,R}, A_{\Omega',R}^\dagger] &= [A_{\Omega,L}, A_{\Omega',L}^\dagger] = \delta(\Omega - \Omega') \\ [a_{\Omega,I}, a_{\Omega',I}^\dagger] &= [a_{\Omega,II}, a_{\Omega',II}^\dagger] = \delta(\Omega - \Omega').\end{aligned}\tag{3.1.4}$$

Commutators for mixed R, L and I, II vanish. One can use the inner product 2.2.28 to find the transformations between the different mode solutions. Between Minkowski and

Unruh modes they read

$$\begin{aligned}
 \phi_{\omega,M} &= \int_0^\infty (\alpha_{\omega\Omega}^R \phi_{\Omega,R} + \alpha_{\omega\Omega}^L \phi_{\Omega,L}) d\Omega \\
 \phi_{\Omega,R} &= \int_0^\infty (\alpha_{\omega\Omega}^R)^* \phi_{\omega,M} d\omega \\
 \phi_{\Omega,L} &= \int_0^\infty (\alpha_{\omega\Omega}^L)^* \phi_{\omega,M} d\omega,
 \end{aligned} \tag{3.1.5}$$

where

$$\begin{aligned}
 \alpha_{\omega\Omega}^R &= \frac{1}{\sqrt{2\pi\omega}} \sqrt{\frac{\Omega \sinh \pi\Omega}{\pi}} \Gamma(-i\epsilon\Omega) (\omega l_\Omega)^{i\epsilon\Omega} \\
 \alpha_{\omega\Omega}^L &= \frac{1}{\sqrt{2\pi\omega}} \sqrt{\frac{\Omega \sinh \pi\Omega}{\pi}} \Gamma(i\epsilon\Omega) (\omega l_\Omega)^{-i\epsilon\Omega}.
 \end{aligned} \tag{3.1.6}$$

From (5.4.3) in [21] we may choose l_Ω such that

$$\begin{aligned}
 \alpha_{\omega\Omega}^R &= \frac{1}{\sqrt{2\pi\omega}} (\omega l)^{i\epsilon\Omega} \\
 \alpha_{\omega\Omega}^L &= \frac{1}{\sqrt{2\pi\omega}} (\omega l)^{-i\epsilon\Omega},
 \end{aligned} \tag{3.1.7}$$

where l is a constant of dimension length, independent of ϵ and Ω . If a choice of units is made, l may be set to one. The transformation between modes gives rise to transformations between field operators. Minkowski operators $a_{\omega,M}$ and Unruh operators $A_{\Omega,L}$, $A_{\Omega,R}$ are related by

$$\begin{aligned}
 a_{\omega,M} &= \int_0^\infty ((\alpha_{\omega\Omega}^R)^* A_{\Omega,R} + (\alpha_{\omega\Omega}^L)^* A_{\Omega,L}) d\Omega \\
 A_{\Omega,R} &= \int_0^\infty \alpha_{\omega\Omega}^R a_{\omega,M} d\omega \\
 A_{\Omega,L} &= \int_0^\infty \alpha_{\omega\Omega}^L a_{\omega,M} d\omega,
 \end{aligned} \tag{3.1.8}$$

where $\alpha_{\omega\Omega}^R, \alpha_{\omega\Omega}^L$ are Bogoliubov coefficients. The transformation between Unruh operators and Rindler operators $a_{\Omega,I}, a_{\Omega,II}$ is

$$\begin{aligned}
 a_{\Omega,I} &= \cosh(r_\Omega) A_{\Omega,R} + \sinh(r_\Omega) A_{\Omega,L}^\dagger \\
 a_{\Omega,II} &= \cosh(r_\Omega) A_{\Omega,L} + \sinh(r_\Omega) A_{\Omega,R}^\dagger.
 \end{aligned} \tag{3.1.9}$$

We can address how to relate the particle states in different coordinates. Since the Unruh annihilation operators are linear combinations of Minkowski annihilation operators only, Minkowski modes and Unruh modes share the common vacuum state $|0\rangle_M = |0\rangle_U$, where

$$A_{\Omega,R}|0_\Omega\rangle_M = A_{\Omega,L}|0_\Omega\rangle_M = 0. \tag{3.1.10}$$

Although states with a completely sharp value of Ω are not normalisable, we may approximate normalisable wave packets that are sufficiently narrowly peaked in Ω by taking a fixed Ω and renormalising the Unruh and Rindler commutators to read

$$\left[A_{\Omega,R}, A_{\Omega,R}^\dagger \right] = \left[A_{\Omega,L}, A_{\Omega,L}^\dagger \right] = 1 \quad (3.1.11)$$

$$\left[a_{\Omega,I}, a_{\Omega,I}^\dagger \right] = \left[a_{\Omega,II}, a_{\Omega,II}^\dagger \right] = 1 \quad (3.1.12)$$

with mixed commutators vanishing. In this idealization of sharp peaking in Ω , the most general creation operator that is of purely positive Minkowski frequency can be written as a linear combination of the two Unruh creation operators, in the form

$$a_{\Omega,U}^\dagger = q_L A_{\Omega,L}^\dagger + q_R A_{\Omega,R}^\dagger, \quad (3.1.13)$$

where $q_R, q_L \in \mathbb{C}$ and

$$|q_R|^2 + |q_L|^2 = 1. \quad (3.1.14)$$

It is trivial to check that

$$\left[a_{\Omega,U}, a_{\Omega,U}^\dagger \right] = 1. \quad (3.1.15)$$

Therefore, a single Unruh particle state corresponds to

$$\begin{aligned} a_{\Omega,U}^\dagger |0\rangle_U &= \sum_{n=0}^{\infty} \sqrt{n+1} \frac{\tanh(r_\Omega)}{\cosh^2(r_\Omega)} |\Phi_\Omega^n\rangle \\ |\Phi_\Omega^n\rangle &= q_L |n_\Omega\rangle_I |(n+1)_\Omega\rangle_{II} + q_R |(n+1)_\Omega\rangle_I |n_\Omega\rangle_{II}. \end{aligned} \quad (3.1.16)$$

We stress that in literature one finds $q_R = 1$ and $q_L = 0$ as a common assumption which corresponds to a very special choice of Unruh modes.

3.2 Entanglement revised beyond the single mode approximation

In the RQI literature, the SMA

$$a_{\omega,M} \approx A_{\Omega,R} \quad (3.2.1)$$

is considered to directly relate Minkowski and Unruh modes. The main argument for taking this approximation is that the distribution

$$a_{\omega,M} = \int_0^\infty \left[(\alpha_{\omega\Omega}^R)^* A_{\Omega,R} + (\alpha_{\omega\Omega}^L)^* A_{\Omega,L} \right] d\Omega \quad (3.2.2)$$

is peaked. However this is not true and (3.2.2) in fact oscillates (see (3.1.7)).

Entanglement in non-inertial frames can be studied provided one considers the state

$$|\Psi\rangle = \frac{1}{\sqrt{2}} (|0_\omega\rangle_M |0_\Omega\rangle_U + |1_\omega\rangle_M |1_\Omega\rangle_U), \quad (3.2.3)$$

where the notation in the right hand side of equation (3.2.3) assumes that the states observed by Alice and Bob are orthogonal to good approximation. We will use the notation where kets are put between Alice and Bob simply for clarity of the distinction between the subsystems. we choose the state (3.2.3) for mathematical simplicity. A single Unruh frequency Ω corresponds to the *same* Rindler frequency Ω . As stated before, when $q_R = 1$ and $q_L = 0$ we recover the results canonically presented in the literature (for example [7]). In this section, we will revise the analysis of entanglement in non-inertial frames starting from a general Unruh mode. However, since Minkowski coordinates are a natural choice for inertial observers we will show in the section 3.3 that the standard results also hold for Minkowski states as long as suitable wavepackets are considered.

Having the expressions for the vacuum and single particle states in the Minkowski, Unruh and Rindler bases enables us to analyze the degradation of entanglement when described by observers in uniform acceleration in the standard scenario. Let us consider the maximally entangled state Eq. (3.2.3) analyzed by two inertial observers. By changing $|q_R|$'s we can pick different initial states. An arbitrary Unruh single particle state has different right and left components with weights $|q_R|$ and $|q_L|$. Therefore, we can view the system as being tripartite and say that Alice's modes with frequency ω are entangled to right Unruh (Alice-Bob) modes Ω . There is no a priori reason to choose a specific value of $|q_R|$. In fact, and as we will see later, feasible choices of Minkowski states are in general linear superpositions of different Unruh modes with different values of $|q_R|$.

We now wish to study the entanglement in the state taking into account that the Ω modes are described by observers in uniform acceleration. Therefore, Unruh states must be transformed into the Rindler basis as usual. The Alice-Bob system, once analyzed by Rob, is a tri-partite system. The Minkowski mode corresponds to the mode studied by Alice and the Rindler modes of the region I are analyzed by Rob. In the limit $a \rightarrow 0$ the Alice-Rob partition corresponds to the Alice-Bob partitions.

We quantify entanglement using negativity \mathcal{N} , (2.3.19), since we are left with mixed states.

In what follows we study the entanglement between the Alice-Rob modes. The Alice-Rob density matrix is obtained by tracing over the region II

$$\rho_{AR} = \frac{1}{2} \sum_{n=0}^{\infty} \left[\frac{T^n}{C} \right]^2 \rho_{AR}^n, \quad (3.2.4)$$

where

$$\begin{aligned} \rho_{AR}^n = & |0n\rangle\langle 0n| + \frac{n+1}{C^2} \left(|q_R|^2 |1n+1\rangle\langle 1n+1| + |q_L|^2 |1n\rangle\langle 1n| \right) + \frac{\sqrt{n+1}}{C} \left(q_R |1n+1\rangle\langle 0n| \right. \\ & \left. + q_L T |1n\rangle\langle 0n+1| \right) + \frac{\sqrt{(n+1)(n+2)}}{C^2} q_R q_L^* T |1n+2\rangle\langle 1n| + (\text{H.c.})_{\text{non-diag.}} \end{aligned} \quad (3.2.5)$$

Here $(\text{H.c.})_{\text{non-diag.}}$ means Hermitian conjugate of only the non-diagonal terms and we defined for convenience

$$\begin{aligned} S &:= \sinh(r_\Omega) \\ C &:= \cosh(r_\Omega) \\ T &:= \tanh(r_\Omega). \end{aligned} \quad (3.2.6)$$

The partial transpose σ_R of ρ_R with respect to Alice is given by

$$\sigma_{AR} = \frac{1}{2} \sum_{n=0}^{\infty} [f(n)]^2 \sigma_{AR}^n \quad (3.2.7)$$

where

$$\begin{aligned} \sigma_{AR}^n = & |0n\rangle\langle 0n| + \frac{n+1}{C^2} \left(|q_R|^2 |1n+1\rangle\langle 1n+1| + |q_L|^2 |1n\rangle\langle 1n| \right) + \frac{\sqrt{n+1}}{C} \left(q_R |0n+1\rangle\langle 1n| \right. \\ & \left. + q_L T |0n\rangle\langle 1n+1| \right) + \frac{\sqrt{(n+1)(n+2)}}{C^2} q_R q_L^* T |1n+2\rangle\langle 1n| + (\text{H.c.})_{\text{non-diag.}} \end{aligned} \quad (3.2.8)$$

The eigenvalues of the partial transpose density matrix are computed numerically. The resulting negativity between the Alice-Rob modes is plotted in Fig. (3.1) for different values of $|q_R| = 1, 0.9, 0.8, 0.7$. $|q_R| = 1$ corresponds to the canonical case studied in the literature [5]. In the bosonic case, the entanglement between the Alice-Rob modes always vanishes in the infinite acceleration limit. Interestingly, there is no fundamental difference in the degradation of entanglement for different choices of $|q_R|$. There is no Unruh state which whose entanglement does not degrade monotonically with acceleration.

3.3 Wave packets: recovering the single mode approximation

The entanglement analyses of section 3.2 take Alice's state to be a Minkowski one particle state with a sharp Minkowski momentum and Rob's state to be an Unruh one particle state with sharp Unruh frequency. The Unruh particle is a linear combination of two Unruh modes specified by q_R and q_L . The Alice and Rob states are further assumed to be orthogonal, so that the system can be treated as bipartite. We now discuss the

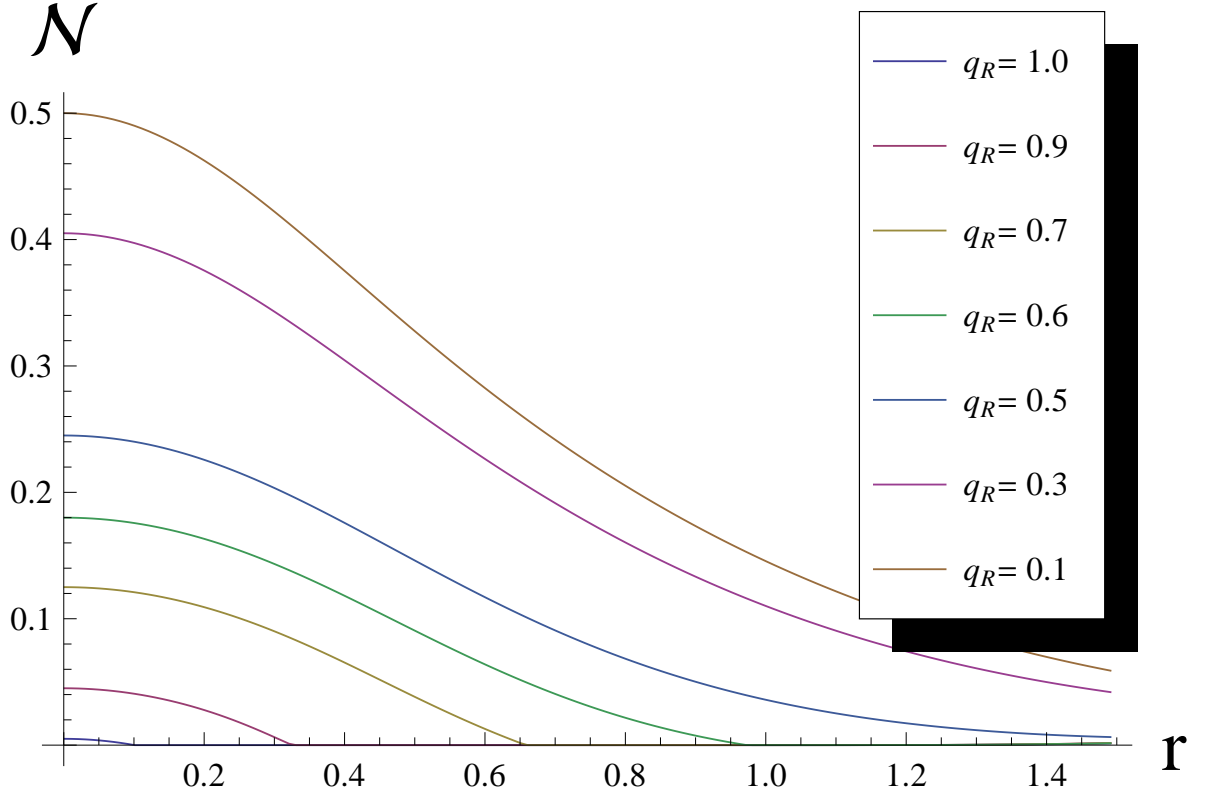


Figure 3.1: Negativity as a function of $r_\Omega = \arctan e^{-\pi\Omega}$ for a sample of values of $|q_R|$.

sense in which these assumptions are a good approximation to Alice and Rob states that can be built as Minkowski wave packets.

Recall that a state with a sharp frequency, be it Minkowski or Unruh, is not normalisable and should be understood as the idealisation of a wave packet that contains a continuum of frequencies with an appropriate peaking. Suppose that the Alice and Rob states are initially set up as Minkowski wave packets, peaked about distinct Minkowski momenta and with negligible overlap, so that the bipartite assumption is a good approximation. The transformation between the Minkowski and Unruh bases is an integral transform: we wish to arrange Rob's state to be peaked about a single Unruh frequency. If we succeed we also wish to understand how the frequency uncertainties on the Minkowski and Unruh sides are related.

For definiteness, we focus on the massless scalar field of section 2.2.4. The massive scalar field is briefly discussed at the end of the section.

We start by considering a packet of Minkowski creation operators $a_{\omega,M}^\dagger$ smeared with some weight function $f(\omega)$. We wish to express this packet in terms of Unruh creation

operators $A_{\Omega,R}^\dagger$ and $A_{\Omega,L}^\dagger$ smeared with the weight functions $g_R(\Omega)$ and $g_L(\Omega)$, so that

$$\int_0^\infty f(\omega) a_{\omega,M}^\dagger d\omega = \int_0^\infty (g_R(\Omega) A_{\Omega,R}^\dagger + g_L(\Omega) A_{\Omega,L}^\dagger) d\Omega. \quad (3.3.1)$$

From (3.1.8) it follows that the smearing functions are related by

$$\begin{aligned} g^R(\Omega) &= \int_0^\infty \alpha_{\omega\Omega}^R f(\omega) d\omega \\ g^L(\Omega) &= \int_0^\infty \alpha_{\omega\Omega}^L f(\omega) d\omega \\ f(\omega) &= \int_0^\infty ((\alpha_{\omega\Omega}^R)^* g_R(\Omega) + (\alpha_{\omega\Omega}^L)^* g_L(\Omega)) d\Omega. \end{aligned} \quad (3.3.2)$$

By (3.1.7), the above equations are recognised as a Fourier transform pair between the variable $\ln(\omega l) \in \mathbb{R}$ on the Minkowski side and the variable $\pm\Omega \in \mathbb{R}$ on the Unruh side: the full real line on the Unruh side has been broken into the Unruh frequency $\Omega \in \mathbb{R}^+$ and the discrete index R, L . All standard properties of Fourier transforms thus apply.

Parseval's theorem takes the form

$$\int_0^\infty |f(\omega)|^2 d\omega = \int_0^\infty (|g_R(\Omega)|^2 + |g_L(\Omega)|^2) d\Omega, \quad (3.3.3)$$

where the two sides are recognised as the norm squared of the one-particle state created from the Minkowski vacuum by the smeared creation operator (3.3.1), evaluated respectively in the Minkowski basis and in the Unruh basis. The classical uncertainty relation reads

$$(\Delta\Omega)(\Delta \ln(\omega l)) \geq \frac{1}{2}, \quad (3.3.4)$$

where $\Delta\Omega$ is understood by combining contributions from $g_R(\Omega)$ and $g_L(\Omega)$ in the sense of (3.1.8) (since there are both contributions Right and Left modes). Note that as equality in (3.3.4) holds only for Gaussian functions, any state in which one of $g_R(\Omega)$ and $g_L(\Omega)$ vanishes will satisfy (3.3.4) with a genuine inequality.

3.3.1 Example: logarithmic Gaussian wave packet

As a concrete example, with a view to optimising the peaking both in Minkowski frequency and in Unruh frequency, consider a Minkowski smearing function that is a Gaussian in $\ln(\omega l)$,

$$f(\omega) = \left(\frac{\lambda}{\pi\omega^2}\right)^{1/4} \exp\left\{-\frac{1}{2}\lambda[\ln(\omega/\omega_0)]^2\right\} (\omega/\omega_0)^{-i\mu}, \quad (3.3.5)$$

where $\omega_0, \lambda > 0$ and $\mu \in \mathbb{R}$. λ and μ are dimensionless and ω_0 has the dimension of inverse length. f is normalised through

$$\int_0^\infty |f(\omega)|^2 d\omega = 1. \quad (3.3.6)$$

The expectation value and uncertainty of $\ln(\omega l)$ are those of a standard Gaussian,

$$\begin{aligned}\langle \ln(\omega l) \rangle &= \ln(\omega_0 l) \\ \Delta \ln(\omega l) &= (2\lambda)^{-1/2},\end{aligned}\tag{3.3.7}$$

while the expectation value and uncertainty of ω are given by

$$\begin{aligned}\langle \omega \rangle &= \exp\left(\frac{1}{4}\lambda^{-1}\right) \\ \Delta\omega &= \langle \omega \rangle \left[\exp\left(\frac{1}{2}\lambda^{-1}\right) - 1\right]^{1/2}.\end{aligned}\tag{3.3.8}$$

The Unruh smearing functions are cropped Gaussians,

$$\begin{aligned}g_R(\Omega) &= \frac{1}{(\pi\lambda)^{1/4}} \exp\left[-\frac{1}{2}\lambda^{-1}(\Omega - \epsilon\mu)^2\right] (\omega_0 l)^{i\epsilon\Omega} \\ g_L(\Omega) &= \frac{1}{(\pi\lambda)^{1/4}} \exp\left[-\frac{1}{2}\lambda^{-1}(\Omega + \epsilon\mu)^2\right] (\omega_0 l)^{-i\epsilon\Omega}.\end{aligned}\tag{3.3.9}$$

We analyze two limits.

$\epsilon\mu \gg \lambda^{1/2}$: $g_L(\Omega)$ is small and $g_R(\Omega)$ is peaked around $\Omega = \epsilon\mu$ with uncertainty $(\lambda/2)^{1/2}$

$\epsilon\mu \ll -\lambda^{1/2}$: $g_R(\Omega)$ is small and $g_L(\Omega)$ is peaked around $\Omega = -\epsilon\mu$ with uncertainty $(\lambda/2)^{1/2}$

Note that the difference in the relative magnitudes of $g_L(\Omega)$ and $g_R(\Omega)$ is consistent with the properties of the smeared mode Minkowski mode function

$$\int_0^\infty f(\omega) u_{\omega,M} d\omega\tag{3.3.10}$$

that corresponds to the smeared creation operator (3.3.1): a contour deformation argument shows the following

$\epsilon\mu \gg \lambda^{1/2}$: the smeared mode function is large in the region $t + x > 0$ and small in the region $t + x < 0$

$\epsilon\mu \ll -\lambda^{1/2}$: the smeared mode function is large in the region $t - x > 0$ and small in the region $t - x < 0$

Now, let Rob's state be the smeared function (3.3.5), and choose for Alice any state that has negligible overlap with Rob's state, for example by taking for Alice and Rob distinct values of ϵ . For $|\mu| \gg \lambda^{1/2}$ and λ not larger than of order unity, the combined state is then well approximated by the single Unruh frequency state of section 3.3 with $\Omega = |\mu|$ and with one of q_R and q_L vanishing. To obtain a state for which q_R and q_L are comparable, we may take for Rob's state a smearing function that is a linear combination of (3.3.5) and its complex conjugate.

3.3.2 Example: non Gaussian wave packet

While the phase factor $(\omega/\omega_0)^{-i\mu}$ in the Minkowski smearing function (3.3.5) is essential for adjusting the location of the peak in the Unruh smearing functions, the choice of a logarithmic Gaussian for the magnitude appears not essential. We have verified that similar results ensue with the choices

$$f(\omega) = \frac{2^\lambda (\omega/\omega_0)^{\lambda-i\mu} \exp(-\omega/\omega_0)}{\sqrt{\omega} \Gamma(2\lambda)} \quad (3.3.11)$$

and

$$f(\omega) = \frac{(\omega/\omega_0)^{-i\mu}}{\sqrt{2\omega} K_0(2\lambda)} \exp\left[-\frac{\lambda}{2} \left(\frac{\omega}{\omega_0} + \frac{\omega_0}{\omega}\right)\right], \quad (3.3.12)$$

for which the respective Unruh smearing functions can be expressed in terms of the gamma-function and a modified Bessel function.

3.4 Conclusions

In this chapter we have revised the SMA typically used in literature in the field of RQI. The SMA attempts to relate a single Minkowski frequency mode (inertial observers) with a single Rindler frequency mode (uniformly accelerated observers). We have shown that the SMA does not hold in general. Furthermore, we show that the states canonically analyzed in the literature correspond to maximally entangled states of Minkowski and Unruh modes. We analyzed the entanglement between two bosonic modes in the case when, as described by inertial observers, the state corresponds to a maximally entangled state between Minkowski modes and Unruh modes. We found that, when a uniform accelerated observer looks at the same states, the entanglement is always degraded with acceleration. It could be argued that the $q_R = 1$ Unruh mode is the most natural choice of Unruh modes since the entanglement for very small accelerations ($a \rightarrow 0$) is mainly contained in the subsystem Alice-Rob. However, other choices of Unruh modes become relevant if one wishes to consider an entangled state described by inertial observers which involves only Minkowski frequencies. We have also shown that a Minkowski wave packet involving a superposition of general Unruh modes can be constructed in such way that the corresponding Rindler state involves (effectively) a single frequency. This result is particularly interesting since it presents an instance where the SMA can be considered recovering the standard results in the literature.

CHAPTER 4

Entanglement redistribution
between charged bosonic field
modes in relativistic settings

In the previous chapter we have addressed the validity of the SMA commonly employed in literature. It is of interest to use the results presented there, in particular the generalization of the concept of Unruh particle, to investigate further the effects of relativity on entanglement. One of the main aims in RQI is to understand how entanglement depends on the motion of an observer. It has been shown that the amount of entanglement initially present in a state of free modes of a relativistic quantum field analyzed by two inertial observers, Alice and Bob, is different when the same state is analyzed by Alice and a uniformly accelerated observer Rob [5–7, 36–47]. In particular, if Alice and Bob share a maximally entangled state of bosonic field modes, Rob will measure entanglement which degrades with increasing acceleration and vanishes in the limit of infinite acceleration [5–7, 36–47, 47, 48]. Surprisingly, when Alice and Bob share a maximally entangled state of fermionic field modes, entanglement is still degraded with acceleration but does not vanish in the limit of infinite acceleration (for example, see [49]). The reasons for this striking difference are not yet understood. In order to address this issue, nonlocal correlations between fermionic particle and antiparticle degrees of freedom have also been taken into account [60]. There the authors considered initially maximally entangled states and three different bipartitions: the first where Rob could not distinguish between particle and antiparticles and two where he could analyze separately particles and antiparticles. They found that the survival of entanglement in the infinite acceleration in the first bipartition could be accounted for by considering the redistribution of entanglement between particle and antiparticle bipartitions. While [60] did improve the understanding of the behavior of fermionic entanglement as described by different observers, the behavior could not be directly compared with that for bosons, as previous work on bosons has focused on real scalar fields in which there is no distinction between particles and antiparticles.

In this chapter we introduce charged bosonic fields. Alice and Bob will analyze a one parameter family of maximally entangled states of Unruh modes. Bob and uniformly accelerated Rob will not agree on the particle content of each of these states. We consider the same bipartitions as in [60] and analyze the bosonic analogues of the states studied therein. We study the entanglement tradeoff between the bipartitions and how entanglement is degraded as a function of the Rob’s proper acceleration.

In spite of the presence of antiparticles, we find that mode entanglement always vanishes in the infinite acceleration limit. The redistribution of entanglement between particles and antiparticles observed in the fermionic case [60] does not occur for charged bosons. This supports the conjecture that the main differences in the behavior of entanglement in the bosonic and fermionic case are due to Fermi-Dirac versus Bose-Einstein

statistics [50].

4.1 Charged bosonic field states for uniformly accelerated observers

4.1.1 Quantization of charged scalar fields

The *charged massive scalar field* is a map

$$\Phi : x^\mu \rightarrow \Phi(x^\nu), \quad (4.1.1)$$

where $\Phi(x^\nu)$ is an operator valued distribution. In this case, $\Phi(x^\nu) \neq \Phi^\dagger(x^\nu)$ and the free Lagrangian reads

$$\mathcal{L} = \partial_\nu \Phi^\dagger \partial^\nu \Phi - \frac{1}{2} \mu^2 \Phi^\dagger \Phi. \quad (4.1.2)$$

Invoking the least action principle one uses (2.2.3) for both Φ, Φ^\dagger and finds the field equations which determine the kinematics:

$$\begin{aligned} (\square - \mu^2)\Phi &= 0, \\ (\square - \mu^2)\Phi^\dagger &= 0, \end{aligned} \quad (4.1.3)$$

where, again, $\mu \geq 0$ is the mass of the field. The conjugate momenta to Φ and Φ^\dagger are defined as

$$\begin{aligned} \Pi &:= \frac{\partial \Phi^\dagger}{\partial x^0}, \\ \Pi^\dagger &:= \frac{\partial \Phi}{\partial x^0} \end{aligned} \quad (4.1.4)$$

and one imposes the algebra relations

$$\begin{aligned} [\Phi(x^0, \mathbf{x}), \Pi(x^0, \mathbf{y})] &= i\delta^3(\mathbf{x} - \mathbf{y}), \\ [\Phi^\dagger(x^0, \mathbf{x}), \Pi^\dagger(x^0, \mathbf{y})] &= i\delta^3(\mathbf{x} - \mathbf{y}), \end{aligned} \quad (4.1.5)$$

We at last notice that while for the uncharged bosonic field the Fourier spectrum carried one type of operator, in this case Φ carries two different types of operators, say a_ω, b_ω where the a s annihilate particle operators and b s annihilate antiparticle operators. The generic expansion of Φ reads

$$\Phi = \int d^{n-1}k_i [a(k_i)u(k_\mu x^\mu) + b^\dagger(k_i)u^*(k_\mu x^\mu)] \quad (4.1.6)$$

where n is the dimensions of the spacetime, u are mode solutions which satisfy (4.1.3) and are normalized through (2.2.28). The four momenta k_μ satisfy

$$k_\mu k^\mu - m^2 = 0 \quad (4.1.7)$$

4.1.2 States of charged bosonic field modes

We consider a free charged scalar field Φ in 1 + 1 Minkowski spacetime and employ the quantization techniques explained in chapters 2 and 3.

We now proceed to expound those features about Unruh modes which will be used in this chapter.

It is well known that the Unruh basis provides an intermediate step between Minkowski and Rindler modes and allows for analytical Bogoliubov transformation between Unruh operators and Rindler operators [8]. Given the set of Minkowski modes $\{u_{\omega,M}^{\pm}\}$, one can obtain the Unruh modes $\{u_{\Omega,\Gamma}^{\pm}\}$ by a simple change of basis. Here Ω is the same label as for the Rindler modes and $\Gamma = R, L$ are extra indices. Positive and negative energy Minkowski modes do not mix when transforming between the two set of modes and therefore the Unruh operators $C_{\Omega,R}, C_{\Omega,L}, D_{\Omega,R}, D_{\Omega,L}$ annihilate the Minkowski vacuum as well. The BVT between Unruh and Rindler operators takes the simple form

$$\begin{aligned} C_{\Omega,R} &= \left(\cosh r_{\Omega} c_{\Omega,I} - \sinh r_{\Omega} d_{\Omega,II}^{\dagger} \right), \\ C_{\Omega,L} &= \left(\cosh r_{\Omega} c_{\Omega,II} - \sinh r_{\Omega} d_{\Omega,I}^{\dagger} \right), \\ D_{\Omega,R}^{\dagger} &= \left(-\sinh r_{\Omega} c_{\Omega,I} + \cosh r_{\Omega} d_{\Omega,II}^{\dagger} \right), \\ D_{\Omega,L}^{\dagger} &= \left(-\sinh r_{\Omega} c_{\Omega,II} + \cosh r_{\Omega} d_{\Omega,I}^{\dagger} \right), \end{aligned} \quad (4.1.8)$$

where the standard definition of r_{Ω} is

$$\tanh r_{\Omega} := e^{-\pi\Omega}. \quad (4.1.9)$$

The transformation between the Minkowski vacuum $|0\rangle_M$ and the Rindler vacuum $|0\rangle_R$ can be found in a standard way. We first introduce the generic Rindler Fock state $|nn, mm\rangle_{\Omega}$ as

$$|pq, rs\rangle_{\Omega} \equiv |pq, rs\rangle := \frac{(c_{\Omega,I}^{\dagger})^p (d_{\Omega,II}^{\dagger})^q (d_{\Omega,I}^{\dagger})^r (c_{\Omega,II}^{\dagger})^s}{\sqrt{p!} \sqrt{q!} \sqrt{r!} \sqrt{s!}} |0\rangle_R \quad (4.1.10)$$

and c, d correspond to particle and antiparticle respectively. The subscript to the operators indicates wether the operator has support in region I or region II . This allows us to write

$$|0_{\Omega}\rangle_M = \frac{1}{C^2} \sum_{n,m=0}^{+\infty} T^{n+m} |nn, mm\rangle_{\Omega}, \quad (4.1.11)$$

where

$$\begin{aligned} T &:= \tanh r_{\Omega}, \\ C &:= \cosh r_{\Omega}, \\ S &:= \sinh r_{\Omega} \end{aligned} \quad (4.1.12)$$

and $|0_\Omega\rangle_M$ is a shortcut notation used to underline that each Unruh Ω is uniquely mapped to the corresponding Rindler Ω .

One particle Unruh states are defined as

$$\begin{aligned} |1_j\rangle_U^+ &= c_{\Omega,U}^\dagger |0\rangle_M, \\ |1_j\rangle_U^- &= d_{\Omega,U}^\dagger |0\rangle_M, \end{aligned} \quad (4.1.13)$$

where the Unruh particle and antiparticle creation operator are defined as a linear combination of the two Unruh operators

$$\begin{aligned} c_{k,U}^\dagger &= q_R C_{\Omega,R}^\dagger + q_L C_{\Omega,L}^\dagger, \\ d_{k,U}^\dagger &= p_R D_{\Omega,R}^\dagger + p_L D_{\Omega,L}^\dagger. \end{aligned} \quad (4.1.14)$$

$q_R, q_L, p_R, p_L \in \mathbb{C}$ and satisfy

$$|q_R|^2 + |q_L|^2 = |p_R|^2 + |p_L|^2 = 1. \quad (4.1.15)$$

The coefficients $p_{R,L}$ and $q_{R,L}$ are not independent. We require that the Unruh particle and antiparticle operators have the same interpretation of particle and antiparticle operators when restricted to the same Rindler wedges. Therefore to be consistent with a particular choice of q_R and q_L , we must choose $p_L = q_R$ and $p_R = q_L$. (4.1.16) reduces to

$$\begin{aligned} c_{k,U}^\dagger &= q_R C_{\Omega,R}^\dagger + q_L C_{\Omega,L}^\dagger, \\ d_{k,U}^\dagger &= q_L D_{\Omega,R}^\dagger + q_R D_{\Omega,L}^\dagger. \end{aligned} \quad (4.1.16)$$

Therefore, Unruh L and R excitations are given by

$$\begin{aligned} |1_k\rangle_U^+ &= c_{k,U}^\dagger |0\rangle_U = q_R |1_{\Omega,R}\rangle + q_L |1_{\Omega,L}\rangle \\ |1_k\rangle_U^- &= d_{k,U}^\dagger |0\rangle_U = q_L |1_{\Omega,R}\rangle + q_R |1_{\Omega,L}\rangle \end{aligned} \quad (4.1.17)$$

4.2 Particle and Anti-particle entanglement in non-inertial frames

We have found the expressions for the vacuum and single Unruh and Rindler particle states. This allows us to analyse the degradation of entanglement from the perspective of observers in uniform acceleration. Unruh modes with sharp frequency are not normalised but are delta-normalised. As discussed in 3.3, one can always consider a superposition of Minkowski modes which will correspond to a distribution of Unruh frequencies Ω . One can then choose the Minkowski distribution in such a way that the Unruh distribution will be peaked around some frequency Ω . In the following we study the idealized case

of Unruh modes that are sharply peaked in Ω , so that the width of the peak may be neglected and we may regard the modes as normalized to a Kronecker (rather than Dirac) delta in Ω 3.1.

We first consider the following one parameter family of maximally entangled states prepared by inertial observers Alice and Bob.

$$|\Psi_+\rangle = \frac{1}{\sqrt{2}} (|0_\omega\rangle_M |0_\Omega\rangle_U + |1_\omega\rangle_M^\sigma |1_\Omega\rangle_U^+) \quad (4.2.1a)$$

$$|\Psi_-\rangle = \frac{1}{\sqrt{2}} (|0_\omega\rangle_M |0_\Omega\rangle_U + |1_\omega\rangle_M^\sigma |1_\Omega\rangle_U^-) \quad (4.2.1b)$$

$$|\Psi_1\rangle = \frac{1}{\sqrt{2}} (|1_\omega\rangle_M^+ |1_\Omega\rangle_U^- + |1_\omega\rangle_M^- |1_\Omega\rangle_U^+) \quad (4.2.1c)$$

where U labels bosonic Unruh modes and $\sigma = \pm$ denotes particle and antiparticle modes as usual. The states are parametrized by dimensionless parameter Ω and again we have split Alice and Bob's subsystems in the right hand side of equations (4.2.1). We also note that, since Alice's subsystem only provides the initial entanglement, the results will be independent of the choice of σ . State (4.2.1a) has only particle excitations in Bob's subsystem, while state (4.2.1b) has only antiparticle excitations. State (4.2.1c) is symmetric under Unruh charge conjugation in Bob's subsystem. For these reasons, we believe that states (4.2.1) are the simplest and most general states we wish to consider, since we will analyze the influence of charge on entanglement. In fact, (4.2.1) cover all possible combinations of charge in Bob's subsystem.

Rob does not naturally describe the states (4.2.1) with Minkowski coordinates but with Rindler coordinates. To take this into account we transform the Unruh modes to Rindler ones using (4.1.17). After this transformation, the total system Alice-Bob becomes effectively a tri-partite system Alice-Region I-Region II.

As is commonplace in the literature, we define the Alice-Rob bi-partition as the Minkowski-region I Rindler modes. We note that the dimensionless Rindler frequency Ω that appears as a label in the states (4.2.1) is not equal to the physical, dimensionful frequency observed in these states by any Rindler observer. As the proper time of a Rindler observer of acceleration A is equal to η/A , this Rindler observer sees the states (4.2.1) to have the physical frequency

$$E = \Omega A. \quad (4.2.2)$$

The parameter r is hence related to the physically observable quantities E and A by

$$\tanh r = e^{-\pi\Omega} = e^{-\pi E/A}. \quad (4.2.3)$$

In particular, if E is considered fixed, the limit $r \rightarrow \infty$ is that in which $A \rightarrow \infty$.

To study distillable entanglement in this context we will employ the negativity \mathcal{N} as usual (2.3.19). Two cases of interest will be considered. In the first case we assume that Alice and Rob cannot distinguish between particles and antiparticles. In this case, particles and antiparticles together are considered to be a subsystem. In the second case we consider that Rob is able to distinguish between particles or antiparticles and therefore antiparticle or particle states must be traced out.

4.2.1 Entanglement in states $|\Psi_+\rangle$ and $|\Psi_-\rangle$

We start with states (4.2.1a) and (4.2.1b). To compute entanglement we first compute Alice-Rob partial density matrix in (4.2.1a) we trace over region II in $|\Psi_+\rangle\langle\Psi_+|$ and perform the partial transposition. We obtain,

$$\begin{aligned} \rho_{A-R}^{PT} = & \frac{1}{2} \frac{1}{C^4} \sum_{n,m} T^{2n+2m} \{ \\ & |0\rangle\langle 0| \otimes |n, m\rangle\langle n, m| \\ & + \frac{1}{C^2} |1\rangle\langle 1| \otimes \left[(n+1)|q_R|^2 |n+1, m\rangle\langle n+1, m| + T\sqrt{(n+1)(m+1)}q_Rq_L^* |n+1, m+1\rangle\langle n, m| + \right. \\ & + T\sqrt{(n+1)(m+1)}q_Lq_R^* |n, m\rangle\langle n+1, m+1| + (m+1)|q_L|^2 |n, m\rangle\langle n, m| \left. \right] \\ & + \frac{1}{C} |1\rangle\langle 0| \otimes \left[\sqrt{(n+1)}q_R^* |n, m\rangle\langle n+1, m| + T\sqrt{(m+1)}q_L^* |n, m+1\rangle\langle n, m| \right] + \text{h.c.} \}. \end{aligned} \quad (4.2.4)$$

A major difference between the fermionic and the bosonic case is that in the latter, the Fock space is infinite dimensional in the particle number degree of freedom. In the present case it is therefore not possible to find the eigenvalues of the partial transpose density matrix analytically. However, we calculate \mathcal{N} numerically and plot our results in Fig.4.1.

We see that entanglement always vanishes in the infinite acceleration limit as for the uncharged bosonic case.

We now analyse the entanglement when Rob only looks at antiparticles. In this case Rob's particle modes are entangled with Alice's subsystem. Since Rob is not interested in antiparticles, we must trace over all antiparticle states and therefore, considering eq. (4.2.4):

$$-\rho_{A-R}^{PT} = \sum_n \langle n_I^- | \rho_{AR}^+ | n_I^- \rangle. \quad (4.2.5)$$

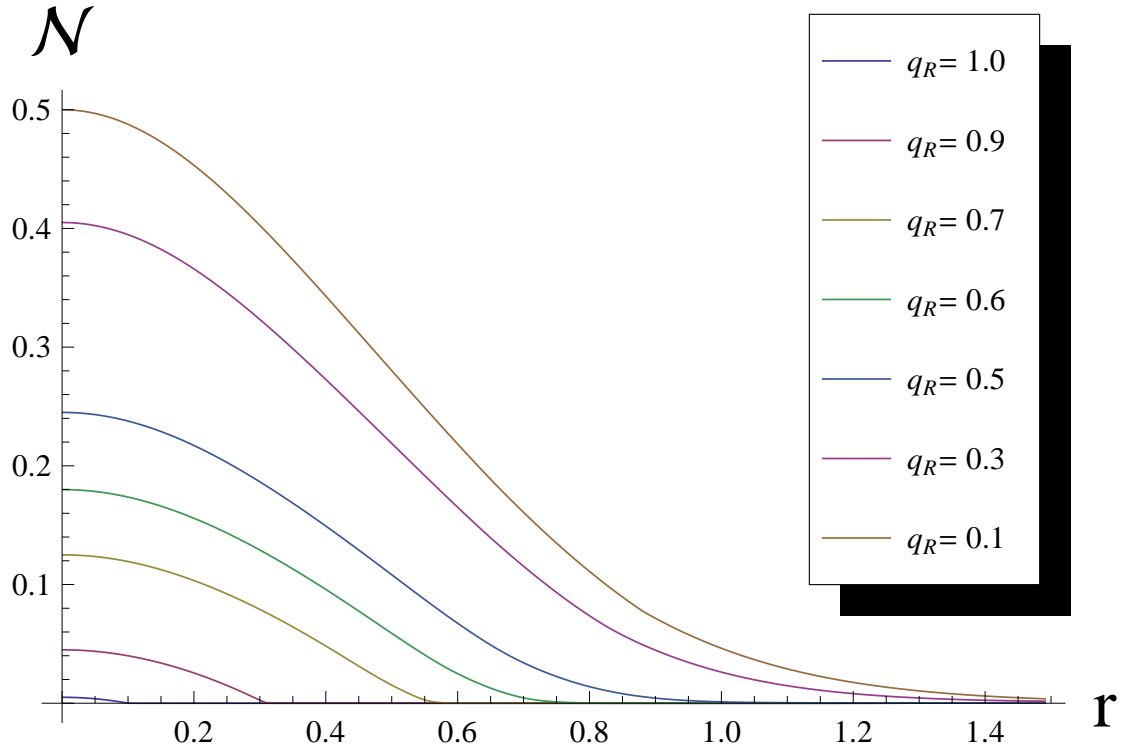


Figure 4.1: Negativity \mathcal{N} as a function of r for the state ρ_{A-R}^{PT} . Curves are for $q_R = 1, 0.9, 0.7, 0.6, 0.5, 0.3, 0.1$ from top to bottom. Entanglement vanishes at finite r in some cases.

This yields

$$\begin{aligned}
 -\rho_{A-R}^{PT} = & \frac{1}{2} \sum_n \frac{T^{2n}}{C^2} \{ |0\rangle \langle 0| \otimes |n\rangle \langle n| + \\
 & + |1\rangle \langle 1| \otimes \left[(n+1) \frac{1}{C^2} |q_R|^2 |n+1\rangle \langle n+1| + |q_L|^2 |n\rangle \langle n| \right] \\
 & + |1\rangle \langle 0| \otimes \left[\frac{1}{C} \sqrt{(n+1)} q_R^* |n\rangle \langle n+1| + \text{h.c.} \right] \}
 \end{aligned} \tag{4.2.6}$$

In this case we find analytical results. One can show that the partially transposed density matrix of the Alice-Rob bipartition has negative eigenvalues iff

$$1 \geq |q_R|^2 > T^2. \tag{4.2.7}$$

This means that entanglement, quantified by \mathcal{N} , vanishes for finite acceleration. We plot the entanglement in this bipartition in Fig. 4.2.

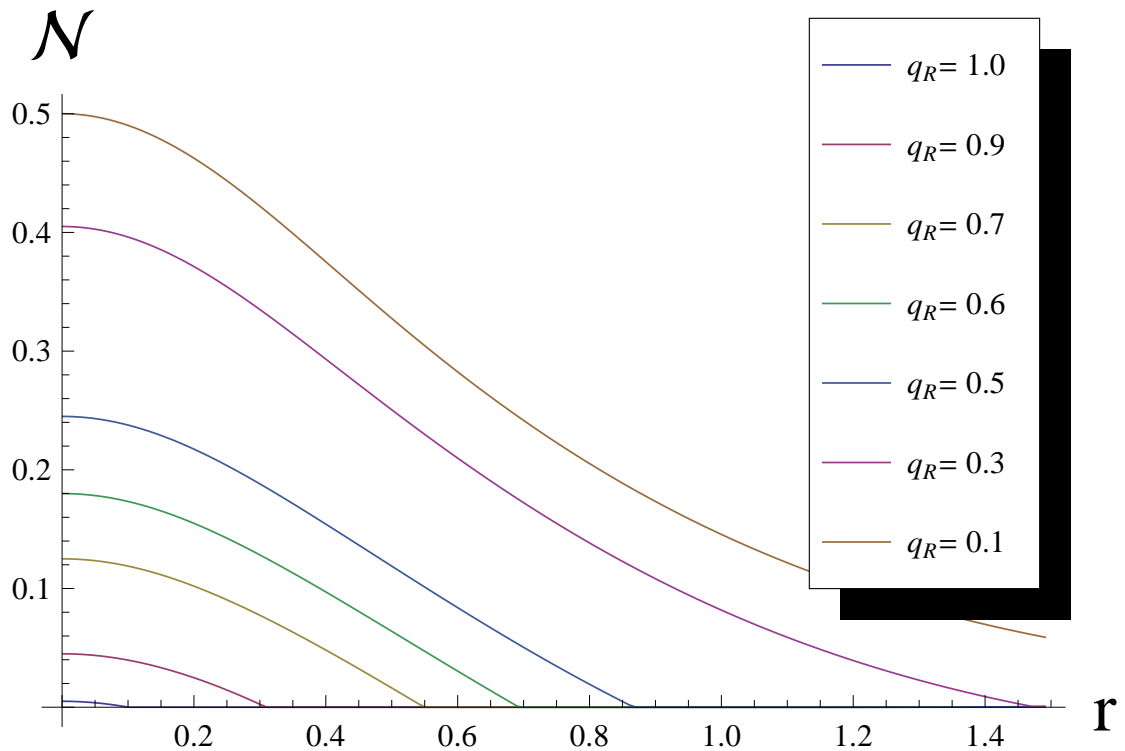


Figure 4.2: Negativity \mathcal{N} as a function of r for the state ${}_{-}\rho_{A-R}^{PT}$. Curves are for $q_R = 1, 0.9, 0.7, 0.6, 0.5, 0.3, 0.1$ from top to bottom.

The entanglement is always degraded and vanishes at finite acceleration A . We will compare these results with those of the last part of section 4.2.2. We stress that in the present case, the cutoff (4.2.7) is the same for every eigenvalue of (4.2.6).

It is interesting to analyze the case where Rob and AntiRob's only consider antiparticles. In this case one must trace over particle states. We consider again eq. (4.2.4) and obtain:

$${}_{+}\rho_{A-R}^{PT} = \sum_n \langle n|_I^{\dagger} \rho_{AR}^+ |n\rangle_I^{\dagger}, \quad (4.2.8)$$

and therefore,

$$\begin{aligned} {}_{+}\rho_{A-R}^{PT} = & \frac{1}{2} \sum_n T^{2n} \left\{ \frac{1}{C^2} |0\rangle \langle 0| \otimes |n\rangle \langle n| \right. \\ & + |1\rangle \langle 1| \otimes \left[(n+1) \frac{|q_L|^2}{C^4} + (T^2 C^2) |q_R|^2 \right] |n\rangle \langle n| \\ & \left. + |1\rangle \langle 0| \otimes \left[\frac{T}{C^3} \sqrt{(n+1)} q_L^* |n+1\rangle \langle n| + \text{h.c.} \right] \right\}. \end{aligned} \quad (4.2.9)$$

In this case negative eigenvalues in the Alice-Rob partial transpose density matrix exist iff

$$|q_L|^2 + T^2 C^2 |q_R|^2 < 0, \quad (4.2.10)$$

which can never be satisfied.

Therefore, entanglement is always zero in this bipartition. This result is in clear contrast with the fermionic case in which entanglement is always created in this bipartition [60]. We therefore conclude that in the bosonic case the redistribution of entanglement between particles and antiparticles does not occur.

The tensor product structure of the Hilbert space in the fermionic and the charged bosonic case plays an important role in the behavior of entanglement in the infinite acceleration limit. In the case of neutral scalar fields there are no antiparticles and entanglement is completely degraded. One could expect that in the charged bosonic case transfer between particles and antiparticles might occur but we find that this is not the case. In the next section we will see more explicitly that the different statistics play a primary role in entanglement behavior. We also notice that, as in [60], these results have been computed for the initial state (4.2.1a). One can easily find the result for the initial state (4.2.1b) by exchanging particle with antiparticle in all the previous calculations and conclusions.

4.2.2 Entanglement in state $|\Psi_1\rangle$

We now study the entanglement in the state (4.2.1c).

The density matrix for the subsystem Alice-Rob is obtained from $|\Psi_1\rangle\langle\Psi_1|$ by tracing over region II :

$$\begin{aligned}
 \rho_{A-R}^{PT} = & \frac{1}{2} \frac{1}{C^6} \sum_{n,m} T^{2n+2m} \{ \\
 & |-\rangle\langle-| \otimes [(n+1)|q_R|^2 |n+1, m\rangle\langle n+1, m| \\
 & + T\sqrt{(n+1)(m+1)}q_Rq_L^* |n+1, m+1\rangle\langle n, m| \\
 & + T\sqrt{(n+1)(m+1)}q_Lq_R^* |n, m\rangle\langle n+1, m+1| + (m+1)|q_L|^2 |n, m\rangle\langle n, m|] \\
 & + |+\rangle\langle+| \otimes [(m+1)|q_R|^2 |n, m+1\rangle\langle n, m+1| \\
 & + T\sqrt{(n+1)(m+1)}q_Rq_L^* |n+1, m+1\rangle\langle n, m| \\
 & + T\sqrt{(n+1)(m+1)}q_Lq_R^* |n, m\rangle\langle n+1, m+1| + (n+1)|q_L|^2 |n, m\rangle\langle n, m|] \\
 & + |-\rangle\langle+| \otimes [T\sqrt{(m+1)(m+2)}q_Rq_L^* |n, m+2\rangle\langle n, m| \\
 & + \sqrt{(n+1)(m+1)}|q_R|^2 |n, m+1\rangle\langle n+1, m| \\
 & + \sqrt{(n+1)(m+1)}T^2|q_L|^2 |n, m+1\rangle\langle n+1, m| \\
 & + T\sqrt{(n+1)(n+2)}q_Lq_R^* |n, m\rangle\langle n+2, m|] + \text{h.c.} \}. \tag{4.2.11}
 \end{aligned}$$

As in subsection 4.2.1, it is not possible to find an analytic expression for the eigenvalues of (4.2.11). We calculate \mathcal{N} numerically. We show our numerical results in Fig. 4.3.

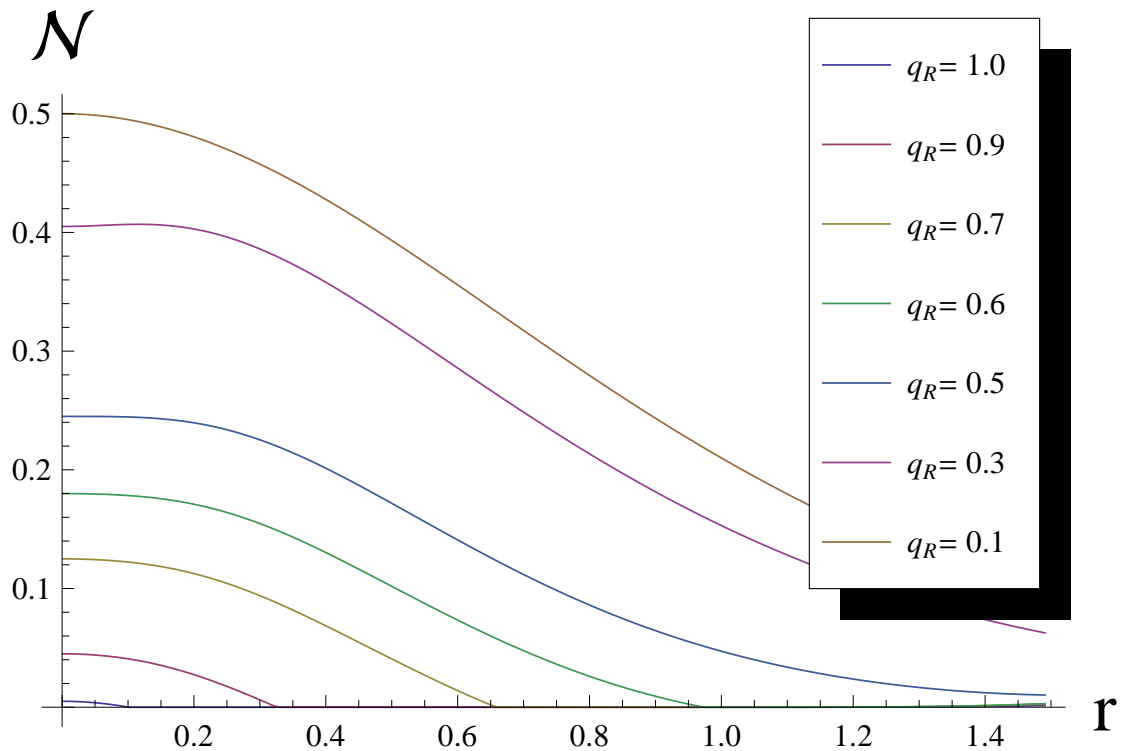


Figure 4.3: Negativity \mathcal{N} as a function of r for the state ρ_{A-R}^{PT} . Curves are for $q_R = 1, 0.9, 0.7, 0.6, 0.5, 0.3, 0.1$ from top to bottom.

We find once more that entanglement is degraded in all cases and vanishes in the limit of infinite acceleration.

The standard result addressing how entanglement behaves as a function of acceleration of one of the two parties have, in the majority of cases, shown that entanglement monotonically decreases. A rare counterexample was found in [51]. There the authors found that, in analogous settings as described in this Chapter and for fermionic systems, there are values of q_R that allow for non-monotonically decrease of entanglement as a function of the acceleration. In the present we find again a similar behavior as in [51]. The physical motivations for such feature to arise are not yet understood, although we might conjecture the following: when $q_R = 1$, there is initial entanglement between Alice and Right Unruh modes as analyzed by Bob, while when $q_R \neq 1$, Alice is entangled with *both* Right Unruh modes (Right Unruh degrees of freedom) and Left Unruh modes (Left Unruh degrees of freedom). On one hand, when $q_R = 1$, we can perform a change of basis from Unruh to Rindler bases and by tracing over degrees of freedom in region II we will always lose entanglement (see (3.1.1)). On the other hand, when $q_R \neq 1$ we can

still perform the same change of basis and trace over degrees of freedom in region II , but in this case, while increasing r decreases the contribution from the Right modes in region I (see (3.1.1)), it also increases the contribution of the Left modes in region I , therefore creating two competing effects. For this reason, one can expect that in principle entanglement is not monotonically degraded¹.

We focus on a region $0 < r < 0.25$ of 4.3. We find numerically that for some values of $|q_R|$ entanglement is not a monotonically decreasing function of r . We choose to show a sample for $|q_R| = 0.9$.

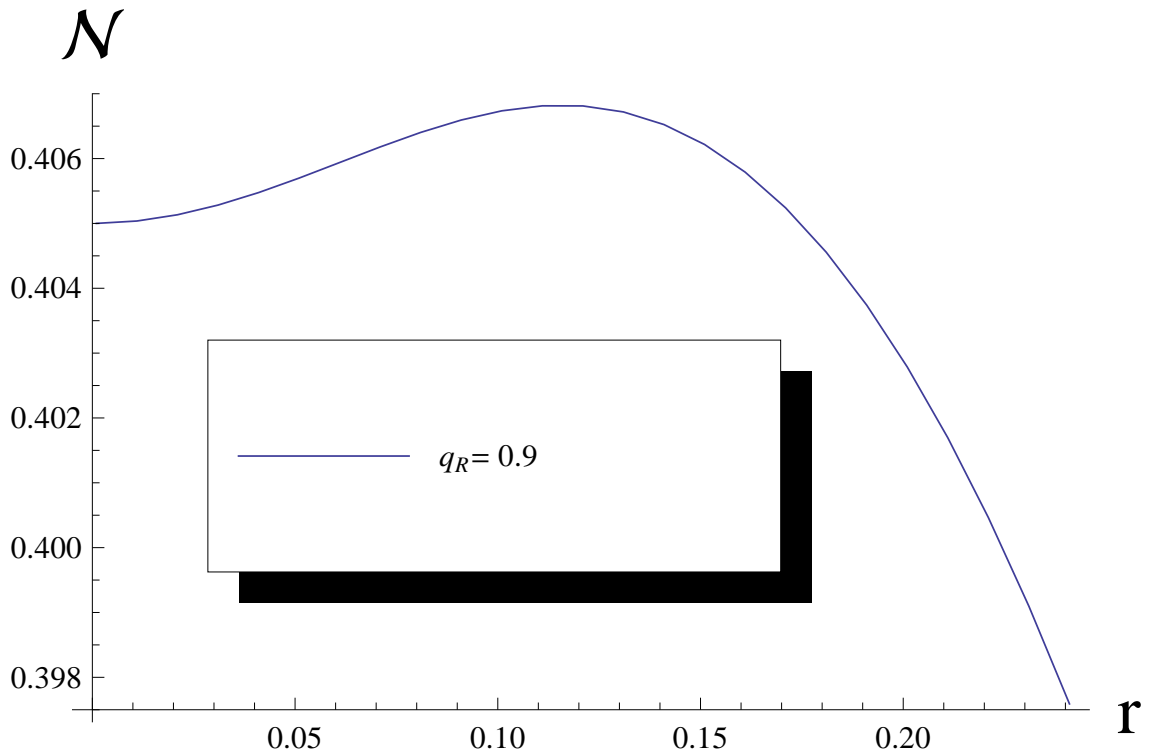


Figure 4.4: Negativity \mathcal{N} as a function of r in the range $0 < r < 0.25$ from figure 4.3. We choose $|q_R| = 0.9$ as a sample.

¹We thank Gerardo Adesso at the University of Nottingham for indicating that this might be the cause and that Local Operations might lie at the basis of such effect

Assuming now that Rob only analyzes particles, we trace over antiparticles in region I and obtain

$$\begin{aligned}
 -\rho_{A-R}^{PT} = & \frac{1}{2} \sum_n T^{2n} \{ \\
 & |+\rangle\langle+| \otimes \left[\frac{|q_R|^2}{C^4} (n+1) |n+1\rangle\langle n+1| + \frac{|q_L|^2}{C^2} |n\rangle\langle n| \right] \\
 & + |-\rangle\langle-| \otimes \left[\frac{|q_L|^2}{C^4} (n+1) + \frac{|q_R|^2}{C^2} \right] |n\rangle\langle n| \\
 & + |+\rangle\langle-| \otimes \left[\frac{T}{C^4} \sqrt{(n+1)(n+2)} q_L q_R^* |n\rangle\langle n+2| + \text{h.c.} \right] \} \quad (4.2.12)
 \end{aligned}$$

We are able to analytically find the eigenvalues of the state (4.2.12). Unlike the case for the state (4.2.6), where *all* the eigenvalues could be negative when (4.2.7) is satisfied, here we find that only a finite subset of the eigenvalues can be negative and this subset depends on r . The entanglement for this scenario is plotted in Fig. 4.5.

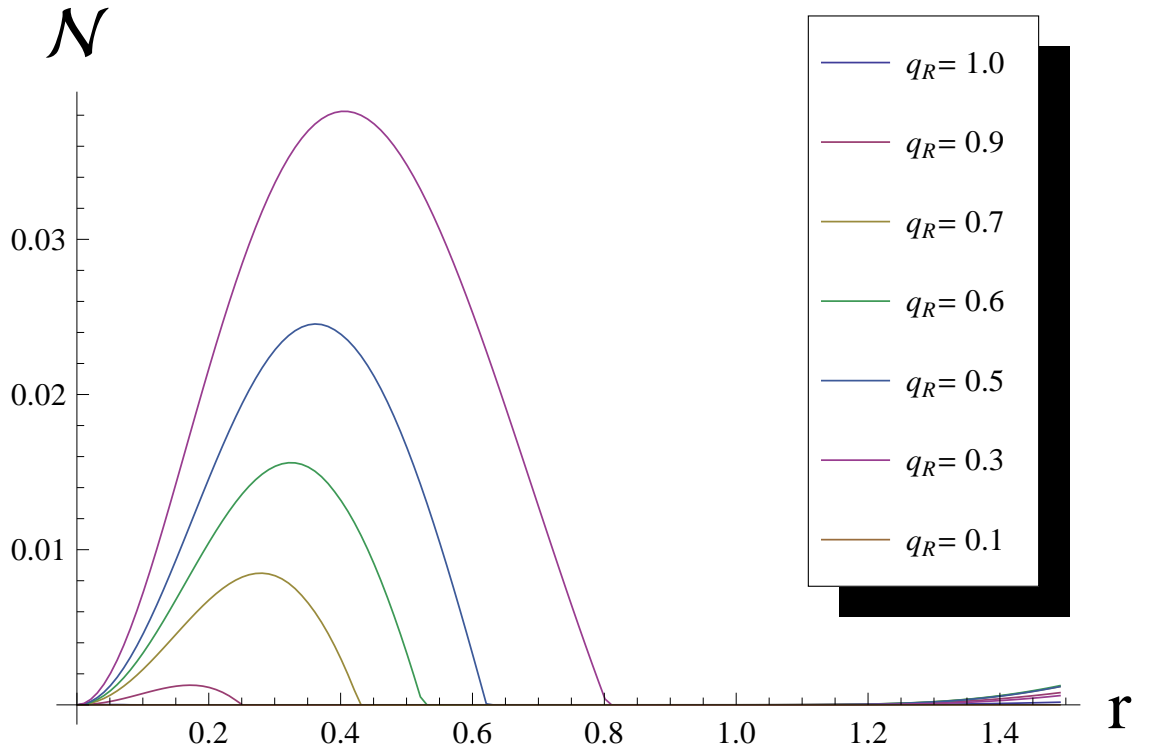


Figure 4.5: Negativity \mathcal{N} as a function of r for the state ρ_{A-R}^{PT} . Curves are for $q_R = 1, 0.9, 0.7, 0.6, 0.5$ from top to bottom.

Assuming that Rob looks only at antiparticles yields analogous results.

We find that entanglement behaves very differently to the corresponding fermionic case

where entanglement between Alice's and Rob's particle (or antiparticle) sector is identically zero [60]. However, here the entanglement grows with acceleration and reaches a maximum value after which it degrades. We trace the difference between the two cases down to extra terms of the form $|n\rangle\langle n+2|$ which appear in (5.2.6). Clearly, no such fermionic Fock state $|(n+2)_{\Omega}^{\pm}\rangle$ can exist due to Pauli exclusion principle. This behavior is again a rare case of non monotonically decrease of entanglement with increasing r .

4.3 Conclusions

In this chapter we have analyzed the entanglement tradeoff between the particles and antiparticles when the initial maximally entangled states are composed by charged bosonic fields. Including antiparticles in the study of field mode entanglement in non-inertial frames has deepened our understanding of key features which explain the difference in behavior of entanglement in the fermionic and bosonic case. It was shown in [60] that in the fermionic case an entanglement redistribution between particle and antiparticle modes is responsible for the finite value of entanglement in the infinite acceleration limit. In particular, the relative redistribution for different particle and antiparticle bipartitions could be used to explain the behavior of the entanglement when particles and antiparticles were considered as a whole system. Here we have analyzed the charged bosonic case and computed the entanglement in the partitions that correspond to those considered for fermions in [60]. We showed that, due to the bosonic statistics, there are substantial differences in the entanglement behavior when particles or antiparticles are not taken into account. We also find rare cases of non-monotonically decrease of entanglement as a function of acceleration. However, we confirmed that entanglement is always degraded in the infinite acceleration limit independently of the redistribution of entanglement between the particle and antiparticle bipartitions.

The main difference with the results found in [60] is the following: while in the fermionic case the redistribution of entanglement between particle and antiparticle sectors can explain the survival of entanglement for infinite accelerations, in the bosonic case such redistribution allows the entanglement to degrade at infinite accelerations. Such behavior is better explained by analyzing Figures 4.3 and 4.5, where the entanglement vanishes in the limit of infinite acceleration for both cases.

Part II

Entanglement degradation of cavity modes due to motion

A common way to implement quantum information tasks involves storing information in cavity field modes. How the motion of the cavities affects the stored information is a question that could be of practical relevance in space-based experiments [52, 53]. At present, there has been no success in concretely addressing this question in the framework of RQI, although a first step was attempted in [11]. From a completely different perspective and for almost four decades, the community working on the dynamical Casimir effect has been seeking an experimentally implementable model which would allow for the demonstration of the creation of particles as predicted by QFT in Casimir-like settings, where the wall of a cavity confining the quantum electromagnetic field in its vacuum state oscillates rapidly and excites the vacuum of the field therefore producing pairs of correlated particles. Any input in this direction could increase corroboration of QFT and provide indication that motion does affect quantum resources.

In this chapter we introduce a scheme that allows us to confine a relativistic quantum field in a cavity and determine how modes before any motion occurs are related to the modes in the cavity after it has undergone non inertial motion. The cavity walls are modeled by Dirichlet boundary conditions on the field. In particular, we find a suitable parameter which enables us to employ perturbation techniques and obtain analytical results to the lowest contributing order. This perturbation parameter is directly related to the physical variables of the problem and controls the size of the cavity vs the magnitude of the proper acceleration.

We use this setup to analyze the degradation of initially maximal entangled state of couples of uncharged scalar field modes each within a cavities in Minkowski space. One cavity will remain inertial while the other will undergo motion that need not be stationary. Our analysis therefore combines the explicit confinement of a quantum field to a finite size cavity and a freely adjustable time-dependence of the cavity's acceleration. This allows observers within the cavities to implement quantum information protocols in a way that is localized both in space and in time [11]. In particular, our system-environment split is manifestly causal and invokes no horizons or other notions that would assume acceleration to persist into the asymptotic, post-measurement future (cf. [54, 55]). By the equivalence principle, the analysis can be regarded as a model of gravity effects on entanglement.

5.1 Cavity prototype configuration

5.1.1 Field quantization inside a Dirichlet box

We start by quantizing a massive scalar field Φ in a $(1 + 1)$ -dimensional cavity in Minkowski spacetime, where $\mu > 0$ is the mass of the field and the left and right cavity walls are placed at $0 < L_0 < R_0$. The choice of boundary conditions is not unique and we employ the *Dirichlet boundary conditions* which require $\Phi = 0$ on the boundaries. We find this choice natural for this type of problem given its simplicity (for example see [12]). It is possible to choose other boundary conditions, for example Von Neumann boundary conditions, but we will restrict ourselves to the Dirichlet ones. When the box is inertial, this implies

$$\Phi(t, L_0) = \Phi(t, R_0) = 0 \quad (5.1.1)$$

and the field has support only within the cavity. In this case, the mode solutions to (2.2.16) take the form

$$\phi_{n,M}^{\pm}(t, x) = \frac{1}{\sqrt{n\pi}} \sin(\omega_n(x - L_0)) e^{\mp i\omega_n t} \quad (5.1.2)$$

where $n > 0$ labels the energy eigenstates, \pm stands for positive or negative frequency,

$$\omega_n = \sqrt{\left(\frac{n\pi}{R_0 - L_0}\right)^2 + \mu^2} \quad (5.1.3)$$

are the dimensional frequencies with respect to the Killing vector ∂_t and

$$i\partial_t \phi_n^{\pm}(t, x) = \pm \omega_n \phi_n^{\pm}(t, x) \quad (5.1.4)$$

The spectrum is therefore discrete and quantization proceeds exactly as in the continuum case, except that now modes are properly normalizable through (2.2.28)

$$(\phi_n^{\pm}, \phi_{n'}^{\pm}) = \delta_{nn'} \quad (5.1.5)$$

Mixed products vanish. The field Φ can be expanded as

$$\Phi = \sum_{n>0} [a_n \phi_n^+ + \text{h.c.}] \quad (5.1.6)$$

where the creation and annihilation operators satisfy the usual commutation relations

$$[a_n, a_m^{\dagger}] = \delta_{nm} \quad (5.1.7)$$

We are interested in a cavity which has constant proper length as measured by a comoving observer. When the cavity is accelerating, the natural coordinates to employ are the Rindler coordinates η, χ introduced in 2.2.36 and the boundaries follow two different

Rindler trajectories. The proper accelerations of the left wall A_{L_0} , the centre A and right A_{R_0} wall of the box are respectively

$$\begin{aligned} A_{L_0} &= \frac{c^2}{L_0} \\ A &= \frac{2c^2}{R_0 + L_0} \\ A_{R_0} &= \frac{c^2}{R_0} \end{aligned} \tag{5.1.8}$$

We take advantage of the invariance under the boost Killing vector ∂_η during the acceleration to write the solutions to (2.2.16) as

$$\phi_{n,R}^\pm(\eta, \chi) = \frac{1}{\sqrt{n\pi}} \sin(\Omega_n \ln(\frac{\chi}{L_0})) e^{\mp i\Omega_n \eta} \tag{5.1.9}$$

where $n \in \mathbb{N}$,

$$\Omega_n = \frac{n\pi}{\ln(\frac{R_0}{L_0})} \tag{5.1.10}$$

is the dimensionless discrete frequency with respect to the boost Killing vector ∂_η and

$$i\partial_\eta \phi_{n,R}^\pm(\eta, \chi) = \pm \Omega_n \phi_{n,R}^\pm(\eta, \chi) \tag{5.1.11}$$

Let Alice and Rob be observers in $(1+1)$ -dimensional Minkowski spacetime, each carrying (or comoving with) a cavity of this type that contains an uncharged scalar field of mass $\mu \geq 0$ with Dirichlet boundary conditions. Alice and Rob are initially inertial with vanishing relative velocity, and each cavity has length $\delta > 0$. As shown above, the field modes in each cavity are discrete, indexed by the quantum number $n \in \mathbb{N}$ and having the frequencies

$$\omega_n := \sqrt{M^2 + \pi^2 n^2} / \delta \tag{5.1.12}$$

where $M := \mu\delta$. We proceed in the following to build trajectories for Rob's cavity.

5.1.2 Basic Building Block

Rob starts inertial, possibly at rest (Alice and Rob will prepare the state at this point and we *do not* address the preparation procedure. We assume that the state has been prepared before the analysis starts). He then uniformly accelerates for a finite interval of his proper time. After accelerating, Rob's cavity is again inertial and has proper length δ in its new rest frame. We call this travel scenario *Basic Building Block* (BBB). Figure 5.1 shows the prototype case.

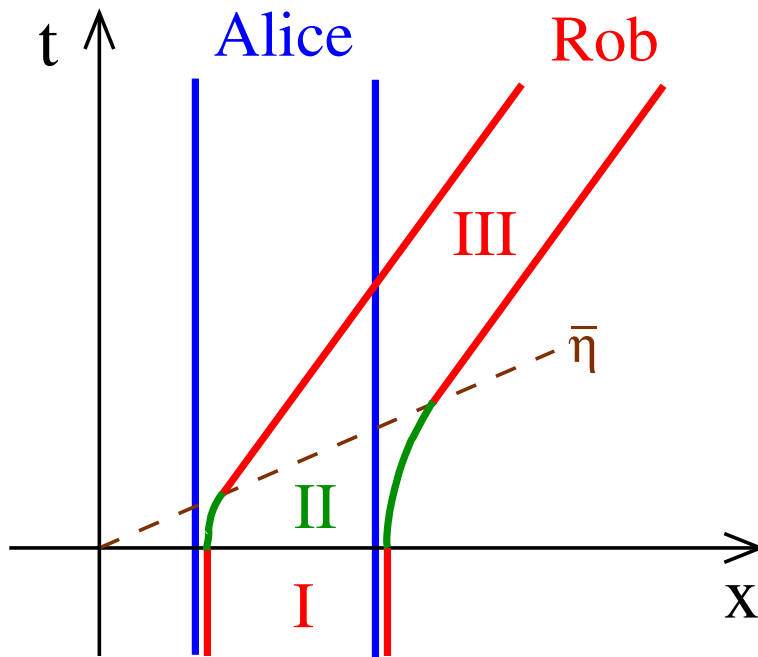


Figure 5.1: Cavity trajectories in Minkowski space. Alice's cavity remains inertial. Rob's cavity is inertial in region I, accelerates in region II and is again inertial in region III. The figure shows the prototype case where Rob's acceleration is to the right and uniform throughout region II, and $\bar{\eta}$ is the duration of the acceleration in Rindler time $\text{atanh}(t/x)$.

By composing BBBs one can obtain a “general” travel scenario, where by general we mean any travel scenario that can be obtained by pasting together segments of uniform acceleration and inertial evolution. It is possible to obtain also the transformations for a small varying accelerations which we omit to present since they involve time ordered integrals which makes them unmanageable when needed for explicit computations.

5.1.3 Bogoliubov transformations

Let $\{\phi_n, \phi_n^*\}$, $n = 1, 2, \dots$, denote Rob’s field modes that are of positive and negative frequency ω_n with respect to his proper time t *before* the acceleration (the star denotes complex conjugation as usual). Similarly, let $\{\bar{\phi}_n, \bar{\phi}_n^*\}$, $n = 1, 2, \dots$ denote Rob’s field modes that are of positive frequency Ω_n with respect to his proper time *during* the acceleration.

The two sets of modes $\{\phi_n, \phi_n^*\}, \{\bar{\phi}_n, \bar{\phi}_n^*\}$ are related by the BVT

$$\begin{aligned}\bar{\phi}_m &= \sum_n (\alpha_{0, mn} \phi_n + \beta_{0, mn} \phi_n^*) \\ \bar{\phi}_m^* &= \sum_n (\alpha_{mn}^* \phi_n^* + \beta_{mn}^* \phi_n)\end{aligned}\tag{5.1.13}$$

where the coefficient matrices α and β are determined by the motion of the cavity during the acceleration [10]. We notice that they encode the entries of the matrix \mathcal{A} in (2.2.64) and can be found using (2.2.28). We denote by \mathcal{A}_0 the matrix for the inertial to accelerated BVT.

Rob might follow an arbitrarily complicated trajectory, which is composed of segments of inertial evolution alternated with segments of uniform acceleration. Let the pre-trip modes be again ϕ_n , $n = 1, 2, \dots$ and the post-trip modes be $\bar{\phi}_n$, $n = 1, 2, \dots$. We find that the coefficients A_{mn}, B_{mn} for the general trajectory can *always* be expressed in terms of the coefficients $\alpha_{0, mn}, \beta_{0, mn}$ of the inertial to accelerated BVT. In general, the resulting expression is complicated but the methods to obtain it are particularly simple and can provide insight into the physics. We use the formalism of the \mathcal{M} matrices developed in chapter 2 to provide a simple tool for computation of travel coefficients.

One starts from a generic BVT matrix \mathcal{A}_0 , which encodes how the modes $\bar{\phi}_m$ during acceleration are related to the modes ϕ_m just before it. The inverse BVT, \mathcal{A}_0^{-1} undoes this transformation. We now introduce two diagonal matrices \mathcal{E}, \mathcal{F} where \mathcal{E} encodes the time evolution of each mode during an inertial segment and \mathcal{F} during an accelerated

segment. Specifically

$$\begin{aligned}\mathcal{E} &= \text{diag}(\dots, e^{i\omega_k t} \dots; \dots e^{-i\omega_k t} \dots) \\ \mathcal{F} &= \text{diag}(\dots, e^{i\Omega_k t} \dots; \dots e^{-i\Omega_k t} \dots)\end{aligned}\quad (5.1.14)$$

We find that

$$\mathcal{A} = \dots E^{(n)} \left(\mathcal{A}_0^{(n)} \right)^{-1} F^{(n)} \mathcal{A}_0^{(n)} \dots E^{(2)} \left(\mathcal{A}_0^{(2)} \right)^{-1} F^{(2)} \mathcal{A}_0^{(2)} E^{(1)} \left(\mathcal{A}_0^{(1)} \right)^{-1} F \mathcal{A}_0^{(1)} \quad (5.1.15)$$

where the expression must be read right to left. Eq. (5.1.15) can be interpreted as follows: one cavity is inertial and then starts accelerating. This is encoded in $\mathcal{A}_0^{(1)}$. The cavity uniformly accelerates, $F^{(1)}$, and then turns off the engines $\left(\mathcal{A}_0^{(1)} \right)^{-1}$. The cavity travels at constant velocity, $\mathcal{E}^{(1)}$ and then repeats the procedure at will. Accelerations and times of acceleration and coasting can be chosen at will. This travel scenario is not the most general and one can design different travel scenarios once the above logic is understood. For example, one can set the proper time of some inertial segment that connects two accelerated ones to zero. In addition, different accelerated segments might have different proper accelerations. For the sake of simplicity and without loss of generality, in the following we will specialize to scenarios where, in case of two or more segments of acceleration, the magnitude of the acceleration is the same.

5.1.4 $h \ll 1$ perturbative expansion

In order to fulfill our aims, it is necessary to be able to compute the Bogoliubov coefficients. Any matrix \mathcal{A} can be written in terms of $\alpha_{0,mn}, \beta_{0,mn}$ which implies that we need to be able to compute these coefficients. It turns out that they do have a closed form which we reproduce below:

$$\alpha_{0,mn} = \frac{1}{\delta} \sqrt{\frac{n}{m}} F_{mn} + \frac{1}{\ln\left(\frac{R_0}{L_0}\right)} \sqrt{\frac{m}{n}} G_{mn} \quad (5.1.16a)$$

$$\beta_{0,mn} = \frac{1}{\delta} \sqrt{\frac{n}{m}} F_{mn} - \frac{1}{\ln\left(\frac{R_0}{L_0}\right)} \sqrt{\frac{m}{n}} G_{mn} \quad (5.1.16b)$$

where

$$\begin{aligned}F_{mn} &:= \int_{L_0}^{R_0} dx \sin(\omega_n(x - L_0)) \sin\left(\Omega_m \ln\left(\frac{x}{L_0}\right)\right) \\ G_{mn} &:= \int_{L_0}^{R_0} \frac{dx}{x} \sin(\omega_n(x - L_0)) \sin\left(\Omega_m \ln\left(\frac{x}{L_0}\right)\right)\end{aligned}\quad (5.1.17)$$

and (5.1.16) cannot be handled in practical computations. We have identified a perturbative regime that allows us to treat analytically the Bogoliubov coefficients (5.1.16).

We introduce the parameter

$$h := \frac{A\delta}{c^2} \quad (5.1.18)$$

where A is the proper acceleration of the center of the cavity, δ is the length of the cavity as measured in its rest frame and we have restored the speed of light c in this definition in order to highlight the role of all the relevant physical constants. The perturbative regime is for $h \ll 1$. We can now expand the \mathcal{A} matrix as

$$\mathcal{A} = \mathcal{A}^{(0)} + \mathcal{A}^{(1)} + \mathcal{A}^{(2)} + \mathcal{O}(h^3) \quad (5.1.19)$$

where the superscript indicates to which order in h do the elements of \mathcal{A} contribute. The matrix $\mathcal{A}^{(0)}$ is the contribution to \mathcal{A} when $h = 0$. It is clear that when $h = 0$ every mode evolves freely and does not mix. We do choose not to write the powers of h explicitly for notational simplicity. Therefore

$$\mathcal{A}^{(0)} = \text{diag}(\dots G_{i-1}, G_i, G_{i+1}, \dots; \dots, G_{i-1}^*, G_i^*, G_{i+1}^*) \quad (5.1.20)$$

G_i satisfies $|G_i| = 1$ and it collects all phases from inertial evolution and accelerated evolution.

In the bosonic case, since \mathcal{A} can be expressed as (2.2.64), we can also write

$$A = A^{(0)} + A^{(1)} + A^{(2)} + \mathcal{O}(h^3), \quad (5.1.21a)$$

$$B = B^{(1)} + B^{(2)} + \mathcal{O}(h^3), \quad (5.1.21b)$$

where the superscripts indicate again the power of h . We now turn to the expansions of ${}_{\circ}\alpha$ and ${}_{\circ}\beta$ which can be written as

$${}_{\circ}\alpha_{nn} = 1 - \frac{1}{240} \pi^2 n^2 h^2 + \mathcal{O}(h^4), \quad (5.1.22a)$$

$$\alpha_{0, mn} = \sqrt{mn} \frac{(-1 + (-1)^{m-n})}{\pi^2 (m-n)^3} h + \mathcal{O}(h^2) \quad (m \neq n), \quad (5.1.22b)$$

$$\beta_{0, mn} = \sqrt{mn} \frac{(1 - (-1)^{m-n})}{\pi^2 (m+n)^3} h + \mathcal{O}(h^2). \quad (5.1.22c)$$

which hold iff $nh \ll 1$. These expressions will be fundamental throughout this and the following chapters.

Note on the role of relative parity of cavity mode numbers

We have found that the Bogoliubov coefficients (5.1.21) in the perturbative regime display dramatic differences when the relative parity of two modes k, k' is even or odd. Such feature will play a key role in Chapter 7 and Chapter 8. The reason for this behavior is not yet understood, although one can make the following observations. First, we remind that the Bogoliubov coefficients are determined by inner products between modes (2.2.57). Any transformation that maps a mode ϕ_k to

$$\phi_k \mapsto (-1)^k \phi_k \quad (5.1.23)$$

is a map that knows about the parity of the mode. We therefore notice that such a map will act on the elements of the Bogoliubov matrix \mathcal{A} as

$$\mathcal{A}_{kk'} \mapsto (-1)^{k+k'} \mathcal{A}_{kk'}. \quad (5.1.24)$$

Therefore, the Bogoliubov coefficients are affected by the relative parity of the modes that define them. We then notice that, since $\hbar > 0$, given the perturbative expansion in (5.1.19) for *rightwards* accelerations, which we reproduce below

$$\mathcal{A} = \mathcal{A}^{(0)} + \mathcal{A}^{(1)} + \mathcal{A}^{(2)} + \mathcal{O}(\hbar^3) \quad (5.1.25)$$

it is possible to obtain the *leftwards* acceleration expansion by means of the map (5.1.23). This accounts for the expansion (5.1.19) to take the form

$$\mathcal{A} = \mathcal{A}^{(0)} - \mathcal{A}^{(1)} + \mathcal{A}^{(2)} + \mathcal{O}(\hbar^3) \quad (5.1.26)$$

which, to all effects, could have been achieved by replacing \hbar with $-\hbar$. This can occur only when $k + k' = 2n + 1$ and therefore we expect all Bogoliubov coefficients $\mathcal{A}_{kk'}$ with $k + k' = 2n$ to vanish $\hbar = 0$.

5.1.5 Pre-trip preparation

Let Alice and Rob initially prepare their two-cavity system in the maximally entangled Bell state

$$|\Psi\rangle = \frac{1}{\sqrt{2}}(|0\rangle_A |0\rangle_R + |1_\omega\rangle_A |1_k\rangle_R) \quad (5.1.27)$$

where the subscripts A and R identify the cavities, $|0\rangle$ is the vacuum and $|1_k\rangle$ is the one-particle state with quantum number k . Experimentally, $|\Psi\rangle$ might be prepared by allowing a single atom to emit an excitation of frequency ω_k over a flight through the two cavities [56, 57], and the assumption of a single k is experimentally justified if δ is so small that cavity's frequency separation $\omega_{n+1} - \omega_n$ is large compared with the frequency separations of the atom.

The subscripts A, R refer to Alice and Rob and the fields in their cavities have support only within the cavity.

5.1.6 Travel techniques

Working in the Heisenberg picture, the state $|\Psi\rangle$ does not change in time, but for late time observations the early time states $|0\rangle_R$ and $|1_k\rangle_R$ need to be expressed in terms of Rob's late time vacuum $|\bar{0}\rangle_R$ and the late time excitations on it, by formulas that involve

the A_{mn}, B_{mn} from (5.1.15). In this sense, the acceleration creates particles in Rob's cavity.

We regard the late time system as tripartite between Alice's cavity, the (late time) mode k in Rob's cavity and the (late time) modes $\{n \mid n \neq k\}$ in Rob's cavity. As any excitations in the $n \neq k$ modes are entirely due to the acceleration, we regard these modes as the environment. We ask: Has the entanglement between Alice's cavity and the mode k in Rob's cavity been degraded after he finishes his travel (and therefore is inertial again), from the maximal value it had before Rob's acceleration?

We quantify the entanglement by the negativity \mathcal{N} (2.3.19), where the reduced density matrix ρ is obtained by tracing the full density matrix $|\Psi\rangle\langle\Psi|$ over Rob's late time frequencies $\{\omega_n \mid n \neq k\}$.

The situation covering all the scenarios below is when

$$\begin{aligned} A &= \text{diag}(G_1, G_2, \dots) + A^{(1)} + \mathcal{O}(h^2) \\ B &= B^{(1)} + \mathcal{O}(h^2), \end{aligned} \quad (5.1.28)$$

where the first-order coefficient matrices $A^{(1)}$ and $B^{(1)}$ are off-diagonal, and each G_n has unit modulus as explained in the subsection 5.1.4. Since we are considering that all accelerations in our travel scenarios are the same, h is the only expansion parameter. We perturbatively expand ρ in terms of h as

$$\rho = \rho^{(0)} + \rho^{(1)} + \rho^{(2)} + \mathcal{O}(h^3). \quad (5.1.29)$$

In order to find the contributions to (5.1.29) we need to find the expressions of $|0\rangle_R$ and $|1_k\rangle_R$ in terms of late-time excitations. We start by the standard expression that relates different vacua [9]

$$|0\rangle_R = N e^W |\bar{0}\rangle_R \quad (5.1.30)$$

$$W := - \sum_{ij} \frac{V_{ij}}{2} \bar{a}_i^\dagger \bar{a}_j^\dagger \quad (5.1.31)$$

$$V = B^* A^{-1}. \quad (5.1.32)$$

where $N \in \mathbb{C}$ is an appropriate normalization constant which in this perturbative regime has the form

$$|N|^2 = 1 - \frac{1}{2} \text{Tr}(V^\dagger V) + \mathcal{O}(h^3), \quad (5.1.33)$$

the matrix V is defined through the full travel scenario beta and alpha Bogoliubov matrices B, A and the ket $|\bar{0}\rangle_R$ is the vacuum annihilated by the post-trip annihilation operators \bar{a}_j . Note that $|N|^2 = 1 + \mathcal{O}(h^2)$.

Given (5.1.28), it is trivial to check that the V matrix has the perturbative expansion

$$V = V^{(1)} + \mathcal{O}(h^2). \quad (5.1.34)$$

This can be immediately verified since $B \sim \mathcal{O}(h)$ and $A \sim \mathcal{O}(1)$, therefore the lowest possible order for V is $\mathcal{O}(h)$. Using (5.1.28),(5.1.27),(5.1.30) and (5.1.33) one obtains the explicit form for $|0\rangle_R$ and $|1_k\rangle_R$ to second order in h . We find:

$$\begin{aligned} |0\rangle_R &= N \left\{ 1 + W + \frac{1}{2}W^2 + \right\} |\bar{0}\rangle_R \\ |1_k\rangle_R &= N \left\{ \Gamma + \Gamma W + \frac{1}{2}\Gamma W^2 + \Delta \right\} |\bar{0}\rangle_R \end{aligned} \quad (5.1.35)$$

where

$$\begin{aligned} \Gamma &:= \sum_j (A^\dagger)_{nj} \bar{a}_j^\dagger \\ \Delta &:= \sum_j (B^T V)_{nj} \bar{a}_j^\dagger. \end{aligned} \quad (5.1.36)$$

One can use (5.1.35) to compute the terms in (5.1.29) and then perform the partial transpose but we do not reproduce such computations explicitly since they are technically involved and not illuminating.

Once (5.1.29) is computed, we observe that the first nontrivial contribution appears to order h^2 and the partial transpose is to this order an 8×8 matrix. When working in perturbation theory one can employ standard techniques to find the eigenvalues of matrices. However, when the unperturbed term in the expansion, $\rho^{(0)}$ in our case, has degenerate eigenvalues, this forces one to use degenerate perturbation theory.

Given the 8×8 matrix ρ that we need to diagonalize in the perturbation regime, we isolate the $\mathcal{O}(2)$ contribution $\rho^{(2)}$. Then, we compute the eigenvalues of the unperturbed part $\rho^{(0)}$. We select a set of eigenvalues $\lambda_i^{(0)}$ that is degenerate and $g > 1$ elements and we find the eigenvectors $v_i | i = 1, \dots, g$ which span the g dimensional subspace associated to such eigenvalues. One then constructs a $g \times g$ square matrix \tilde{N} where the elements \tilde{N}_{ij} can be found by

$$\tilde{N}_{ij} = v_i^T \cdot M^{(2)} \cdot v_j \quad (5.1.37)$$

and T denotes partial transposition. The $\mathcal{O}(2)$ corrections to the eigenvalues λ_i can be found by diagonalizing the matrix \tilde{N} , whose eigenvalues we denote by $\tilde{\lambda}_i \sim \mathcal{O}(h^2)$. Therefore, we find the corrected degenerate eigenvalues λ_i of ρ as

$$\lambda_i = \lambda_i^{(0)} + \tilde{\lambda}_i. \quad (5.1.38)$$

We choose to work to the first non-trivial contributing order which is $\mathcal{O}(h^2)$. Using these techniques we find that the partial transpose to this order has exactly one negative

eigenvalue. The formula for the negativity reads to this order

$$\mathcal{N} = \frac{1}{2} - \sum'_n \left(\frac{1}{2} |A_{nk}^{(1)}|^2 + |B_{nk}^{(1)}|^2 \right), \quad (5.1.39)$$

where the prime on the sum means that the term $n = k$ is omitted. In order to plot the dependence of (5.1.39) as a function of the parameters, one needs to specify the details of the travel scenario considered. Such details will appear in the explicit expression of $A_{nk}^{(1)}$ and $B_{nk}^{(1)}$.

We emphasize that the decrease of the negativity is due *only* with the mixing of the modes. The BVT act as a local operation in Rob's cavity and therefore will in general decrease the initial entanglement between Alice and Bob.

5.2 Massless field.

In this section we specialise to a massless scalar field. Nonzero mass or extra dimensions will be included in section 5.3.

5.2.1 Basic Building Block travel scenario

Let I, II and III denote respectively the initial inertial region, the region of acceleration and the final inertial region. As a first travel scenario, we consider the BBB depicted in Figure 5.1. Let the proper acceleration at the centre of the cavity be h/δ . In region II, the field modes that are positive frequency with respect to η and their frequencies with respect to the proper time τ at the centre of the cavity are

$$\tilde{\Omega}_n = \frac{n\pi h}{2\delta \operatorname{arctanh}(h/2)}. \quad (5.2.1)$$

We notice that (5.2.1) follows from

$$\tilde{\Omega}_n = A\Omega_n \quad (5.2.2)$$

As a special case of (5.1.15), we can now write the Bogoliubov transformation from region I to region III as the composition of three individual transformations.

The first comes with the coefficient matrices $({}_o\alpha, {}_o\beta)$ from I to II. The second is with the coefficient matrices

$$\mathcal{F} = \left(\operatorname{diag}(p, p^2, p^3, \dots), \operatorname{diag}(p^{-1}, p^{-2}, p^{-3}, \dots) \right) \quad (5.2.3)$$

where

$$p := \exp(i\tilde{\Omega}_1\bar{\tau}) \quad (5.2.4)$$

and $\bar{\tau}$ is the proper duration of the acceleration: this undoes the phases that the modes $\bar{\phi}_n$ develop over region II. The third is the inverse of the first, from II to III, with the coefficient matrices $({}_o\alpha^\dagger, -{}_o\beta^T)$.

Collecting, we find that the negativity \mathcal{N}_1 is given to order h^2 by

$$\mathcal{N}_1 = \frac{1}{2} - 2[Q(k, 1) - Q(k, p)]h^2 = \frac{1}{2} - h^2 \sum_{r=0}^{\infty} a_{kr} |p^{1+2r} - 1|^2, \quad (5.2.5)$$

where

$$Q(n, z) := \frac{4n^2}{\pi^4} \operatorname{Re} \left(\operatorname{Li}_6(z) - \frac{1}{64} \operatorname{Li}_6(z^2) \right) + \frac{6n}{\pi^4} \sum_{r=\lfloor \frac{n}{2} \rfloor}^{\infty} \operatorname{Re}(z^{1+2r}) \left(\frac{1}{(1+2r)^5} - \frac{n}{(1+2r)^6} \right) \quad (5.2.6)$$

Here Li_6 is the polylogarithm [21], the square brackets in the lower limit of the sum in (5.2.6) denote the integer part, and a_{nr} are all strictly positive. The sum term in (5.2.6) is $O(n^{-3})$ as $n \rightarrow \infty$, and numeric shows that the sum term contribution to $Q(n, z)$ is less than 1.1% already for $n = 1$ and less than 0.25% for $n \geq 2$.

The negativity \mathcal{N}_1 (5.2.5) is periodic in $\bar{\tau}$ with period $2\pi\tilde{\Omega}_1^{-1}$ and attains its unique minimum at half-period, with a shape that is close to a pure cosine curve. The behavior is plotted for one period in Fig. 5.2

The full time evolution of the field in Rob's cavity during the accelerated segment is periodic with period since the frequencies $\tilde{\Omega}_n$ are integer multiples of the fundamental frequency $\tilde{\Omega}_1$: hence, the periodic behavior of Fig. 5.2. The negativity \mathcal{N}_1 is therefore periodic not just in the small h approximation of (5.2.5) but exactly for arbitrary h . More generally, the same periodicity occurs for all cavity trajectories that contain a uniformly accelerated segment. We note that the period can be written as

$$2\delta (h/2)^{-1} \operatorname{arctanh}(h/2) : \quad (5.2.7)$$

this is the proper time elapsed at the centre of the cavity between sending and recapturing a light ray that bounces off each wall once.

5.2.2 One way trip travel scenario

As a second travel scenario, suppose that Rob blasts off as above, coasts inertially for proper time $\bar{\tau}'$ and then performs a braking manoeuvre that is the reverse of the initial acceleration, bringing him to rest (at, say, Alpha Centauri). Composing the segments

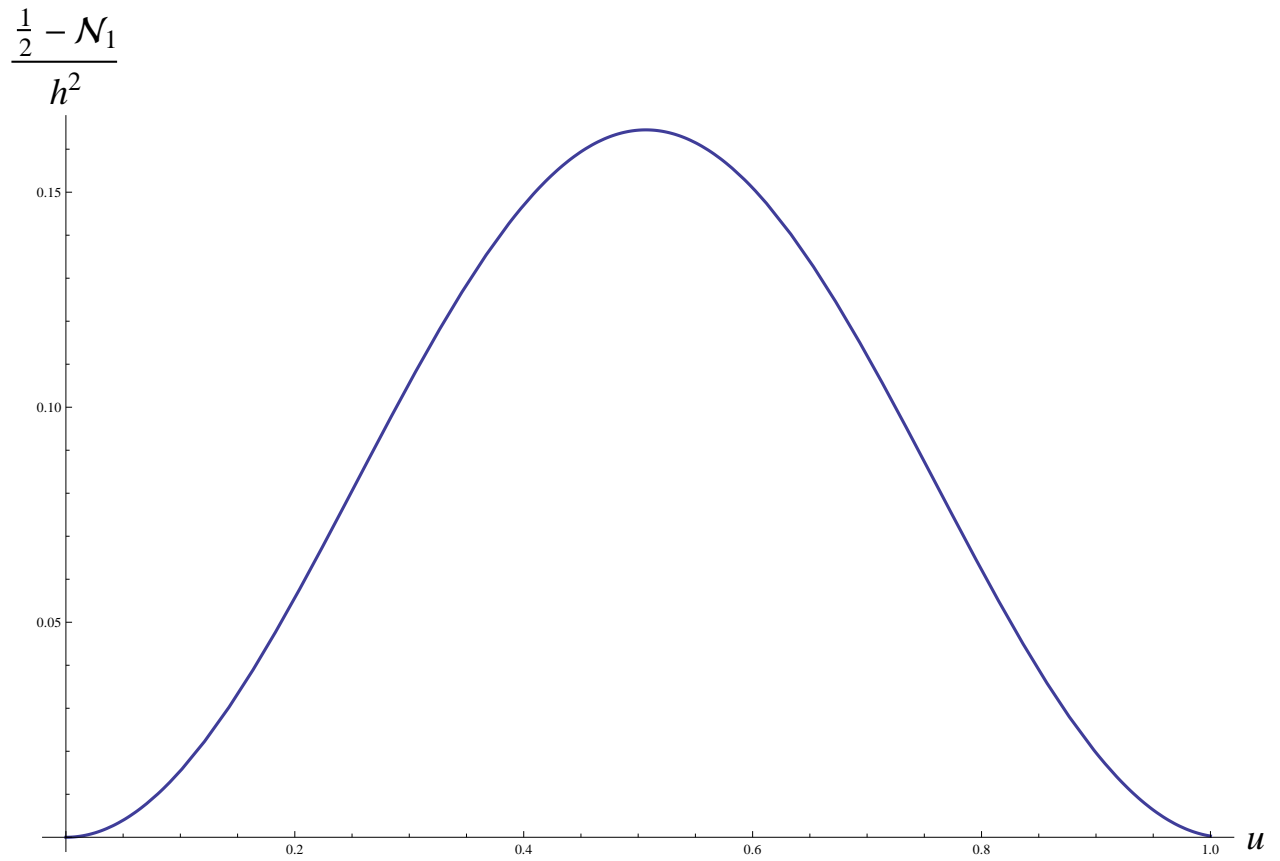


Figure 5.2: We plot $(\frac{1}{2} - \mathcal{N}_1) h^{-2}$ with $k = 1$ as a function of $u := \tilde{\Omega}_1 \bar{\tau}$ over the full period $0 \leq u \leq 2\pi$

as above, we see that the negativity \mathcal{N}_2 is periodic in $\bar{\tau}'$ with period 2δ . Noting that for leftward acceleration (5.1.22) holds with negative h , we find to order h^2 the formula

$$\begin{aligned}\mathcal{N}_2 &= \frac{1}{2} - h^2 \sum_{r=0}^{\infty} a_{kr} |p^{1+2r} - 1|^2 |(pp')^{1+2r} - 1|^2 \\ &= \frac{1}{2} - 2[2Q(k, 1) - 2Q(k, p) + Q(k, p') - 2Q(k, pp') + Q(k, p^2 p')] h^2,\end{aligned}\quad (5.2.8)$$

where

$$p' := \exp(i\pi\bar{\tau}'/\delta), \quad (5.2.9)$$

[cf. the expression of \mathcal{N}_1 in terms of two Q s in (5.2.5)]. In addition to displaying the periodicities in $\bar{\tau}$ and $\bar{\tau}'$, (5.2.8) shows that the coefficient of h^2 vanishes iff

$$p = 1 \text{ or } pp' = 1. \quad (5.2.10)$$

This implies that to order h^2 , any entanglement degradation caused by the accelerated segments can be cancelled by fine-tuning the duration of the coasting segment. The time scales for a $1m$ long cavity are of the order of $ms - ns$. A plot is shown in Figure 5.3.

5.2.3 Return trip travel scenario

As a third scenario, suppose Rob travels to Alpha Centauri as above, rests there for proper time $\bar{\tau}''$ and then returns to Alice by reversing the outward maneuvers. Again composing the segments, we see that the negativity \mathcal{N}_3 is periodic in $\bar{\tau}''$ with period 2δ , and to order h^2 we find

$$\mathcal{N}_3 = \frac{1}{2} - h^2 \sum_{r=0}^{\infty} a_{kr} |p^{1+2r} - 1|^2 \cdot |(pp')^{1+2r} - 1|^2 \cdot |(p^2 p' p'')^{1+2r} - 1|^2, \quad (5.2.11)$$

where

$$p'' := \exp(i\pi\bar{\tau}''/\delta), \quad (5.2.12)$$

and the sum can be expressed as a sum of 14 Q s if desired. The periodicities in $\bar{\tau}$, $\bar{\tau}'$ and $\bar{\tau}''$ are manifest in (5.2.11). The coefficient of h^2 vanishes iff

$$p = 1, \quad pp' = 1 \text{ or } p^2 p' p'' = 1, \quad (5.2.13)$$

so that to order h^2 any entanglement degradation caused by the accelerated segments can be cancelled by fine-tuning the duration of either of the independent inertial segments. Plots are not illuminating and resemble those of Fig. 5.3. Selected plots for the current scenario can be found in [58].

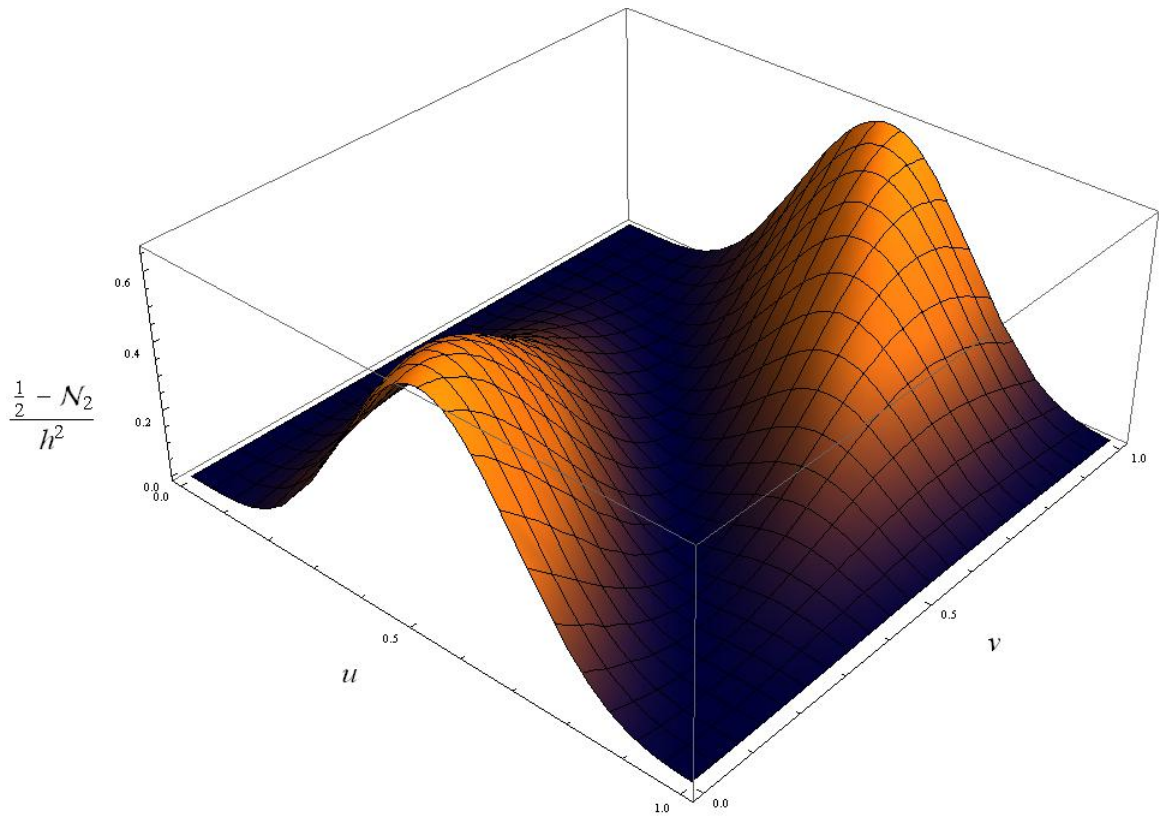


Figure 5.3: The plot shows $(\frac{1}{2} - \mathcal{N}_2) h^{-2}$ with $k = 1$ as a function of $u := \tilde{\Omega}_1 \bar{\tau}$ and $v := \pi \bar{\tau}' / \delta$ over the full periods $0 \leq u \leq 2\pi$ and $0 \leq v \leq 2\pi$. Note the zeroes at $u \equiv 0 \pmod{2\pi}$ and at $u + v \equiv 0 \pmod{2\pi}$.

5.2.4 Validity of the perturbation regime $h \ll 1$

Four comments are in order.

I Should one wish to consider noninertial initial or final states for Rob, our small h analysis is applicable whenever the assumptions leading to formula (5.1.39) still hold. For example, in a kick-start scenario that contains just regions I and II of Fig. 5.1, so that Rob's final state is uniformly accelerating, we find

$$\mathcal{N}_{kick} = \frac{1}{2} - Q(k, 1)h^2 \quad (5.2.14)$$

- II Second, the validity of our perturbative treatment requires the negativity to remain close to its initial value $1/2$ which in our scenarios happens when $kh \ll 1$. As the expansions (5.1.22) are not uniform in the indices, the treatment could potentially have missed even in this regime effects due to very high energy modes. However, we have verified that when the h^2 terms are included in the expansions (5.1.22), these expansions satisfy the Bogoliubov identities (2.2.50) perturbatively to order h^2 and the products of the order h matrices in the identities are unconditionally convergent. This gives confidence in our order h^2 negativity formulas, whose infinite sums come from similar products of order h matrices.
- III Third, the matrices (5.1.22) can be self-consistently truncated to the lowest 2×2 block provided the rows and columns are renormalised by suitable factors of the form $1 + \mathcal{O}(h^2)$ to preserve the Bogoliubov identities to order h^2 . Taking Rob's initial excitation to be in the lower frequency, we find that all the above negativity results hold with the replacement

$$Q(1, z) \rightarrow a_{10}\text{Re}(z) + \frac{1}{2}a_{11}\text{Re}(z^3) \quad (5.2.15)$$

and the error in this replacement is less than 0.7%. The high frequency effects on the entanglement are hence very strongly suppressed.

- IV The analysis can be adapted to a fermionic field and to scenarios where mode entanglement is generated from an initially unentangled state; such settings are the main object of study of the following three chapters

5.3 Massive field

For a massive field the frequencies are not uniformly spaced and the negativity is no longer periodic in the durations of the inertial and uniformly accelerated segments. The

massive counterparts of the expansions (5.1.22) can be found using uniform asymptotic expansions of modified Bessel functions [21, 59], with the result

$$\alpha_{0,nn} = 1 - \left(\frac{\pi^2 n^2}{240} + \frac{M^2}{120} + \frac{M^2(M^2 - 5)}{240 \pi^2 n^2} + \frac{M^2(M^2 - 24)}{96 \pi^4 n^4} \right) h^2 + O(h^4), \quad (5.3.1a)$$

$$\alpha_{0, m \neq n} + \beta_{0, mn} = \frac{2mn(-1 + (-1)^{m-n})[\pi^2(n^2 + 3m^2) + 4M^2](M^2 + \pi^2 n^2)^{1/4}}{\pi^4(m^2 - n^2)^3(M^2 + \pi^2 m^2)^{1/4}} h + O(h^2), \quad (5.3.1b)$$

$$\alpha_{0, m \neq n} - \beta_{0, mn} = \frac{2mn(-1 + (-1)^{m-n})[\pi^2(m^2 + 3n^2) + 4M^2](M^2 + \pi^2 m^2)^{1/4}}{\pi^4(m^2 - n^2)^3(M^2 + \pi^2 n^2)^{1/4}} h + O(h^2) \quad (5.3.1c)$$

where

$$M := \frac{\mu}{\delta} \quad (5.3.2)$$

and we have again verified that the Bogoliubov identities are satisfied perturbatively to order h^2 .

The perturbative treatment is now valid provided $h \ll 1$ and $hM^2 \lesssim 100$, allowing the possibility that M may be large. When $k \ll M$, a qualitatively new feature is that the order h contribution in ${}_0\alpha$ is proportional to M^2 , resulting in an overall enhancement factor M^4 in the negativity. In the travel scenario with one accelerated segment, the negativity takes in this limit the form

$$\mathcal{N}_1 = \frac{1}{2} - h^2 M^4 \times \frac{256k^2}{\pi^8} \sum_n'' \frac{n^2}{(k^2 - n^2)^6} \left\{ 1 - \cos \left[\left(\sqrt{M^2 + \pi^2 k^2} - \sqrt{M^2 + \pi^2 n^2} \right) (\bar{\tau}/\delta) \right] \right\}, \quad (5.3.3)$$

where the double prime means that the sum is over positive n with $n \equiv k+1 \pmod{2}$. The negativity \mathcal{N}_1 (5.3.3) is approximately periodic in $\bar{\tau}$ with period $4M\delta/\pi$, but it contains also significant higher frequency components. Plots are shown in Figure 5.4.

5.4 (3 + 1) dimensions.

The above (1 + 1)-dimensional entanglement degradation analysis extends immediately to linear acceleration in (3 + 1)-dimensional Minkowski space, where the transverse momentum merely contributes to the effective (1 + 1)-dimensional mass (see chapter 2). For a massless field in a cavity of length $\delta = 10\text{m}$ and acceleration 10ms^{-2} , an effect of

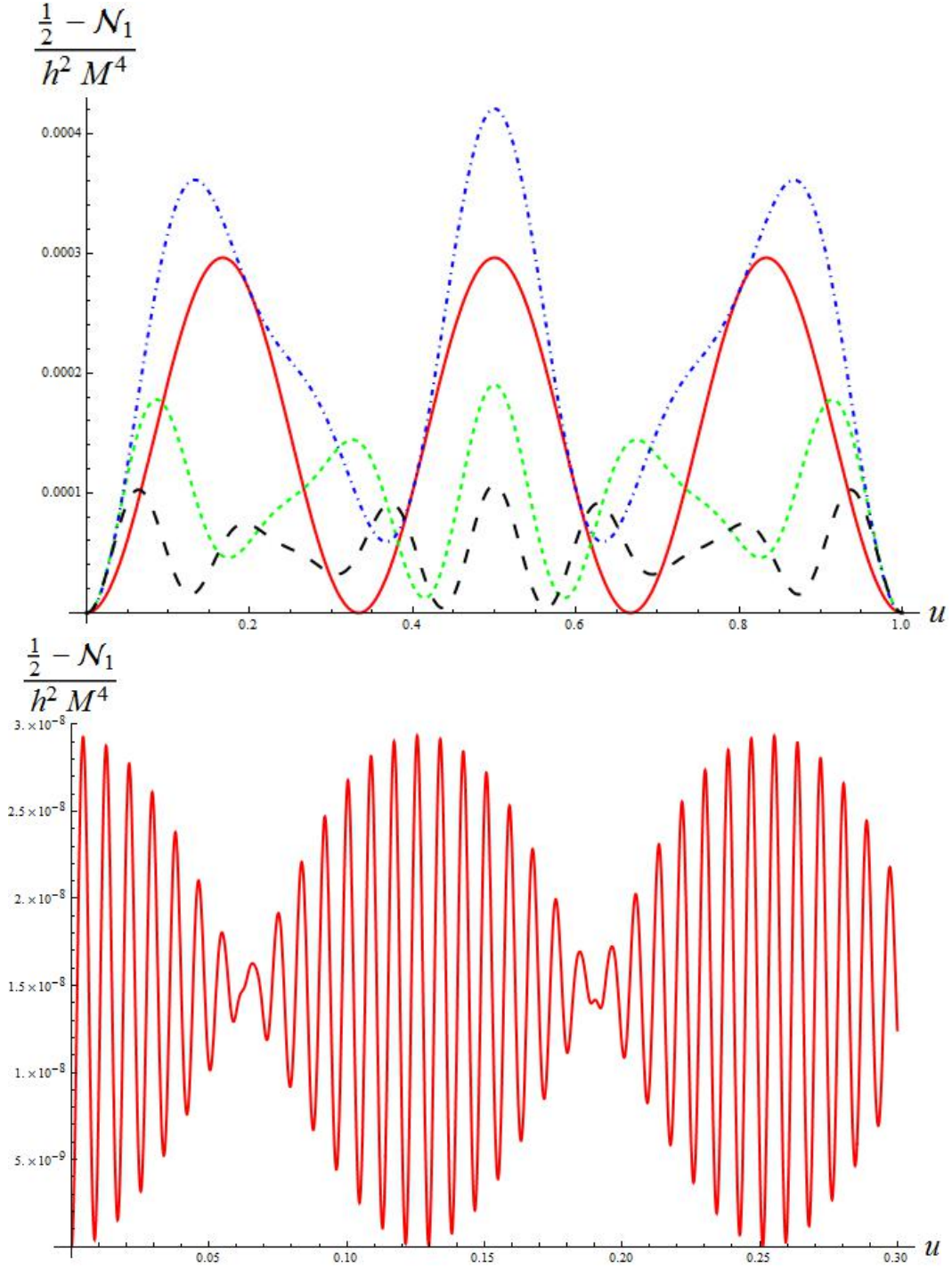


Figure 5.4: The plots show $(\frac{1}{2} - \mathcal{N}_1) h^{-2} M^{-4}$ (5.3.3) for $M = 10^3$ as a function of $u = \pi \bar{\tau} / (4M\delta)$, in the upper figure with $k = 1, 2, 3, 4$ (solid, dashed, dash-dotted, wide-dashed) and in the lower figure with $k = 30$.

observable magnitude can be achieved by trapping quanta of optical wavelengths provided the momentum is highly transverse so that $k \ll M \approx 10^8$. Were it possible to trap and stabilise massive quanta of kaon mass $\mu = 10^{-27}$ kg in a cavity of length $\delta = 10$ cm, the effect would become observable already at the extreme microgravity acceleration of 10^{-10} ms^{-2} .

5.5 Conclusions

In this chapter we have introduced the techniques that allow us to quantize an uncharged massive or massless scalar field in a 1+1 or 3+1 cavity and to compute explicitly the BVT between initial and final modes of the traveling cavity in the low \hbar regime. Our techniques allow for “general” trajectories which are composed by inertial and uniform accelerated segments. We find that the entanglement present in an initial maximally entangled state between two modes, one in each inertial cavity, is degraded when one of the two cavities travels. The degradation of entanglement is quantified by negativity and we find that for 1+1 massless bosons it is periodic. Exact periodicity occurs because every mode acquires a phase during the inertial or accelerated segments which are multiples of the fundamental one. The degradation of entanglement is not exactly periodic for 1+1 massive or 3+1 massless or massive fields. In this case, the degradation can be enhanced by entangling highly transverse photons (with high momentum transverse to the direction of the acceleration) or massive bosons (which cannot be realized with current technologies). The enhancement cannot be so large that the overall correction to the negativity will exceed 5-10% of the maximum value. Over this amount, we exit the perturbative regime. This chapter provides the basics tools for understanding the work presented in the following three where we analyze fermionic field modes entanglement and creation of entanglement within a single cavity.

CHAPTER 6

**Kinematic entanglement
degradation of fermionic cavity
modes**

In the previous chapter we have introduced techniques for analyzing how motion of cavities that contain bosonic quantum fields affects the initial entanglement between modes of the fields in different cavities. Studies of uniform acceleration in Minkowski spacetime (see [5, 7, 15, 36, 48, 60] for a small selection and [61] for a recent review) have revealed significant differences in the degradation that occurs for bosonic and fermionic fields. There are in particular clear qualitative differences in the bosonic versus fermionic particle-antiparticle entanglement swapping (see [60] and Chapter 4 for an example) and in the infinite acceleration residual entanglement and nonlocality [48].

The analyses of uniform acceleration mentioned above involve two ingredients that make it difficult to compare the theoretical predictions to experimentally realisable situations. The first is that while the uniformly-accelerated observers are considered to be pointlike and perfectly localised on a trajectory of prescribed acceleration, the field excitations are nevertheless usually treated as delocalised field modes of plane wave type, normalised in the sense of Dirac rather than Kronecker deltas. This may seem a technicality, perhaps remediable by use of appropriate wave packets [15], but at present it appears unexplored how localised observers would in practice perform measurements to probe the correlations in the delocalised states.

The second concern lies in the time evolution of the correlations. An inertial trajectory in Minkowski space is stationary, in the sense that it is the integral curve of a Minkowski time translation Killing vector. A uniformly-accelerated trajectory is also stationary, in the sense that it is the integral curve of a boost Killing vector. However, the combined system of the two trajectories is not stationary, as the two Killing vectors do not commute. For example, in the $(1+1)$ -dimensional setting there is a unique moment at which the two trajectories are parallel, and the trajectories may or may not intersect depending on their relative spatial location. Yet the analyses mentioned above regard the correlations between observers on the two trajectories as stationary and the relative location of the trajectories as irrelevant, observing just that the spacetime has a quadrant causally disconnected from the uniformly-accelerated worldline and noting that the field modes confined in this quadrant are inaccessible to the accelerated observer. While the acceleration horizon that is responsible for this inaccessibility may be seen as the basis of the Unruh effect [8, 22], the horizon exists only if the uniform acceleration persists from the asymptotic past to the asymptotic future. In this setting it is not clear how to address motion on trajectories that remain uniformly accelerated only up to the moment at which localised observers might make their measurements on the quantum state.

Both of these concerns have been addressed in the previous chapter by means of bosonic quantum fields. In this chapter we shall undertake the first steps of investigating fermionic entanglement in accelerated cavities by adapting the scalar field analysis developed in chapter 5 to a Dirac fermion. When considering fermions, the presence of positive and negative charges allows a broader range of initial Bell-type states to be considered. Another difference is that in a fermionic Fock space the entanglement between the cavities can be characterised not just by the negativity but also by the violation of the Clauser-Horne-Shimony-Holt (CHSH) version of Bell's inequality [62, 63], physically interpretable as nonlocality. New technical issues arise from the boundary conditions that are required to keep the fermionic field confined in the cavities.

In this chapter we focus on a massless fermion in $(1 + 1)$ dimensions. In this setting another new technical issue arises from a zero mode that is present in the cavity under boundary conditions that may be considered physically preferred. This zero mode needs to be regularised in order to apply usual Fock space techniques.

6.1 Quantization of fermions within an inertial cavity

As a first step we quantize the fermionic field in the cavity.

Let (t, x) be standard Minkowski coordinates in $(1 + 1)$ dimensional Minkowski space with standard Minkowski metric.

The massless Dirac equation reads

$$i \gamma^\mu \partial_\mu \psi = 0, \quad (6.1.1)$$

where the 4×4 matrices γ^μ form the usual Dirac-Clifford algebra,

$$\{\gamma^\mu, \gamma^\nu\} = 2\eta^{\mu\nu}. \quad (6.1.2)$$

A standard basis of plane wave solutions reads

$$\psi_{\omega, \epsilon, \sigma}(t, x) = A_{\omega, \epsilon, \sigma} e^{-i\omega(t - \epsilon x)} U_{\epsilon, \sigma}, \quad (6.1.3)$$

where $\omega \in \mathbb{R}$, $\epsilon \in \{1, -1\}$, $\sigma \in \{1, -1\}$, the constant spinors $U_{\epsilon, \sigma}$ satisfy

$$\alpha_3 U_{\epsilon, \sigma} = \epsilon U_{\epsilon, \sigma}, \quad (6.1.4a)$$

$$\gamma^5 U_{\epsilon, \sigma} = \sigma U_{\epsilon, \sigma}, \quad (6.1.4b)$$

$$U_{\epsilon, \sigma}^\dagger U_{\epsilon', \sigma'} = \delta_{\epsilon\epsilon'} \delta_{\sigma\sigma'}, \quad (6.1.4c)$$

The solutions (6.1.3) satisfy the eigenvalue equations

$$\begin{aligned} i\partial_t\psi_{\omega,\epsilon,\sigma}(t,x) &= \omega\psi_{\omega,\epsilon,\sigma}(t,x) \\ \alpha_3\psi_{\omega,\epsilon,\sigma} &= \gamma^0\gamma^3\psi_{\omega,\epsilon,\sigma} = \epsilon\psi_{\omega,\epsilon,\sigma} \\ \gamma^5\psi_{\omega,\epsilon,\sigma} &= i\gamma^0\gamma^1\gamma^2\gamma^3\psi_{\omega,\epsilon,\sigma} = \sigma\psi_{\omega,\epsilon,\sigma} \end{aligned} \quad (6.1.5)$$

where ω is the frequency of the mode, ϵ labels right-movers ($\epsilon = 1$) and a left-movers ($\epsilon = -1$), σ is the eigenvalue that labels helicity/chirality [18] and the right-handed ($\sigma = +1$) and left-handed ($\sigma = -1$) solutions are decoupled because $m = 0$ in (6.1.1).

We confine the field in the inertial cavity

$$L_0 \leq x \leq R_0, \quad (6.1.6)$$

where $0 < L_0 < R_0$ and $\delta := R_0 - L_0$ is the usual length of the box. The fermionic inner product reads

$$(\psi, \psi') = \int_{L_0}^{R_0} dx \psi^\dagger \psi', \quad (6.1.7)$$

where the integral is evaluated on a hyper-surface $t = \text{const}$. To ensure unitarity of the time evolution, so that the inner product (6.1.7) is conserved in time, the Hamiltonian must be defined as a self-adjoint operator by introducing suitable boundary conditions at $x = L_0$ and $x = R_0$ [64, 65]. We specialise to boundary conditions that do not couple right-handed and left-handed spinors. For concreteness, we consider from now on only left-handed spinors, and we drop the index σ . The analysis for right-handed spinors is similar.

We seek the eigenfunctions of the Hamiltonian in the form

$$\psi_\omega(t,x) = A_\omega e^{-i\omega(t-x)} U_+ + B_\omega e^{-i\omega(t+x)} U_-, \quad (6.1.8)$$

where $A_\omega, B_\omega \in \mathbb{C}$. In order to retain unitarity, one choice of boundary conditions would be to allow probability to flow out through one of the cavity walls and instantaneously reappear at the other wall; physically, this would correspond to a spatial surface being a circle, possibly with one marked point. However, we wish to regard the spatial surface as a genuine interval with two spatially separated endpoints, and we hence specialise to boundary conditions that ensure vanishing of the probability current independently at each wall. The boundary condition on the eigenfunctions thus reads

$$\left(\bar{\psi}_\omega \gamma^3 \psi_{\omega'}\right)_{x=L_0} = 0 = \left(\bar{\psi}_\omega \gamma^3 \psi_{\omega'}\right)_{x=R_0}, \quad (6.1.9)$$

where $\bar{\psi} = \psi^\dagger \gamma^0$.

Following the procedure of [64, 65], we find from (6.1.8) and (6.1.9) that the self-adjoint extensions of the Hamiltonian are specified by two independent phases, characterising the phase shifts of reflection from the two walls. We encode these phases in the parameters $\theta \in [0, 2\pi)$ and $s \in [0, 1)$, which can be understood respectively as the normalised sum and difference of the two phases. Choosing the value of the phases leads to (in principle) different quantizations. The quantum theories then fall into two qualitatively different cases, the generic case $0 < s < 1$ and the special case $s = 0$.

In the generic case $0 < s < 1$, the orthonormal eigenfunctions are

$$\psi_n(t, x) = \frac{1}{\sqrt{2\delta}} \left[e^{-i\omega_n(t-x+L_0)} U_+ + e^{i\theta} e^{-i\omega_n(t+x-L_0)} U_- \right] \quad (6.1.10a)$$

where

$$\omega_n = (n + s)\pi/\delta, n \in \mathbb{Z}. \quad (6.1.11)$$

Note that $\omega_n \neq 0$ for all n , and positive (respectively negative) frequencies are obtained for $n \geq 0$ ($n < 0$). A Fock space quantisation can be performed in a standard manner [18].

The special case $s = 0$ corresponds to assuming that the two walls are of identical physical build. In this case $\omega_n \neq 0$ for $n \neq 0$ but $\omega_0 = 0$. It follows that a Fock quantisation can proceed as usual for the $n \neq 0$ modes, but $n = 0$ is a zero mode that does not admit a Fock space quantisation. In what follows we consider the $s = 0$ quantum theory to be defined by first quantising with $s > 0$ and at the end taking the limit $s \rightarrow 0_+$. All our entanglement measures will be seen to remain well defined in this limit.

6.2 Uniformly accelerated cavity

We proceed to quantize the fermionic field contained in a cavity, as in the section 6.1, when the latter accelerates and is rigid in its rest frame. We consider a cavity whose ends move on the worldlines

$$\begin{aligned} x_L &= \sqrt{L_0^2 + t^2}, \\ x_R &= \sqrt{R_0^2 + t^2}, \end{aligned} \quad (6.2.1)$$

where the notation is as above.

The proper accelerations of the ends are $1/L_0$ and $1/R_0$ respectively, and the cavity as a whole is static in the sense that it is dragged along the boost Killing vector

$$\Xi := x\partial_t + t\partial_x. \quad (6.2.2)$$

At $t = 0$ the accelerated cavity overlaps precisely with the inertial cavity of Sec. 6.1.

Coordinates convenient for the accelerated cavity are the standard Rindler coordinates (2.2.36) in the RRW. The metric reads

$$ds^2 = -\chi^2 d\eta^2 + d\chi^2 \quad (6.2.3)$$

The cavity is at

$$L_0 \leq \chi \leq R_0, \quad (6.2.4)$$

and the boost Killing vector Ξ along which the cavity is dragged has the expression $\Xi = \partial_\eta$.

In Rindler coordinates the massless Dirac equation (6.1.1) takes the form [10, 66]

$$i \partial_\eta \psi(\eta, \chi) = \left(-i \alpha_3 (\chi \partial_\chi + \frac{1}{2}) \right) \psi(\eta, \chi), \quad (6.2.5)$$

and the inner product for a field enclosed in the accelerated cavity reads

$$(\psi, \psi') = \int_{L_0}^{R_0} d\chi \psi^\dagger \psi', \quad (6.2.6)$$

where the integral is evaluated on a hyper surface $\eta = \text{const}$. Working as in Sec. 6.1, we find that the orthonormal energy eigenfunctions are

$$\widehat{\psi}_n(\eta, \chi) = \frac{e^{-i\Omega_n \eta}}{\sqrt{2\chi \ln(R_0/L_0)}} \left(\left(\frac{\chi}{a} \right)^{i\Omega_n} U_+ + e^{i\theta} \left(\frac{\chi}{a} \right)^{-i\Omega_n} U_- \right) \quad (6.2.7)$$

where the R frequencies are defined as

$$\Omega_n = \frac{(n + s)\pi}{\ln(R_0/L_0)} \quad (6.2.8)$$

and $n \in \mathbb{Z}$. θ and s have the same meaning and values as above: we consider the microphysical build of the cavity walls not to be affected by their acceleration. For $s \neq 0$ a Fock space quantisation can be performed in a standard manner. For $s = 0$ the mode $n = 0$ is again a zero mode, and we consider the $s = 0$ quantum theory to be defined as the limit $s \rightarrow 0_+$.

6.3 Quantization and BVT

We now turn to a cavity whose trajectory consists of inertial and uniformly accelerated segments.

The prototype cavity configuration is the same as in the previous chapter and we reproduce it here shown in Fig. 6.1. Again, Alice and Rob will be initially inertial and

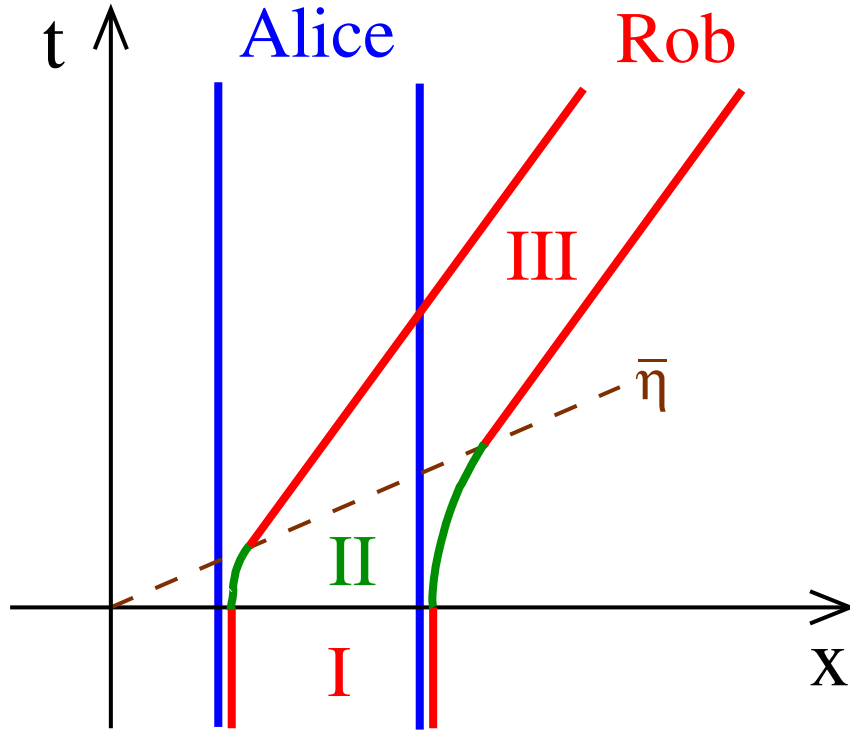


Figure 6.1: Space-time diagram of cavity motion is shown. Rob's cavity is at rest initially (Region I), then undergoes a period of uniform acceleration from $t = 0$ to $\eta = \bar{\eta}$ (Region II) and is thereafter again inertial (Region III). Alice's cavity overlaps with Rob's cavity in Region I and remains inertial throughout.

at $t = 0$ Rob will start a trip. Trajectories are again planned using the techniques in Chapter 5.

The Dirac field Ψ in Rob's cavity before the trip starts may be expanded as

$$\Psi = \sum_{n \geq 0} a_n \psi_n + \sum_{n < 0} b_n^\dagger \psi_n \quad (6.3.1)$$

while after the trip it may be expanded as

$$\Psi = \sum_{n \geq 0} \hat{a}_n \hat{\psi}_n + \sum_{n < 0} \hat{b}_n^\dagger \hat{\psi}_n \quad (6.3.2)$$

where the nonvanishing anticommutators are

$$\{a_m, a_n^\dagger\} = \{b_m, b_n^\dagger\} = \delta_{mn}, \quad (6.3.3a)$$

$$\{\hat{a}_m, \hat{a}_n^\dagger\} = \{\hat{b}_m, \hat{b}_n^\dagger\} = \delta_{mn}. \quad (6.3.3b)$$

We again employ the formalism of \mathcal{A} matrices for the BVT and we can express the final

modes in terms of the initial ones through

$$\widehat{\psi}_m = \sum_n \mathcal{A}_{mn} \psi_n, \quad \psi_n = \sum_m \mathcal{A}_{mn}^* \widehat{\psi}_m, \quad (6.3.4)$$

where the coefficients of \mathcal{A} are given by

$$\mathcal{A}_{mn} = (\psi_n, \widehat{\psi}_m) \quad (6.3.5)$$

Once more, the matrix \mathcal{A} can be expressed in terms of the BVT between inertial and accelerated modes that we denote by A .

The perturbation parameter is again

$$h := \frac{2\delta}{R_0 + L_0}, \quad (6.3.6)$$

satisfying $0 < h < 2$. Expanding A in a Maclaurin series in h , we find

$$A = A^{(0)} + A^{(1)} + A^{(2)} + O(h^3), \quad (6.3.7)$$

where the superscript indicates the power of h and the explicit expressions for $A^{(0)}$, $A^{(1)}$ and $A^{(2)}$ read

$$A_{mn}^{(0)} = \delta_{mn}, \quad (6.3.8a)$$

$$A_{nn}^{(1)} = 0, \quad (6.3.8b)$$

$$A_{mn}^{(1)} = \frac{[(-1)^{m+n} - 1](m+n+2s)}{2\pi^2(m-n)^3} h, \quad (m \neq n) \quad (6.3.8c)$$

$$A_{nn}^{(2)} = -\left(\frac{1}{96} + \frac{\pi^2(n+s)^2}{240}\right) h^2, \quad (6.3.8d)$$

$$A_{mn}^{(2)} = \frac{[(-1)^{m+n} + 1]}{8\pi^2(m-n)^4} [(m+s)^2 + 3(n+s)^2 + 8(m+s)(n+s)] h^2. \quad (m \neq n) \quad (6.3.8e)$$

The expressions (6.3.8) show that the small h expansion of A_{mn} is not uniform in the indices, but it is easy to verify that the expansion maintains the unitarity of A perturbatively to order h^2 and the products of the order h matrices in the unitarity identities are unconditionally convergent.

The perturbative unitarity of A persists in the limit $s \rightarrow 0_+$. Had we set $s = 0$ at the outset and dropped the zero mode from the system by hand, the resulting truncated A would not be perturbatively unitary to order h^2 .

6.3.1 Pre-trip to post-trip Bogoliubov transformations

After the trip, we expand the Dirac field in Rob's cavity as

$$\Psi = \sum_{n \geq 0} \tilde{a}_n \tilde{\psi}_n + \sum_{n < 0} \tilde{b}_n^\dagger \tilde{\psi}_n, \quad (6.3.9)$$

where the mode functions $\tilde{\psi}_n$ are as in (6.1.10) but (t, x) are replaced by the Minkowski coordinates (\tilde{t}, \tilde{x}) adapted to the cavity's new rest frame, with the surface $\tilde{t} = 0$ coinciding with $\eta = \eta_1$. The nonvanishing anticommutators are

$$\{\tilde{a}_m, \tilde{a}_n^\dagger\} = \{\tilde{b}_m, \tilde{b}_n^\dagger\} = \delta_{mn}. \quad (6.3.10)$$

The BVT between the modes before and after the journey can then be written as

$$\tilde{\psi}_m = \sum_n \mathcal{A}_{mn} \psi_n, \quad \psi_n = \sum_m \mathcal{A}_{mn}^* \tilde{\psi}_m. \quad (6.3.11)$$

We proceed as before and expand \mathcal{A} in a Maclaurin series in h as

$$\mathcal{A} = \mathcal{A}^{(0)} + \mathcal{A}^{(1)} + \mathcal{A}^{(2)} + O(h^3), \quad (6.3.12)$$

where the superscript again indicates the power of h . Given a specific travel scenario one can express every term in (6.3.12) as functions of \mathcal{A} .

6.3.2 Relations between operators and vacua

We denote the Fock vacua of the field before the trip by $|0\rangle$ and after the trip by $|\tilde{0}\rangle$. As for the bosonic case [9], we make the following ansatz for the transformation between the two

$$|0\rangle = N e^W |\tilde{0}\rangle, \quad (6.3.13)$$

where

$$W = \sum_{p \geq 0, q < 0} V_{pq} \tilde{a}_p^\dagger \tilde{b}_q^\dagger \quad (6.3.14)$$

and the V matrix entries V_{pq} and the normalisation constant N are to be determined. Note that the two indices of V take values in disjoint sets.

It follows from (6.3.9) and (6.3.11) that the creation and annihilation operators before and after the voyage are related by

$$n \geq 0: a_n = (\psi_n, \psi) = \sum_{m \geq 0} \tilde{a}_m \mathcal{A}_{mn} + \sum_{m < 0} \tilde{b}_m^\dagger \mathcal{A}_{mn}, \quad (6.3.15a)$$

$$n < 0: b_n^\dagger = (\psi_n, \psi) = \sum_{m \geq 0} \tilde{a}_m \mathcal{A}_{mn} + \sum_{m < 0} \tilde{b}_m^\dagger \mathcal{A}_{mn}. \quad (6.3.15b)$$

Using (6.3.13) and (6.3.15a), the condition $a_n |0\rangle = 0$ reads

$$\left(\sum_{m \geq 0} \tilde{a}_m \mathcal{A}_{mn} + \sum_{m < 0} \tilde{b}_m^\dagger \mathcal{A}_{mn} \right) e^W |\tilde{0}\rangle = 0. \quad (6.3.16)$$

From the anticommutators (6.3.10) it follows that

$$[W, \tilde{a}_m] = -\sum_{q<0} V_{mq} \tilde{b}_q^\dagger, \quad (6.3.17a)$$

$$[W, [W, \tilde{a}_m]] = 0. \quad (6.3.17b)$$

Using (6.3.17) and the Hadamard lemma,

$$e^A B e^{-A} = B + [A, B] + \frac{1}{2}[A, [A, B]] + \dots, \quad (6.3.18)$$

(6.3.16) reduces to

$$\sum_{m \geq 0} \mathcal{A}_{mn} V_{mq} = -\mathcal{A}_{qn} \quad (n \geq 0, q < 0). \quad (6.3.19)$$

A similar computation shows that the condition $b_n |0\rangle = 0$ reduces to

$$\sum_{m < 0} \mathcal{A}_{mn}^* V_{pm} = \mathcal{A}_{pn}^* \quad (n < 0, p \geq 0). \quad (6.3.20)$$

If the block of \mathcal{A} where both indices are non-negative is invertible, Eq. (6.3.19) determines V uniquely. Similarly, if the block of \mathcal{A} where both indices are negative is invertible, Eq. (6.3.20) determines V uniquely. If both blocks are invertible, it can be verified using unitarity of \mathcal{A} that the ensuing two expressions for V are equivalent. Working perturbatively in \hbar , the invertibility assumptions hold, and using ((6.3.12)) we find

$$V = V^{(1)} + O(\hbar^2), \quad (6.3.21)$$

where

$$V_{pq}^{(1)} = -\mathcal{A}_{qp}^{(1)} G_p^* = \mathcal{A}_{pq}^{(1)*} G_q \quad (p \geq 0, q < 0). \quad (6.3.22)$$

We shall show in Section 6.4 that the normalisation constant N has the small \hbar expansion

$$N = 1 - \frac{1}{2} \sum_{p,q} |V_{pq}|^2 + O(\hbar^3). \quad (6.3.23)$$

6.4 Evolution of entangled states

In this section we study the evolution of Bell-type quantum states of modes within two cavities. We shall work perturbatively to quadratic order in \hbar .

We specialize to the scenario where Rob is initially inertial, accelerates uniformly and then turns the engines off and travels with constant velocity. More complicated scenarios can be analyzed in a similar fashion adopting the techniques developed in the previous

chapter. Focusing first on Rob's cavity only, we write out in Sec. 6.4.1 the pre-trip vacuum and states with a single (anti-)particle in terms of post-trip excitations on the appropriate vacuum. In Sec. 6.4.2 we address an entangled state where one field mode is controlled by Alice and one by Rob. In Sec. 6.4.3 we address a state of the type analysed in [60] where the entanglement between Alice and Rob is in the charge of the field modes.

6.4.1 Rob's cavity: vacuum and single-particle states

Consider the initial vacuum $|0\rangle$ in Rob's cavity before the journey starts. We shall use (6.3.13) to express this state in terms of post-trip excitations over the post-trip vacuum $|\tilde{0}\rangle$.

We expand the exponential in (6.3.13) as

$$e^W = \mathbb{1} + \sum_{p,q} V_{pq} \tilde{a}_p^\dagger \tilde{b}_q^\dagger + \frac{1}{2} \sum_{p,q,i,j} V_{pq} V_{ij} \tilde{a}_p^\dagger \tilde{b}_q^\dagger \tilde{a}_i^\dagger \tilde{b}_j^\dagger + O(\hbar^3). \quad (6.4.1)$$

We denote the final single-particle states by

$$|\tilde{1}_k\rangle^+ := \tilde{a}_k^\dagger |\tilde{0}\rangle \quad (6.4.2)$$

for $k \geq 0$ and by

$$|\tilde{1}_k\rangle^- := \tilde{b}_k^\dagger |\tilde{0}\rangle \quad (6.4.3)$$

for $k < 0$, so that the superscript \pm indicates particles and antiparticles respectively. From (6.4.1) we obtain

$$\begin{aligned} e^W |\tilde{0}\rangle = & \quad |\tilde{0}\rangle + \sum_{p,q} V_{pq} |\tilde{1}_p\rangle^+ |\tilde{1}_q\rangle^- \\ & - \frac{1}{2} \sum_{p,q,i,j} V_{pq} V_{ij} (1 - \delta_{pi})(1 - \delta_{qj}) |\tilde{1}_p\rangle^+ |\tilde{1}_i\rangle^+ |\tilde{1}_q\rangle^- |\tilde{1}_j\rangle^- + O(\hbar^3), \end{aligned} \quad (6.4.4)$$

where the ordering of the single-particle kets encodes the ordering of the fermion creation operators. It follows that the normalisation constant N is given by (6.3.23), and (6.3.13) gives

$$\begin{aligned} |0\rangle = & \left(1 - \frac{1}{2} \sum_{p,q} |V_{pq}|^2\right) |\tilde{0}\rangle + \sum_{p,q} V_{pq} |\tilde{1}_p\rangle^+ |\tilde{1}_q\rangle^- \\ & - \frac{1}{2} \sum_{p,q,i,j} V_{pq} V_{ij} (1 - \delta_{pi})(1 - \delta_{qj}) |\tilde{1}_p\rangle^+ |\tilde{1}_i\rangle^+ |\tilde{1}_q\rangle^- |\tilde{1}_j\rangle^- + O(\hbar^3). \end{aligned} \quad (6.4.5)$$

Consider then in Rob's cavity the state with exactly one pre-trip particle,

$$\begin{aligned} |1_k\rangle^- & := b_k^\dagger |0\rangle \text{ for } k < 0 \text{ or} \\ |1_k\rangle^+ & := a_k^\dagger |0\rangle \text{ for } k \geq 0. \end{aligned} \quad (6.4.6)$$

Acting on the initial vacuum (6.4.5) by (6.3.15b) and the Hermitian conjugate of (6.3.15a) respectively, we find

$$\begin{aligned}
 k < 0: \quad |1_k\rangle^- &= \sum_{p,q} V_{pq} \mathcal{A}_{pk} |\tilde{1}_q\rangle^- \\
 &+ \sum_{m < 0} \mathcal{A}_{mk} \left[\left(1 - \frac{1}{2} \sum_{p,q} |V_{pq}|^2 \right) |\tilde{1}_m\rangle^- + \sum_{p,q} V_{pq} (1 - \delta_{mq}) |\tilde{1}_p\rangle^+ |\tilde{1}_q\rangle^- |\tilde{1}_m\rangle^- \right. \\
 &\left. - \frac{1}{2} \sum_{p,q,i,j} V_{pq} V_{ij} (1 - \delta_{pi})(1 - \delta_{qj})(1 - \delta_{mq})(1 - \delta_{mj}) |\tilde{1}_p\rangle^+ |\tilde{1}_i\rangle^+ |\tilde{1}_q\rangle^- |\tilde{1}_j\rangle^- |\tilde{1}_m\rangle^- \right] \\
 &+ O(\hbar^3), \tag{6.4.7a}
 \end{aligned}$$

$$\begin{aligned}
 k > 0: \quad |1_k\rangle^+ &= - \sum_{p,q} V_{pq} \mathcal{A}_{qk}^* |\tilde{1}_p\rangle^+ \\
 &+ \sum_{m \geq 0} \mathcal{A}_{mk}^* \left[\left(1 - \frac{1}{2} \sum_{p,q} |V_{pq}|^2 \right) |\tilde{1}_m\rangle^+ + \sum_{p,q} V_{pq} (1 - \delta_{mp}) |\tilde{1}_m\rangle^+ |\tilde{1}_p\rangle^+ |\tilde{1}_q\rangle^- \right. \\
 &\left. - \frac{1}{2} \sum_{p,q,i,j} V_{pq} V_{ij} (1 - \delta_{pi})(1 - \delta_{qj})(1 - \delta_{mp})(1 - \delta_{mi}) |\tilde{1}_m\rangle^+ |\tilde{1}_p\rangle^+ |\tilde{1}_i\rangle^+ |\tilde{1}_q\rangle^- |\tilde{1}_j\rangle^- \right] \\
 &+ O(\hbar^3). \tag{6.4.7b}
 \end{aligned}$$

6.4.2 Entangled two-mode states

We wish to consider a state where one cavity field mode is controlled by Alice and one by Rob. Concretely, we take

$$|\phi_{\text{init}}^\pm\rangle_{AR^+} = \frac{1}{\sqrt{2}} \left(|0_{\hat{k}}\rangle_A |0_k\rangle_R \pm |1_{\hat{k}}\rangle_A^\kappa |1_k\rangle_R^+ \right), \tag{6.4.8a}$$

$$|\phi_{\text{init}}^\pm\rangle_{AR^-} = \frac{1}{\sqrt{2}} \left(|0_{\hat{k}}\rangle_A |0_k\rangle_R \pm |1_{\hat{k}}\rangle_A^\kappa |1_k\rangle_R^- \right), \tag{6.4.8b}$$

where the superscripts \pm indicate particles or antiparticles, so that $\kappa = +$ for $\hat{k} \geq 0$ and $\kappa = -$ for $\hat{k} < 0$. Furthermore, we consider the two particle basis state of the two mode Hilbert space, corresponding to one excitation each in the modes \hat{k} in Alice's cavity and k in Rob's cavity, to be ordered as in (6.4.8). As pointed out in Ref. [67], making such a choice can lead to ambiguities in the entanglement. In fact, the fermionic Fock space is not naturally equipped with a tensor product structure. When defining vectors in the Fock space, the ordering of fermionic operators is uniquely defined upto an overall sign difference. In our case, the ambiguity amounts to a relative phase shift of π , i.e., a sign change, in (6.4.8), which does not affect the amount of entanglement. In other words, the states (6.4.8) are pure, bipartite, maximally entangled states of mode \hat{k} in Alice's cavity and mode k in Rob's cavity.

We form the density matrix for each of the states (6.4.8), express the density matrix in terms of Rob's post-trip basis to order h^2 using (6.4.5) and (6.4.7), and take the partial trace over all of Rob's modes except the reference mode k . All of Rob's modes except k are thus regarded as environment, to which information is lost due to the acceleration. The relevant partial traces of Rob's matrix elements depend on the sign of the mode label k . Throughout this work, we use the notation Tr_{-k} to emphasize that we are performing a trace over all degrees of freedom (mode numbers) except k and analogously for $\text{Tr}_{-k,k'}$. For $k \geq 0$, corresponding to (6.4.8a), we find

$$\text{Tr}_{-k} |0_k\rangle \langle 0_k| = (1 - f_k^-) |\tilde{0}_k\rangle \langle \tilde{0}_k| + f_k^- |\tilde{1}_k\rangle \langle \tilde{1}_k|, \quad (6.4.9a)$$

$$\text{Tr}_{-k} |0_k\rangle \langle 1_k| = \left(G_k + \mathcal{A}_{kk}^{(2)}\right) |\tilde{0}_k\rangle \langle \tilde{1}_k|, \quad (6.4.9b)$$

$$\text{Tr}_{-k} |1_k\rangle \langle 1_k| = (1 - f_k^+) |\tilde{1}_k\rangle \langle \tilde{1}_k| + f_k^+ |\tilde{0}_k\rangle \langle \tilde{0}_k|, \quad (6.4.9c)$$

where we have used (6.3.22) and introduced the abbreviations

$$f_k^+ := \sum_{p \geq 0} |\mathcal{A}_{pk}^{(1)}|^2, \quad f_k^- := \sum_{q < 0} |\mathcal{A}_{qk}^{(1)}|^2. \quad (6.4.10)$$

For $k < 0$, corresponding to (6.4.8b), we find similarly

$$\text{Tr}_{-k} |0_k\rangle \langle 0_k| = (1 - f_k^+) |\tilde{0}_k\rangle \langle \tilde{0}_k| + f_k^+ |\tilde{1}_k\rangle \langle \tilde{1}_k|, \quad (6.4.11a)$$

$$\text{Tr}_{-k} |0_k\rangle \langle 1_k| = \left(G_k^* + \mathcal{A}_{kk}^{(2)*}\right) |\tilde{0}_k\rangle \langle \tilde{1}_k|, \quad (6.4.11b)$$

$$\text{Tr}_{-k} |1_k\rangle \langle 1_k| = (1 - f_k^-) |\tilde{1}_k\rangle \langle \tilde{1}_k| + f_k^- |\tilde{0}_k\rangle \langle \tilde{0}_k|. \quad (6.4.11c)$$

6.4.3 States with entanglement between opposite charges

We finally consider the state in the initial region of the form

$$|\chi_{\text{init}}^\pm\rangle_{AR} = \frac{1}{\sqrt{2}} \left(|1_k\rangle_A^+ |1_{k'}\rangle_R^- \pm |1_{k'}\rangle_A^- |1_k\rangle_R^+ \right), \quad (6.4.12)$$

where the meaning of the subscripts and superscripts is as described for Eq. (6.4.8), indicating that $k \geq 0$ and $k' < 0$. In this state Alice and Rob each have access to both of the modes k and k' , and the entanglement is in the *charge* of the field modes, similarly to the states considered in [60]. While superselection rules do not allow for states with linear combinations of different charges, our cavity scenario does not lead to inconsistencies. In fact, it is easy to see that the state (6.4.12) is not a superposition of different charges in any of the cavities.

We form the reduced density matrix to order h^2 as in Sec. 6.4.2, but now the partial tracing over Rob's modes excludes both mode k and mode k' . The relevant matrix

elements take the form

$$\begin{aligned} \text{Tr}_{-k,k'} |1_{k'}\rangle\langle 1_{k'}| &= f_{k'}^- |\tilde{0}_k\rangle\langle 0_{k'}| \langle \tilde{0}_{k'}| \langle \tilde{0}_k| + (1 - f_{k'}^- - f_k^- + |\mathcal{A}_{kk'}^{(1)}|^2) |\tilde{0}_k\rangle\langle 1_{k'}| \langle \tilde{1}_{k'}| \langle \tilde{0}_k| \\ &+ (f_k^- - |\mathcal{A}_{kk'}^{(1)}|^2) |\tilde{1}_k\rangle\langle 1_{k'}| \langle \tilde{1}_{k'}| \langle \tilde{1}_k| + \left(\sum_{q<0} G_k G_{k'}^* \mathcal{A}_{qk}^{(1)*} \mathcal{A}_{qk'}^{(1)} |\tilde{0}_k\rangle\langle 0_{k'}| \langle \tilde{0}_{k'}| \langle \tilde{1}_k| + h.c. \right), \end{aligned} \quad (6.4.13a)$$

$$\begin{aligned} \text{Tr}_{-k,k'} |1_k\rangle\langle 1_k| &= f_k^+ |\tilde{0}_k\rangle\langle 0_{k'}| \langle \tilde{0}_{k'}| \langle \tilde{0}_k| + (1 - f_{k'}^+ - f_k^+ + |\mathcal{A}_{kk'}^{(1)}|^2) |\tilde{1}_k\rangle\langle 0_{k'}| \langle \tilde{0}_{k'}| \langle \tilde{1}_k| \\ &+ (f_{k'}^+ - |\mathcal{A}_{kk'}^{(1)}|^2) |\tilde{1}_k\rangle\langle 1_{k'}| \langle \tilde{1}_{k'}| \langle \tilde{1}_k| - \left(\sum_{p\geq 0} G_k G_{k'}^* \mathcal{A}_{pk}^{(1)*} \mathcal{A}_{pk'}^{(1)} |\tilde{0}_k\rangle\langle 0_{k'}| \langle \tilde{0}_{k'}| \langle \tilde{1}_k| + h.c. \right), \end{aligned} \quad (6.4.13b)$$

$$\text{Tr}_{-k,k'} |1_k\rangle\langle 1_{k'}| = \left(G_k^* G_{k'}^* |\mathcal{A}_{kk'}^{(1)}|^2 + \mathcal{A}_{kk}^* \mathcal{A}_{k'k'}^* \right) |\tilde{1}_k\rangle\langle 0_{k'}| \langle \tilde{0}_{k'}| \langle \tilde{1}_k|, \quad (6.4.13c)$$

where in (6.4.13c) $\mathcal{A}_{kk}^* \mathcal{A}_{k'k'}^*$ is kept only to order h^2 in the small h expansion

$$\mathcal{A}_{kk}^* \mathcal{A}_{k'k'}^* = G_k^* G_{k'}^* + G_{k'}^* \mathcal{A}_{kk}^{(2)*} + G_k^* \mathcal{A}_{k'k'}^{(2)*} + O(h^3). \quad (6.4.14)$$

6.5 Entanglement degradation and nonlocality

We are now in a position to study the entanglement and the nonlocality of the states after Rob has undergone his trip.

6.5.1 Entanglement of two-mode states

Consider the states $|\phi_{\text{init}}^\pm\rangle_{AR+}$ and $|\phi_{\text{init}}^\pm\rangle_{AR-}$ (6.4.8), in which Alice and Rob control one mode each. We shall quantify the entanglement by the negativity \mathcal{N} (2.3.19) and the nonlocality by a possible violation of the CHSH inequality [62, 63].

The unperturbed part of $\rho_{AR\pm}^{\pm PT}$ has the triply degenerate eigenvalue $\frac{1}{2}$ and the non-degenerate eigenvalue $-\frac{1}{2}$. In a perturbative treatment the positive eigenvalues remain positive and the only correction to the negativity comes from the perturbative correction to the negative eigenvalue. A straightforward computation using (6.4.9) and (6.4.11) shows that the leading correction to the negativity comes in order h^2 , and to this order the negativity formula reads

$$\mathcal{N}[\rho_{AR\pm}^\pm] = \frac{1}{2} (1 - f_k) \quad (6.5.1)$$

where $f_k := f_k^+ + f_k^-$ and f_k can be expressed as

$$f_k = \sum_{p=-\infty}^{\infty} |E_1^{k-p} - 1|^2 |\mathcal{A}_{kp}^{(1)}|^2 = 2[Q(2k+s, 1) - Q(2k+s, E_1)] h^2, \quad (6.5.2)$$

where

$$Q(\alpha, z) := \frac{2}{\pi^4} \operatorname{Re} \left[\alpha^2 \left(\operatorname{Li}_6(z) - \frac{1}{64} \operatorname{Li}_6(z^2) \right) + \operatorname{Li}_4(z) - \frac{1}{16} \operatorname{Li}_4(z^2) \right], \quad (6.5.3)$$

the function Li is the polylogarithm (see [21]) and

$$E_1 := \exp \left(\frac{i\pi\eta_1}{\ln(b/a)} \right) = \exp \left(\frac{i\pi h\tau_1}{2\delta \operatorname{arctanh}(h/2)} \right). \quad (6.5.4)$$

We see from (6.5.1) that acceleration does degrade the initially maximal entanglement, and the degradation is determined by the function f_k (6.5.2). f_k is periodic in τ_1 with period

$$2\delta(h/2)^{-1} \operatorname{arctanh}(h/2), \quad (6.5.5)$$

that is the proper time measured at the centre of Rob's cavity between sending and recapturing a light ray that is allowed to bounce off each wall once. f_k is non-negative, and it vanishes only at integer multiples of the period. f_k is not an even function of k for generic values of s , but it is even in k in the limiting case $s = 0$ in which the spectrum is symmetric between positive and negative charges. f_k diverges at large $|k|$ proportionally to k^2 , and the domain of validity of our perturbative analysis is

$$|k|h \ll 1. \quad (6.5.6)$$

Plots for $k = \pm 1$ are shown in Fig. 6.2.

We now turn to nonlocality, as quantified by the violation of the CHSH inequality [62, 63]

$$|\langle \mathcal{B}_{\text{CHSH}} \rangle_\rho| \leq 2, \quad (6.5.7)$$

where $\mathcal{B}_{\text{CHSH}}$ is the bipartite observable

$$\mathcal{B}_{\text{CHSH}} := \mathbf{a} \cdot \underline{\sigma} \otimes (\mathbf{b} + \mathbf{b}') \cdot \underline{\sigma} + \mathbf{a}' \cdot \underline{\sigma} \otimes (\mathbf{b} - \mathbf{b}') \cdot \underline{\sigma}, \quad (6.5.8)$$

\mathbf{a} , \mathbf{a}' , \mathbf{b} and \mathbf{b}' are unit vectors in \mathbb{R}^3 , and $\underline{\sigma}$ is the vector of the Pauli matrices. The inequality (6.5.7) is satisfied by all local realistic theories, but quantum mechanics allows the left-hand side to take values up to $2\sqrt{2}$. The violation of (6.5.7) is hence a sufficient (although not necessary [48, 68]) condition for the quantum state to be entangled.

To look for violations of (6.5.7), we proceed as in [48], noting that the maximum value of the left-hand-side in the state ρ is given by [63]

$$\langle \mathcal{B}_{\text{max}} \rangle_\rho = 2\sqrt{\mu_1 + \mu_2}, \quad (6.5.9)$$

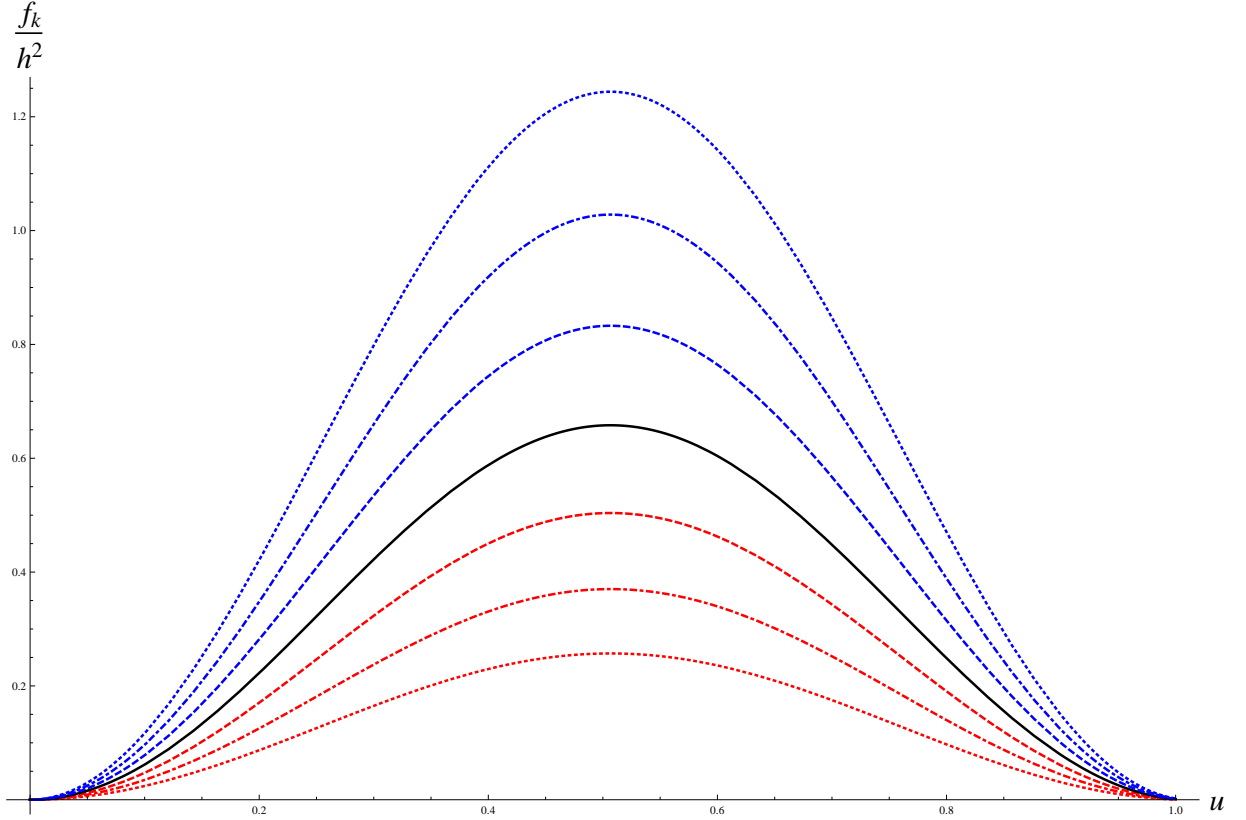


Figure 6.2: The plot shows f_k/h^2 as a function of $u := \frac{1}{2}\eta_1/\ln(b/a) = h\tau_1/[4\delta\text{arctanh}(h/2)]$, over the full period $0 \leq u \leq 1$. The solid curve (black) is for $s = 0$ with $k = \pm 1$. The dashed, dash-dotted and dotted curves are respectively for $s = \frac{1}{4}$, $s = \frac{1}{2}$ and $s = \frac{3}{4}$, for $k = 1$ above the solid curve and for $k = -1$ below the solid curve.

where μ_1 and μ_2 are the two largest eigenvalues of the matrix $U(\rho) = T_\rho^T T_\rho$ and the elements of the correlation matrix $T = (t_{ij})$ are given by $t_{ij} = \text{Tr}[\rho \sigma_i \otimes \sigma_j]$. In our scenario

$$U(\rho_{AR\pm}^\pm) = \begin{pmatrix} 1 - f_k & 0 & 0 \\ 0 & 1 - f_k & 0 \\ 0 & 0 & \frac{1}{4} - f_k \end{pmatrix} + O(h^4), \quad (6.5.10)$$

and working to order h^2 we hence find

$$\langle \mathcal{B}_{\max} \rangle_{\rho_{AR\pm}^\pm} = 2\sqrt{2} \left(1 - \frac{1}{2}f_k \right). \quad (6.5.11)$$

The acceleration thus degrades the initially maximal violation of the CHSH inequality, and the degradation is again determined by the function f_k . Such effect arises again because of the coherence introduced by the BVT between the inertial cavity and the modes within the cavity different from k .

6.5.2 Entanglement between opposite charges

We finally turn to the entanglement between opposite charges in the state (6.4.12).

Expressing the density matrix in the post-trip basis, tracing over Rob's unobserved modes and working perturbatively to order \hbar^2 , we find that the only nonvanishing elements of the reduced density matrix are within a 6×6 block. Partially transposing Rob's subsystem replaces the last lines in (6.4.13a) and (6.4.13b) by their respective conjugates and shifts the particle-antiparticle off-diagonals (6.4.13c) away from the diagonal. The only nonvanishing elements of the partial transpose are thus within an 8×8 block, which decomposes further into two 3×3 blocks that correspond respectively to (6.4.13a) and (6.4.13b) and the 2×2 block

$$\pm \frac{1}{2} \begin{pmatrix} 0 & G_k G_{k'} |\mathcal{A}_{kk'}^{(1)}|^2 + \mathcal{A}_{kk} \mathcal{A}_{k'k'} \\ G_k^* G_{k'}^* |\mathcal{A}_{kk'}^{(1)}|^2 + \mathcal{A}_{kk}^* \mathcal{A}_{k'k'}^* & 0 \end{pmatrix}, \quad (6.5.12)$$

where the off-diagonal components are kept only to order \hbar^2 in their small \hbar expansion (6.4.14).

The only negative eigenvalue comes from the 2×2 block (6.5.12). We find that \mathcal{N} is given by

$$\mathcal{N}[\rho_\chi^\pm] = \frac{1}{2} - \frac{1}{4} \sum_{p \neq k'} |\mathcal{A}_{kp}^{(1)}|^2 - \frac{1}{4} \sum_{p \neq k} |\mathcal{A}_{k'p}^{(1)}|^2 = \frac{1}{2} - \frac{1}{4} (f_k + f_{k'}) + \frac{1}{2} |E_1^{k-k'} - 1|^2 |\mathcal{A}_{kk'}^{(1)}|^2. \quad (6.5.13)$$

The entanglement is hence again degraded by the acceleration, and the degradation has the same periodicity in τ_1 as in the cases considered above. The degradation now depends however on k and k' not just through the individual functions f_k and $f_{k'}$ but also through the term proportional to $|\mathcal{A}_{kk'}^{(1)}|^2$ in (6.5.13): this interference term is nonvanishing iff k and k' have different parity, and when it is nonvanishing, it diminishes the degradation effect. In the charge-symmetric special case of $s = 0$ and $k = -k'$, the degradation coincides with that found in (6.5.1) for the two-mode states (6.4.8).

6.6 One-way journey

Our analysis for the trajectory followed by Rob that comprises being inertial, uniformly accelerating and traveling inertial again can be generalised in a straightforward way to any trajectory obtained by grafting inertial and uniformly-accelerated segments, with arbitrary durations and proper accelerations. The only delicate point is that the phase conventions of our mode functions distinguish the left boundary of the cavity

from the right boundary, and in Sec. 6.3 we set up the Bogoliubov transformation from Minkowski to Rindler assuming that the acceleration is to the right. It follows that the Bogoliubov transformation from Minkowski to leftward-accelerating Rindler is obtained from that in Sec. 6.3 by inserting the appropriate phase factors, $A_{mn} \rightarrow (-1)^{m+n} A_{mn}$, and in the expansions (6.3.8) this amounts to the replacement $h \rightarrow -h$.

As an example, consider Rob's cavity trajectory that starts inertial, accelerates to the right for proper time τ_1 as above, coasts inertially for proper time τ_2 and finally performs a braking manoeuvre that is the reverse of the initial acceleration, ending in an inertial state that has vanishing velocity with respect to the initial inertial state. Denoting the mode functions in the final inertial state by $\tilde{\psi}_n$, and writing

$$\tilde{\psi}_m = \sum_n \mathcal{B}_{mn} \psi_n, \quad (6.6.1)$$

we find

$$|\mathcal{B}_{mn}^{(1)}|^2 = |E_1^{m-n} - 1|^2 |(E_1 E_2)^{m-n} - 1|^2 |A_{mn}^{(1)}|^2 \quad (6.6.2)$$

where $E_2 := \exp(i\pi\tau_2/\delta)$. For the two-mode initial states $|\phi_{\text{init}}^\pm\rangle_{AR+}$ and $|\phi_{\text{init}}^\pm\rangle_{AR-}$ (6.4.8), the negativity and the maximum violation of the CHSH inequality hence read respectively

$$\mathcal{N}[\rho_{AR\pm}^\pm] = \frac{1}{2} (1 - \tilde{f}_k), \quad (6.6.3a)$$

$$\langle \mathcal{B}_{\text{max}} \rangle_{\rho_{AR\pm}^\pm} = 2\sqrt{2} \left(1 - \frac{1}{2} \tilde{f}_k \right), \quad (6.6.3b)$$

where

$$\begin{aligned} \tilde{f}_k &= \sum_{p=-\infty}^{\infty} |\mathcal{B}_{kp}^{(1)}|^2 \\ &= 2 \left[2Q(2k+s, 1) - 2Q(2k+s, E_1) + Q(2k+s, E_2) - 2Q(2k+s, E_1 E_2) + Q(2k+s, E_1^2 E_2) \right] h^2. \end{aligned} \quad (6.6.4)$$

The negativity in the state $|\chi_{\text{init}}^\pm\rangle_{AR}$ (6.4.12) reads

$$\mathcal{N}[\rho_\chi^\pm] = \frac{1}{2} - \frac{1}{4} (\tilde{f}_k + \tilde{f}_{k'}) + \frac{1}{2} |E_1^{k-k'} - 1|^2 |(E_1 E_2)^{k-k'} - 1|^2 |A_{kk'}^{(1)}|^2. \quad (6.6.5)$$

The degradation caused by acceleration is thus again periodic in τ_1 with period

$$2\delta(h/2)^{-1} \operatorname{atanh}(h/2), \quad (6.6.6)$$

and it is periodic in τ_2 with period 2δ . The degradation vanishes iff $E_1 = 1$ or $E_1 E_2 = 1$, so that any degradation caused by the accelerated segments can be cancelled by fine-tuning the duration of the inertial segment, to the order h^2 in which we are working. A plot of \tilde{f}_k is shown in Fig. 6.3.

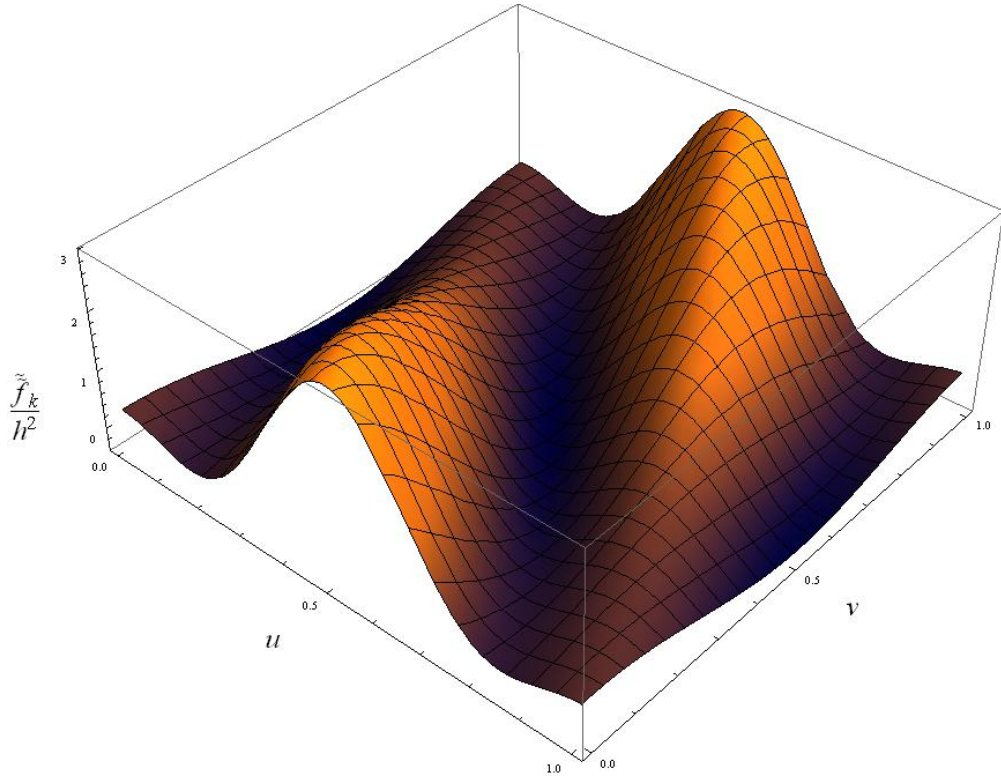


Figure 6.3: The plot shows \tilde{f}_k as a function of $u := h\tau_1/[4\delta \operatorname{atanh}(h/2)]$ and $v := \tau_2/(2\delta)$ over the full period $0 \leq u \leq 1$ and $0 \leq v \leq 1$, for $s = 0$ and $k = 1$. Note the zeroes at $u \equiv 0 \pmod{1}$ and at $u + v \equiv 0 \pmod{1}$.

6.7 Conclusions

We have employed the machinery developed in the previous chapter to analyse the entanglement degradation for a massless Dirac field between two cavities in $(1+1)$ -dimensional Minkowski spacetime, one cavity inertial and the other moving along some “arbitrary” trajectory (that can be obtained by composing segments of inertial coasting and uniform acceleration). Working in the approximation of small accelerations but arbitrarily long travel times, we found that the degradation is qualitatively similar to that found in Chapter 5. The degradation is periodic in the durations of the individual inertial and accelerated segments, and we identified a travel scenario where the degradation caused by accelerated segments can be undone by fine-tuning the duration of an inertial segment. The presence of charge allows however a wider range of initial states of interest to be analysed. As an example, we identified a state where the entanglement degradation contains a contribution due to interference between excitations of opposite charge.

Compared with bosons, working in a fermionic Fock space led both to technical simplifications and complications. A technical simplification was that the relevant reduced density matrices act in a lower-dimensional Hilbert space because of the fermionic

statistics, and this made it possible to quantify the entanglement not just in terms of the negativity but also in terms of the CHSH inequality.

A technical complication was that when the boundary conditions at the cavity walls were chosen in an arguably natural way that preserves charge conjugation symmetry, the spectrum contained a zero mode. This zero mode could not be consistently omitted by hand, but we were able to regularise the zero mode by treating the charge-symmetric boundary conditions as a limiting case of charge-nonsymmetric boundary conditions. All our entanglement measures remained manifestly well defined when the regulator was removed.

Another technical complication occurring for fermions is the ambiguity [67] in the choice of the basis of the two-fermion Hilbert space in (6.4.13). An alternative valid choice of basis is obtained by reversing the order of the single particle kets in (6.4.13), which amounts to a change of the signs in the off-diagonal elements of (6.4.13a) and (6.4.13b). While our treatment does not remove this ambiguity, all of our results for the entanglement and the nonlocality of these states are independent of the chosen convention.

Our analysis contained two significant limitations. First, while our Bogoliubov transformation technique can be applied to arbitrarily complicated graftings of inertial and uniformly accelerated cavity trajectory segments, the treatment is perturbative in the accelerations and hence valid only in the small acceleration limit. We were thus not able to address the large acceleration limit, in which striking qualitative differences between bosonic and fermionic entanglement have been found for field modes that are not confined in cavities [5, 7, 15, 48, 60].

Second, a massless fermion in a $(1+1)$ -dimensional cavity is unlikely to be a good model for systems realisable in a laboratory. A fermion in a linearly-accelerated rectangular cavity in $(3+1)$ dimensions can be reduced to the $(1+1)$ -dimensional case by separation of variables, but for generic field modes the transverse quantum numbers then contribute to the effective $(1+1)$ -dimensional mass; further, any foreseeable experiment would presumably need to use fermions that have a positive mass already in $(3+1)$ dimensions before the reduction. It would be possible to analyse our $(1+1)$ -dimensional system for a massive fermion, and we anticipate that the mass would enhance the magnitude of the entanglement degradation as in the bosonic situation.

We stress that the maximum value of h allowed within the perturbative regime is no greater than 0.01.

CHAPTER 7

Generation of entanglement within
a moving cavity

In the previous chapters we have shown that maximally entangled states of bosonic or fermionic fields confined in (two) cavities are affected by the non inertial motion of one of the cavities. In particular, the entanglement is degraded and we were able to quantify the magnitude of the degradation and its dependence on the different travels scenarios.

It is natural to ask at this point if relativistic effects in this context only degrade the initial entanglement. Such effect would imply that communication protocols that use cavity mode entanglement as a resource would never be improved by the motion of cavities through spacetime. We wish to understand if any entanglement can be created at all through motion and to quantify it.

In this chapter we investigate entanglement creation between different modes of a bosonic and fermionic quantum field confined in a single cavity when the initial state is pure and separable in the field mode degree of freedom. We develop a general quantitative analysis for a scalar field and we refer for the complete work available in [69] for the complete parallel analysis of fermionic field. We give detailed results for a sample travel scenario and mention that the particle statistics has a significant effect on the entanglement.

We work in $(1 + 1)$ -dimensional Minkowski space: additional transverse dimensions can be included via their contribution to the effective field mass as already explained. The length of the cavity in its instantaneous rest frame is again $\delta > 0$. The cavity is assumed to be inertial outside a finite time interval, but the initial and final velocities need not coincide.

In this Chapter we will address matters regarding how to detect entanglement creation but not how to extract the entanglement that is created. Such goals are part of research in progress.

7.1 Bosons

7.1.1 Cavity configuration

We consider the setting of chapter 5 for a massive scalar field Φ . Let $\{\phi_n \mid n = 1, 2, \dots\}$ be a complete orthonormal set of mode solutions that are of positive frequency with respect to the cavity's proper time at early times (pre-trip), and let $\{\tilde{\phi}_n \mid n = 1, 2, \dots\}$ be a similar set at late times (post-trip). Each set has an associated set of creation and annihilation operators, with the commutation relations

$$[a_n, a_m^\dagger] = [\tilde{a}_n, \tilde{a}_m^\dagger] = \delta_{nm} \quad (7.1.1)$$

and a vacuum state, denoted respectively by $|0\rangle$ and $|\tilde{0}\rangle$. The two sets of modes are related by the BVT encoded in the matrix \mathcal{A} while the set of operators are related by the BVT encoded in the matrix \mathcal{A}^{-1} .

The vacua are related by (5.1.30) and (5.1.31) as usual.

7.1.2 Pre-trip preparation

We prepare the system in the pre-trip region in a separable state in the mode degree of freedom. We ask: does the cavity's motion generate mode entanglement when analyzed in the post-trip region, where the particle content of the state has changed?

To answer this question we proceed as follows. We first specify the pre-trip region state and express it in the post-trip basis using (5.1.30) and subsequent equations. We then use equation (2.2.49) to express the BVT between the pre-trip modes and the post-trip modes. These allow us to rewrite the part of the initial state possessed by Rob in terms of post-trip excitations.

We then trace over all post-trip modes except those labelled by two distinct quantum numbers k and k' . We quantify the entanglement in the resulting reduced density matrix by the negativity \mathcal{N} (2.3.19).

As usual, the proper acceleration at Rob's cavity centre is proportional to h/δ . We then work perturbatively in h and we can write the relation between the different vacua to order h^2 . Then

$$N = 1 - \frac{1}{4} \sum_{p,q} |V_{pq}^{(1)}|^2 \quad (7.1.2)$$

and

$$|0\rangle = \left(1 - \frac{1}{4} \sum_{pq} |V_{pq}^{(1)}|^2\right) |\tilde{0}\rangle + \frac{1}{2} \sum_{pq} V_{pq} \tilde{a}_p^\dagger \tilde{a}_q^\dagger |\tilde{0}\rangle + \frac{1}{8} \sum_{pqij} V_{pq}^{(1)} V_{ij}^{(1)} \tilde{a}_p^\dagger \tilde{a}_q^\dagger \tilde{a}_i^\dagger \tilde{a}_j^\dagger |\tilde{0}\rangle + O(h^3). \quad (7.1.3)$$

7.1.3 Initial state: $|0\rangle$

As a first example, we take the in-region state to be the in-vacuum $|0\rangle$.

To order h^2 , the partially-transposed reduced density matrix vanishes outside a 6×6 block. Among the six eigenvalues, the only possibly negative ones are

$$\lambda_4 = -|B_{kk'}^{(1)}|^2, \quad (7.1.4a)$$

$$\lambda_6 = f_{k-k'}^\beta + f_{k'-k}^\beta - \left((f_{k-k'}^\beta - f_{k'-k}^\beta)^2 + |V_{kk'}|^2 \right)^{1/2}, \quad (7.1.4b)$$

where

$$f_{m-n}^\beta := \frac{1}{2} \sum_{q \neq n} |B_{qm}^{(1)}|^2 \quad (7.1.5)$$

and $V_{kk'}$ is kept to order h^2 . λ_4 arises from coherence between $|\tilde{0}\rangle$ and $|\tilde{1}_k\rangle|\tilde{1}_{k'}\rangle$, while λ_6 arises from coherence between $|\tilde{0}\rangle$ and $|\tilde{2}_k\rangle|\tilde{2}_{k'}\rangle$.

Specialising to the usual travel scenario that is composed of inertial and uniformly-accelerated segments, we find that a qualitative difference emerges depending on the relative parity of k and k' . If k and k' have opposite parity, the expansions (5.1.22) show that ${}_o\beta_{kk'}^{(1)}$ is nonvanishing but $V_{kk'}^{(2)} = 0$. It follows that

$$|V_{kk'}|^2 = |B_{kk'}^{(1)}|^2 + O(h^4). \quad (7.1.6)$$

The leading term in the negativity is then *linear* in h and given by $|B_{kk'}^{(1)}|$. If, by contrast, k and k' have the same parity, we have $B_{kk'}^{(1)} = 0$ and $V_{kk'} = V_{kk'}^{(2)} + O(h^3)$. The leading term in the negativity comes then from λ_6 and is of order h^2 . Sample negativity plots for both cases are shown in Fig. 7.1 for a massless field and the BBB travel scenario.

7.1.4 Initial state: $|1_k\rangle$

As a second example, we take the pre-trip state to be $|1_k\rangle$, containing exactly one in-particle. Using (7.1.3) we find

$$\begin{aligned} |1_k\rangle &= \sum_m \left(A_{mk}^* + \sum_p B_{pk}^{(1)} V_{pm}^{(1)} - \frac{1}{4} \delta_{mk} G_k^* \sum_{pq} |V_{pq}^{(1)}|^2 \right) \tilde{a}_m^\dagger |\tilde{0}\rangle \\ &+ \frac{1}{2} \sum_{mpq} \left(A_{mk}^* + G_k^* \delta_{mk} \right) V_{pq} \tilde{a}_m^\dagger \tilde{a}_p^\dagger \tilde{a}_q^\dagger |\tilde{0}\rangle \\ &+ \frac{1}{8} G_k^* \sum_{pqij} V_{pq} V_{ij} \tilde{a}_k^\dagger \tilde{a}_p^\dagger \tilde{a}_q^\dagger \tilde{a}_i^\dagger \tilde{a}_j^\dagger |\tilde{0}\rangle + O(h^3). \end{aligned} \quad (7.1.7)$$

To order h^2 , the partially-transposed reduced density matrix now vanishes outside an 8×8 block. Among the first five eigenvalues, the only possibly negative one is

$$\mu_3 = -\sqrt{3} |B_{kk'}^{(1)}|^2, \quad (7.1.8)$$

which arises from coherence between $|\tilde{1}_k\rangle$ and $|\tilde{3}_k\rangle|\tilde{2}_{k'}\rangle$. The last three eigenvalues are the roots of a cubic polynomial, analytically cumbersome for generic values of the parameters but readily amenable to numerical work.

Specialising to a cavity worldtube that is grafted from inertial and uniformly-accelerated segments, we again find a qualitative difference depending on the relative parity of k

and k' . In particular, if k and k' have opposite parity, the leading contribution to negativity comes from the eigenvalue

$$\mu_8 = -\sqrt{|A_{kk'}^{(1)}|^2 + 2|B_{kk'}^{(1)}|^2} \quad (7.1.9)$$

and is *linear* in h . The negativity is in this case higher than the corresponding negativity for the in-region state $|0\rangle$. We have found that this is a common feature of the results in the cavity settings. The physical reason for this phenomenon is yet not completely understood. Sample negativity plots are shown in Fig. 7.1 for a massless field for the BBB travel scenario.

Fermions

The analysis for fermionic modes has been pursued by N. Friis at Nottingham. For a more detailed analysis we refer to [69].

7.2 Conclusions

We have demonstrated that non-uniform motion of a cavity generates entanglement between modes of a bosonic quantum field confined to the cavity. Working to quadratic order in the cavity's acceleration, and quantifying the entanglement by the negativity, we found that the entanglement generation depends on the initial state of the field, on the relative parity of the mode pair that is observed at late times and from [69] we know it depends also on the bosonic versus fermionic statistics. For both bosons and fermions, we found situations where the entanglement generation can be enhanced by placing particles in the initial state. For fermions, however, charge conservation and the Pauli exclusion principle require the choice of the considered out-region modes to be consistent with the initial state to generate entanglement, while the bosonic statistics allow the modes to be freely populated without hindering entanglement generation.

Compared with the motion-induced entanglement degradation between a static cavity and a moving cavity analyzed in Chapters 5 and 6, we found that the entanglement generation can occur already in linear order in the cavity's acceleration, while the entanglement degradation is a second-order effect. The prospects of experimental verification [58] could hence be significantly better for phenomena signalling entanglement generation than entanglement degradation. Experimental proposals in this direction are currently under investigation.

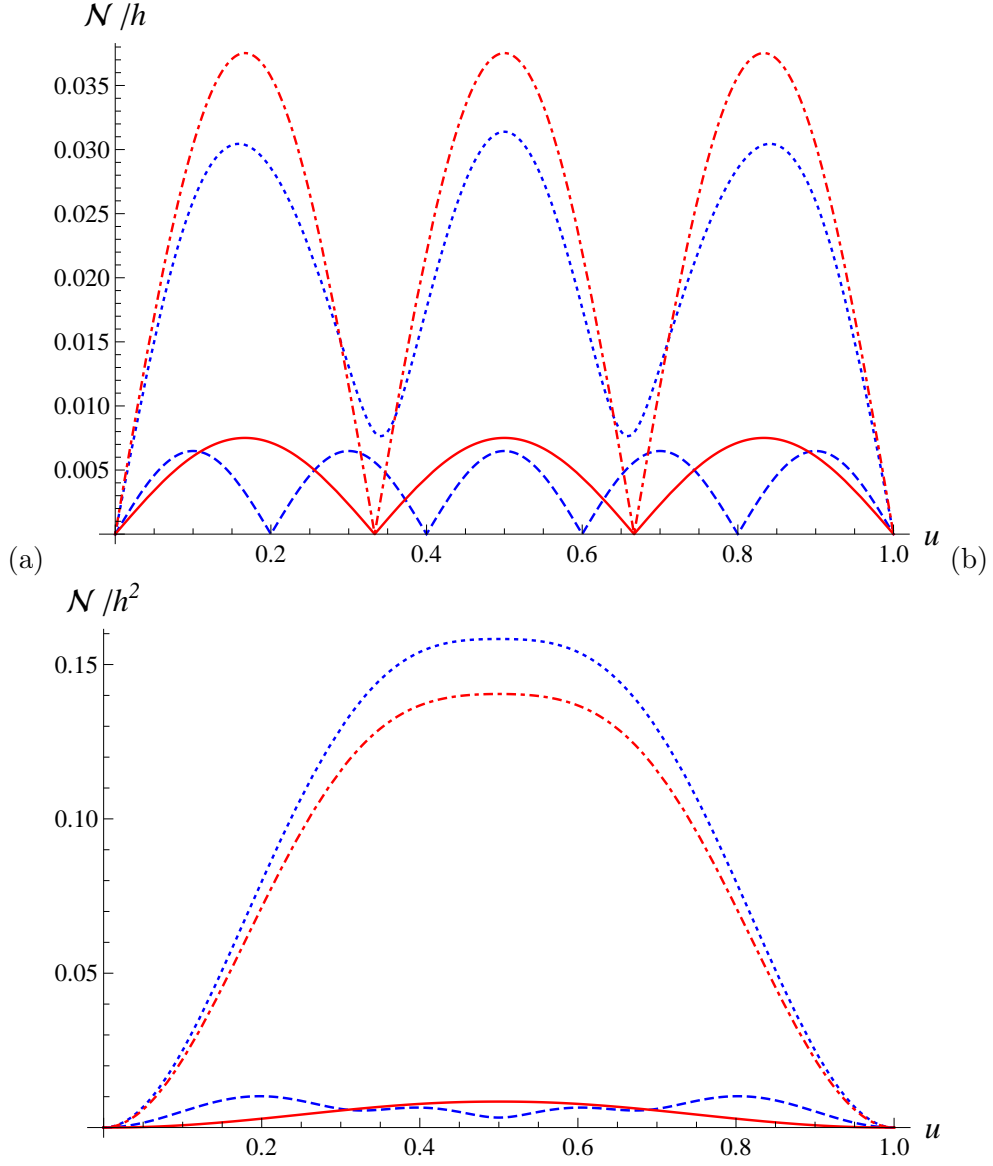


Figure 7.1: The leading order contribution to the negativity is shown for a massless scalar field and a massless Dirac field. The travel scenario has a single accelerated segment, of acceleration h/δ as measured at the cavity's centre and of duration $\tau = (4\delta/h) \operatorname{atanh}(h/2)u$ in the cavity's proper time τ . The negativity is periodic in u with period 1. Fig. 7.1(a) shows \mathcal{N}/h , in dashed for a scalar field with in-region vacuum and $(k, k') = (1, 4)$, in dotted for a scalar field with in-region state $|1_k\rangle$ and $(k, k') = (1, 4)$, in solid for a Dirac field with in-region vacuum and $(\kappa, \kappa') = (2, -1)$ with $s = 0$, and in dotted-dashed for a Dirac field with in-region state $\|1_\kappa\rangle\rangle$ and $(\kappa, \hat{\kappa}) = (1, 4)$ with $s = 0$ in the notation of Chapter 6. Fig. 7.1(b) shows the corresponding curves for \mathcal{N}/h^2 with the scalar field modes $(k, k') = (1, 3)$ and the fermionic modes $(\kappa, \kappa') = (1, -1)$ and $(\kappa, \hat{\kappa}) = (1, 3)$.

The motion-induced entanglement effects that we have analysed have technical similarities with the creation of squeezed states in resonators with oscillating walls, known as the dynamical Casimir effect [70, 71]. In this context, we emphasize that our only approximation was to work in the small acceleration regime, meaning that the product of the cavity's length and acceleration is small compared with the speed of light squared [58, 72]. Our analysis hence covers as a special case cavities that oscillate rapidly with a small amplitude: such cavities are often introduced in theoretical analyses of the dynamical Casimir effect but are experimentally problematic [70].

Our analysis however covers also cavities that accelerate in a given direction for finite but arbitrarily long times, with travel distances that may be arbitrarily large. Further, as the equivalence principle implies that gravitational acceleration can be locally modeled by acceleration in Minkowski space-time, our results suggest that a gravitational field can produce entanglement. Experiments for entanglement generation could hence be sought in setups that span macroscopic distances, including quantum communication through near-Earth satellite orbits.

CHAPTER 8

**Entanglement resonances within a
moving cavity**

In the previous Chapters we have analyzed how motion of cavities through spacetime degrades entanglement between initially entangled modes of quantum fields contained in two separate cavities or creates entanglement between modes of a quantum field within a single cavity. We found a regime where we could explicitly compute the decrease or increase of the negativity as a function of the acceleration of the cavity h (normalized to the width of the cavity itself) and the time of acceleration. In particular, we showed that the degradation and creation effects are typically of second order in h ; in some cases, creation effects can occur to first order in h . Although it appears that the influence of motion of devices is negligible, it is of paramount interest to show that such effects are of impact when considering quantum communication protocols. It would therefore be fundamental to find a situation where they can be greatly enhanced.

In this Chapter we introduce the mathematical techniques that allow us to efficiently study entanglement for different travel scenarios avoiding cumbersome analytical computations as presented in the previous chapters. We work in the small h regime. We start by developing the “two mode truncation” (TMT) which allows us to consider only two arbitrary modes of the energy spectrum of the field contained within a cavity and to effectively reduce the full BVT between all the modes to BVT between these two modes only. We show that this can occur up to corrections to third order in h . The BVT are Gaussian transformations since they are exponentials of quadratic operators. If we start from Gaussian states, for example the vacuum or squeezed states, we find that the natural language to use in our problem is that of Covariance Matrices (CM) within the formalism of Continuous Variables (CV). Gaussian states and gaussian transformations are represented by finite dimensional matrices (for an extensive introduction see [73] and references therein) and there are many manageable tools within the formalism that allow for computation of entanglement.

We proceed to show that one can pick an arbitrary travel scenario, called building block. In general, by repeating the building block any number of times it is possible to fine-tune the total duration of the single building block such that entanglement generated at the end of the trip grows linearly with the number of repetitions. We find analytical conditions for such phenomenon to occur and show that as a particular case we can describe dynamical Casimir-like scenarios where the cavity oscillates as a whole. The importance of our results is emphasized by the following: a resonant enhancement of particle creation occurs in the dynamical Casimir effect [71] which was recently demonstrated in the laboratory in a superconducting circuit consisting of a coplanar transmission line with a tunable electrical length which produces an effective moving boundary [13]. Two-mode squeezed states were detected in the radiation emitted in this

experiment. Previously it was shown that single-mode squeezed states, which contain no entanglement, can also be produced in these scenarios [71].

8.1 Setup and development of the Two Mode Truncation technique

In this chapter we consider a real massless scalar field Φ confined in (1+1)-dimensional cavity in Minkowski spacetime, with Dirichlet boundary conditions modeling the walls. Transverse dimensions can be included as a positive contribution to μ as usual and the field has support only inside the cavity.

We choose a set of Minkowski coordinates (t, x) to describe the cavity that is resting at times $t < 0$. The modes in the cavity are (5.1.2) labeled by $k \in \mathbb{N}$. The field is expanded as (5.1.6). When the cavity is accelerated we employ Rindler coordinates and the modes take the form (5.1.9) also labeled by natural numbers $k \in \mathbb{N}$.

To employ the full BVT, even in the perturbative regime, leads to cumbersome computations. For example, if one wishes to perform partial tracing the complexity of the operation grows extremely fast. When employable, CV techniques allow for simple and straightforward analytical results. Such techniques can be applied to efficiently solve problems when a (small) finite number of modes is used. In addition, gaussian states such as two mode squeezed states or coherent states are typical states that can be produced in laboratory. We therefore aim at finding a finite set of modes which can be treated within our perturbative regime and employ the CM formalism.

The BVT mix all modes. The matrix relation $\mathcal{A}^{-1}\mathcal{A}$ encodes the Bogoliubov identities that are satisfied by *all* the modes together. In our perturbative regime, if one picks two arbitrary modes k, k' and computes the relation $\mathcal{A}_{k,k'}^{-1}\mathcal{A}_{k,k'}$ for such two modes, this will not satisfy the standard Bogoliubov identities as in (2.2.50). This is of course expected since eliminating by hand all other modes will introduce errors in the process. A natural set of questions to ask is:

“Is there a choice of two modes that allows for BVT which mix “only” such modes to some good approximation? Is there any self consistent procedure which allows for this choice? If this is possible, to which order is it safe to ignore the errors introduced?”

In this section we will show that such questions have a positive answer. The procedure we will developed is called *two mode truncation* (TMT). We have verified that such procedure is possible *only* for modes k, k' separated by an odd integer $k - k' = 2n + 1$. In order to conserve probabilities, one cannot arbitrarily pick any number of modes and

ignore the relations between such modes and the rest without introducing errors. We wish to show that is possible to “renormalize” every mode by an appropriate factor such that for any two oddly separated modes, the Bogoliubov coefficients that relate such modes satisfy the Bogoliubov identities to second order in h . Such procedure is self consistent. This means that assuming the two modes to satisfy Bogoliubov identities after the renormalization is viable.

We proceed to develop the TMT: we multiply any mode, say ϕ_k , by a factor $1 + C_k h^2$ which just changes the normalization of the mode. We proceed to choose $\{C_k\}$ as follows: the elements of the \mathcal{A} matrix are uniquely determined by inner products of field modes. Therefore, if

$$\phi_k \longrightarrow \phi'_k = (1 + C_k h^2) \phi_k \quad (8.1.1)$$

then, using (2.2.16) one finds that

$$\mathcal{A}_{kk'} \longrightarrow \mathcal{A}'_{kk'} = (1 + \tilde{C}_k h^2 + C_{k'}^* h^2) \mathcal{A}_{kk'}, \quad (8.1.2)$$

where, in general, C_k and \tilde{C}_k need not to be equal. In fact, $\{C_k\}$ is the set of constants used to renormalize the pre-trip modes while $\{\tilde{C}_k\}$ is the set used to renormalize the post-trip modes. One can now employ (8.1.2) to analyze the effect of such renormalization on the Bogoliubov coefficients A, B . We find that

$$\begin{aligned} A_{kk'} &\rightarrow A'_{kk'} = A_{kk'} \times (1 + \tilde{C}_k h^2 + C_{k'}^* h^2) \\ B_{kk'} &\rightarrow B'_{kk'} = B_{kk'} \times (1 + \tilde{C}_k h^2 + C_{k'}^* h^2). \end{aligned} \quad (8.1.3)$$

One realizes that, since ${}_o\alpha_{k,k'}^{(1)}$ and ${}_o\beta_{k,k'}^{(1)}$ vanish for even mode separation (see (5.1.22)), one can *always choose* $\{C_k\}$ such that

$$\mathcal{A}\mathcal{A}^{-1} = \text{id} + \mathcal{O}(h^3) \quad (8.1.4)$$

for any arbitrary travel scenario. This means that the Bogoliubov identities (2.2.50) are satisfied at first and second order. The consistency of this procedure holds only for modes k, k' separated by and pod integer $k - k' = 2n + 1$.

In addition, analyzing expression (9.2.38) we notice that the operator W has the expression

$$W = - \sum_{i,j} \frac{V_{ij}}{2} a_i^\dagger a_j^\dagger, \quad (8.1.5)$$

where

$$V = B^* A^{-1}. \quad (8.1.6)$$

To first order, we notice that the contributions to V come in the form of

$$V \sim B^{(1)*} A^{(0)*} + \mathcal{O}(h^2), \quad (8.1.7)$$

where we suppress all the indices for the sake of simplicity.

Therefore, the first order corrections to the vacuum $|0\rangle$ in (9.2.38) will have the form

$$W|0\rangle \sim A^{(0)}B^{(1)}(\dots)|0\rangle, \quad (8.1.8)$$

which shows that when the TMT is employed, the vacuum is not affected by the renormalization procedure to first order.

8.2 Techniques for Gaussian states

We make the following observation: in this chapter, we analyze only two modes and employ the TMT which is a unitary operation (up to $\mathcal{O}(\hbar^3)$ corrections). All operators that will act on the states are gaussian. We can choose the initial states to be gaussian, therefore the natural formalism to employ to address this setting is the formalism of Covariance Matrices in continuous variables. In the next two subsections we explain how to translate the techniques developed in the previous three chapters into this new language.

8.2.1 Continuous variables

A *continuous variable* system is described by a Hilbert space

$$\mathcal{H} = \otimes_{i=1}^n \mathcal{H}_i \quad (8.2.1)$$

resulting from the tensor product structure of infinite dimensional Fock spaces \mathcal{H}_i 's. The operator a_i is the annihilation operator that acts on \mathcal{H}_i . We now define

$$\begin{aligned} \hat{q}_i &:= a_i + a_i^\dagger, \\ \hat{p}_i &:= \frac{1}{i} [a_i - a_i^\dagger], \end{aligned} \quad (8.2.2)$$

which are the *quadrature phase operators* and we denote the corresponding *phase-space variables* by q_i and p_i . Let us introduce

$$\hat{X} = (\hat{q}_1, \hat{p}_1, \dots, \hat{q}_n, \hat{p}_n), \quad (8.2.3)$$

which denotes the vector of the operators \hat{q}_i and \hat{p}_i . The canonical commutation relations can be expressed in terms of

$$[\hat{X}_i, \hat{X}_j] = 2i\Omega_{ij}, \quad (8.2.4)$$

where we define the *symplectic form* as

$$\Omega = \oplus_{i=1}^n \omega_i \quad (8.2.5)$$

and

$$\omega = \begin{pmatrix} 0 & 1 \\ -1 & 0 \end{pmatrix}. \quad (8.2.6)$$

The states of a CV system can be equivalently described by the density matrix or by quasi probability distributions [73]. States with Gaussian characteristic functions and quasiprobability distributions are referred to as *Gaussian states*. An example of a non gaussian state is the Fock state $|1_k\rangle$ while an example of gaussian state is a coherent state. We introduce the vector of first moments

$$\bar{X} = (\langle \hat{X}_1 \rangle, \langle \hat{X}_1 \rangle, \dots, \langle \hat{X}_n \rangle, \langle \hat{X}_n \rangle) \quad (8.2.7)$$

and the *covariance matrix* (CM)

$$\sigma = \frac{1}{2} \langle \hat{X}_i \hat{X}_j + \hat{X}_j \hat{X}_i \rangle - \langle \hat{X}_i \rangle \langle \hat{X}_j \rangle, \quad (8.2.8)$$

which completely characterize the Gaussian state ρ .

The positivity of the density matrix ρ and the canonical commutation relations imply

$$\sigma + i\Omega \geq 0 \quad (8.2.9)$$

and such inequality is the necessary and sufficient constraint which σ has to satisfy to be a CM corresponding to a physical physical Gaussian state [73].

Unitary operations that preserve the Gaussian character of the states on which they act and are generated by Hamiltonian terms at most quadratic in the field operators, correspond, in phase space, to a linear *symplectic transformation*. Given a symplectic transformation S , it preserves the symplectic form Ω

$$\Omega = S^T \Omega S. \quad (8.2.10)$$

Symplectic transformations on a $2n$ -dimensional phase space form the real *symplectic group* $\text{Sp}_{(2n, \mathbb{R})}$ and act linearly on the first moments and by

$$\sigma \rightarrow \sigma' = S^T \sigma S \quad (8.2.11)$$

on covariance matrices. In addition,

$$\text{Det}(S) = 1, \quad \forall S \in \text{Sp}_{(2n, \mathbb{R})}. \quad (8.2.12)$$

8.2.2 Evolution of the initial state

As explained in subsection 8.2.1, in gaussian CV a state can be totally described by its first and second moments [74, 75]. The key point is to realise that unitary transformations of a state ρ are represented by a similarity transformation i.e.

$$U^\dagger \rho U \rightarrow S^T \sigma S, \quad (8.2.13)$$

where S is a symplectic matrix which represent U in the formalism and σ is a covariance matrix of the Gaussian state ρ .

We consider only two modes confined in one cavity and we will change from the a, a^\dagger basis to the \hat{q}, \hat{p} basis.

States and transformations will be represented by 4×4 matrices. In particular, the vacuum state is represented by the identity 1. The ‘‘evolution’’ of our state is encoded in the BVT. We start from an initial state, the vacuum in this case, and wish to look for the state after some travel scenario. and working to order h^2 , we find that the matrix that represents our truncated BVT $B(h)$ between the two lowest modes in this formalism reads:

$$B(h) = \begin{pmatrix} 1 - A_-^{(1)} h^2 & 0 & -Ch & 0 \\ 0 & 1 - A_+^{(1)} h^2 & 0 & -Dh \\ Dh & 0 & 1 - A_-^{(2)} h^2 & 0 \\ 0 & Ch & 0 & 1 - A_+^{(2)} h^2 \end{pmatrix},$$

$$A_\pm^{(k)} = \frac{32(16M^4 + 80M^2\pi^2 + 91\pi^4)}{729\pi^8} \pm \frac{1/16}{M^2 + k^2\pi^2},$$

$$D = \frac{8(4M^2 + 7\pi^2)}{27\pi^4} \left(\frac{M^2 + \pi^2}{M^2 + 4\pi^2} \right)^{-1/4},$$

$$C = \frac{8(4M^2 + 13\pi^2)}{27\pi^4} \left(\frac{M^2 + \pi^2}{M^2 + 4\pi^2} \right)^{1/4}, \quad (8.2.14)$$

and $M = \mu\delta$ is dimensionless mass of the field. The matrix $B(h)$ transforms the Minkowski $\{X_1, P_1, X_2, P_2\}$ to the Rindler $\{\tilde{X}_1, \tilde{P}_1, \tilde{X}_2, \tilde{P}_2\}$.

Evolution of the system in this formalism is obtained as follows.

Suppose the initial state in the cavity is σ_i and the cavity undergoes some unitary inertial evolution represented by $U(\tau)$. Then the final state σ_f is

$$\sigma_f = S^T(\tau) \sigma_i S(\tau), \quad (8.2.15)$$

where our task is to find the symplectic matrix $S(\tau)$ which represents the evolution induced by $U(\tau)$. Now the cavity might start accelerating and therefore we need to

transform the operators into R operators. This is taken care of by $B(h)$. The state then takes the form

$$\sigma_f = B^T(h)E^T(\tau)\sigma_i E(\tau)B(h). \quad (8.2.16)$$

The state then evolves “freely” during the acceleration, $F(h, \tau)$ and then stops accelerating. $B^{-1}(h)$. The final state after this trip is

$$\sigma_f = (B^{-1})^T(h)F^T(h, \tau)B^T(h)E^T(\tau)\sigma_i E(\tau)B(h)F(h, \tau)B^{-1}(h) \quad (8.2.17)$$

It is clear how to proceed further by “sandwiching” the state with appropriate matrices. The symplectic matrices E, F correspond to the evolution operators in (5.1.14). As an initial state σ_i we consider a pure state: in this formalism $\det(\sigma_i) = 1$. Since we apply unitary transformations, it follows that $\det(\sigma_f) = 1$. This gives us a way to check that the TMT does maintain the unitarity of the transformations.

We will use the *logarithmic negativity* $E_{\mathcal{N}}$ to quantify entanglement. Given a state σ , one first computes the partial transpose which in this language takes the form

$$\tilde{\sigma} = P\sigma P \quad (8.2.18)$$

where the matrix

$$P = \text{diag}(1, 1, 1, -1)$$

performs the partial transposition. Clearly, $P^2 = \text{id}$ and $P^\dagger = P$.

One now defines the *symplectic version* of $\tilde{\sigma}$ as

$$\tilde{\sigma}_s = i\Omega\tilde{\sigma} \quad (8.2.19)$$

where Ω is the symplectic matrix. The eigenvalues of $\tilde{\sigma}_s$ come into two pairs $\{\pm\tilde{\nu}_-, \pm\tilde{\nu}_+\}$ where $0 < \tilde{\nu}_-, \tilde{\nu}_+$. From now on, $-\tilde{\nu}_-$ will denote the smallest positive symplectic eigenvalue of $\tilde{\sigma}_s$. If $\tilde{\nu}_- < 1$ then there is entanglement (see [76]) and it is quantified by the *logarithmic negativity* $E_{\mathcal{N}}$ which is defined as

$$E_{\mathcal{N}} := \text{Max}(0, -\ln(\tilde{\nu}_-)) \quad (8.2.20)$$

Another measure that could be chosen is the *negativity*. In this formalism it is defined as

$$\mathcal{N} := \max\left\{0, \frac{1 - \tilde{\nu}_-}{2\tilde{\nu}_-}\right\} \quad (8.2.21)$$

When $\tilde{\nu}_- = 1 - \tilde{\nu}_-^{(1)}$ and $0 < \tilde{\nu}_-^{(1)} \ll 1$, it is easy to see that first order in $\tilde{\nu}_-^{(1)}$

$$\begin{aligned} E_{\mathcal{N}} &\sim \tilde{\nu}_-^{(1)} \\ \mathcal{N} &\sim \frac{\tilde{\nu}_-^{(1)}}{2} \sim \frac{E_{\mathcal{N}}}{2} \end{aligned} \quad (8.2.22)$$

8.3 Resonance condition

We look for a condition where the entanglement generated after any travel scenario, which we call Building Block (BB), can be increased by repeating the BB an arbitrary amount of times.

Let the initial state be the vacuum: in this case $\sigma_{in} = \text{id}$. The transformation to the final state is represented by the matrix S and therefore we can write the final state as

$$\sigma_{out} = S^T \sigma_{in} S = S^T S \quad (8.3.1)$$

The matrix S may represent any desired travel scenario and we need not specify it a priori. It encodes the inertial evolutions, the uniformly accelerated evolutions and the BVT. Notice that for transformations that *do not* preserve the energy of the system, such as two mode squeezing or single mode squeezing, $S^T S \neq \mathbb{1}$. Once the travel scenario is fixed, we can repeat it any number of times, say N , using the techniques described in the section 8.2. We have

$$\begin{aligned} \sigma_1 &= S^T S \\ \sigma_N &= (S^T)^N S^N \end{aligned} \quad (8.3.2)$$

where σ_1 is the final state after one BB and σ_N is the final state after the BB has been repeated N times.

We notice that if

$$[S^T, S] = 0 \quad (8.3.3)$$

then

$$\sigma_N = \sigma_1^N \quad (8.3.4)$$

We call (8.3.3) the *resonance condition*. This is the central part of the chapter. From now on we proceed to show that the resonance condition allows for a linear increase of the entanglement created after a single BB, as a function of the number of repetitions, when we repeat the BB any number of times.

We work in the $\hbar \ll 1$ approximation and therefore we can expand our states in power series.

$$\begin{aligned} \sigma_1 &= \sigma_1^{(0)} + \sigma_1^{(1)} + \mathcal{O}(\hbar^2) \\ \sigma_N &= \sigma_N^{(0)} + \sigma_N^{(1)} + \mathcal{O}(\hbar^2) \end{aligned} \quad (8.3.5)$$

where the superscript stands for the relevant order in \hbar and we are interested to truncate at first order. From this point, it is understood that higher than first orders do not

contribute.

We know that the zeroth order contribution must be the identity, since when $h = 0$ the modes undergo free evolution. Therefore we get

$$\begin{aligned}\sigma_1 &= \text{id} + \sigma_1^{(1)} \\ \sigma_N &= \text{id} + \sigma_N^{(1)}\end{aligned}\tag{8.3.6}$$

On resonance, we have that

$$\sigma_N = \sigma_1^N = \left(\text{id} + \sigma_1^{(1)}\right)^N = \text{id} + N\sigma_1^{(1)}\tag{8.3.7}$$

which, when we compare with the second line of (8.3.6) implies that

$$\sigma_N^{(1)} = N\sigma_1^{(1)}.\tag{8.3.8}$$

To compute the logarithmic negativity (2.3.21), we need the symplectic eigenvalues of the symplectic version (8.2.19) of our final state. Therefore, we need to look at the eigenvalues of the matrices

$$\begin{aligned}\tilde{\sigma}_1 &= i\Omega P\sigma_1 P \\ \tilde{\sigma}_N &= i\Omega P\sigma_N P.\end{aligned}\tag{8.3.9}$$

Again, on resonance we can use (8.3.6) and (8.3.8) to write

$$\begin{aligned}\tilde{\sigma}_1 &= i\Omega + i\Omega P\sigma_1^{(1)} P \\ \tilde{\sigma}_N &= i\Omega + iN\Omega P\sigma_1^{(1)} P.\end{aligned}\tag{8.3.10}$$

We wish to diagonalize both matrices in (8.3.10). We first notice that the zeroth order in their expansion $\tilde{\sigma}_1^{(0)}$ and $\tilde{\sigma}_N^{(0)}$ is

$$\tilde{\sigma}_1^{(0)} = \tilde{\sigma}_N^{(0)} = i\Omega,\tag{8.3.11}$$

which has two couples of degenerate eigenvalues $\{1, 1, -1, -1\}$ which forces us to employ degenerate perturbation theory. The procedure is described in detail in [77] in the context of Covariance Matrixes and we shall briefly review it here.

Let $|v_1\rangle, |v_2\rangle$ be the two eigenvectors of the degenerate eigenvalue 1. Therefore

$$\begin{aligned}\tilde{\sigma}_N^{(0)} |v_1\rangle &= |v_1\rangle \\ \tilde{\sigma}_N^{(0)} |v_2\rangle &= |v_2\rangle.\end{aligned}\tag{8.3.12}$$

We now employ the first order correction $\tilde{\sigma}_N^{(1)}$ to compute the corrections to the eigenvalues. We construct the 2×2 matrix $M(N)$ after N shakes whose elements are defined by

$$M_{ij}(N) := \langle v_i | \tilde{\sigma}_N^{(1)} | v_j \rangle.\tag{8.3.13}$$

The eigenvalues of M will be denoted by $\tilde{\nu}_{\pm}^{(1)}(N)$ and are the corrections to the unperturbed eigenvalues 1 of $\tilde{\sigma}_N^{(0)}$. On resonance

$$\tilde{\sigma}_N^{(1)} = N\tilde{\sigma}_1^{(1)}, \quad (8.3.14)$$

which implies

$$M_{ij}(N) = \langle v_i | \tilde{\sigma}_N^{(1)} | v_j \rangle = N \langle v_i | \tilde{\sigma}_1^{(1)} | v_j \rangle = NM_{ij}(1). \quad (8.3.15)$$

Therefore

$$\text{Eigen}[M_{ij}(N)] = N\text{Eigen}[M_{ij}(1)]. \quad (8.3.16)$$

Which translates to

$$\tilde{\nu}_{\pm}^{(1)}(N) = N\tilde{\nu}_{\pm}^{(1)}(1) \quad (8.3.17)$$

Therefore, we have found that the two corrected positive eigenvalues of $\tilde{\sigma}_N$ are related to the corrected positive eigenvalues of $\tilde{\sigma}_1$. We reproduce the expansion of smallest positive eigenvalue after N shakes $\tilde{\nu}_-(N)$ below

$$\tilde{\nu}_-(N) = 1 - \tilde{\nu}_-^{(1)}(N) \quad (8.3.18)$$

where

$$\tilde{\nu}_-^{(1)}(N) = N\tilde{\nu}_-^{(1)}(1) \quad (8.3.19)$$

We can compute the logarithmic negativity $E_{\mathcal{N}}$ for both $\tilde{\sigma}_1$ and $\tilde{\sigma}_N$ where it takes the expression $E_{\mathcal{N}}(1)$ and $E_{\mathcal{N}}(N)$ respectively. We get

$$\begin{aligned} E_{\mathcal{N}}(1) &= -\ln(\tilde{\nu}_-(1)) = -\ln(1 - \tilde{\nu}_-^{(1)}(1)) \approx \tilde{\nu}_-^{(1)}(1) \\ E_{\mathcal{N}}(N) &= -\ln(\tilde{\nu}_-(N)) = -\ln(1 - \tilde{\nu}_-^{(1)}(N)) = -\ln(1 - N\tilde{\nu}_-^{(1)}(1)) \approx N\tilde{\nu}_-^{(1)}(1) \end{aligned} \quad (8.3.20)$$

provided that $N\tilde{\nu}_-^{(1)}(1) \ll 1$. Therefore

$$E_{\mathcal{N}}(N) = NE_{\mathcal{N}}(1) \quad (8.3.21)$$

which is the linear increase of entanglement we were looking for.

8.4 Position of the resonance

We have found that the condition for the resonance to exist is (8.3.3). One can express S in terms of general Bogoliubov coefficients between pre-trip and post-trip modes. We use the results from [77] and find that in general $[S^T, S]$ has the following form

$$[S^T, S] = \begin{pmatrix} 0 & C \\ C^T & 0 \end{pmatrix} + \mathcal{O}(\hbar^2)$$

where C has the expression

$$C = 2 \begin{pmatrix} C_{11} & C_{12} \\ C_{12} & -C_{11} \end{pmatrix}$$

and the elements can be expressed in terms of the B coefficients of \mathcal{A} for the overall trip.

$$\begin{aligned} C_{11} &= ((\cos(\phi_k) - \cos(\phi_{k'}))\text{Re}(B_{kk'}^{(1)}) + (\sin(\phi_k) + \sin(\phi_{k'}))\text{Im}(B_{kk'}^{(1)})) \\ C_{12} &= ((-\cos(\phi_k) + \cos(\phi_{k'}))\text{Im}(B_{kk'}^{(1)}) + (\sin(\phi_k) + \sin(\phi_{k'}))\text{Re}(B_{kk'}^{(1)})) \end{aligned} \quad (8.4.1)$$

The coefficient $B_{kk'}^{(1)}$ is the first order correction to the beta for the *full* travel scenario,

$$\begin{aligned} G_k &= \exp[i\phi_k] \\ G_{k'} &= \exp[i\phi_{k'}] \end{aligned} \quad (8.4.2)$$

are the zero order corrections to the alphas for the *full* travel scenario; these coefficients are all elements of the \mathcal{A} matrix which encodes the TMT truncation version of the BVT. $k, k' \in \mathbb{N}$. We also know that

$$\begin{aligned} \phi_k &= \omega_k T \\ \phi_{k'} &= \omega_{k'} T \end{aligned} \quad (8.4.3)$$

where T is the *total proper time* of the BB and

$$\omega_k = \frac{k\pi}{\delta} \quad (8.4.4)$$

is the frequency of the mode k and δ is the length of the cavity as usual. To first order, the inertial frequency $\omega_k = (k\pi)/\delta$ and the R frequency

$$\tilde{\Omega}_k = (k\pi h)/(2\delta \tanh^{-1}(h/2)) \quad (8.4.5)$$

coincide since

$$\tilde{\Omega}_k = \frac{k\pi h}{2\delta \tanh^{-1}(h/2)} = \frac{k\pi}{\delta} (1 + \mathcal{O}(h^2)) = \omega_k (1 + \mathcal{O}(h^2)) \quad (8.4.6)$$

Therefore,

$$\omega_k T = \omega_k \sum_i T_i \quad (8.4.7)$$

where T_i is the individual proper time of the i -th segment which composes the travel scenario. This might be a Rindler proper time or a Minkowski proper time. In general, the expression will be complicated.

In order for $[S^T, S] = 0$ we find that (8.4) implies

$$B_{kk'}^{(1)} [G_k^* - G_{k'}] = 0. \quad (8.4.8)$$

A sufficient condition for this is

$$G_k^* - G_{k'} = 0. \quad (8.4.9)$$

This occurs when

$$T_n = \frac{2n\pi}{\omega_k + \omega_{k'}}, \quad (8.4.10)$$

which we call *total resonance time*.

There might be extra resonance conditions determined by $B_{kk'}^{(1)} = 0$ but it is possible to find these conditions explicitly only once the specific travel-plan of the scenario is given. In (8.6) we give an example and an explicit computation.

8.5 General description of the increase of entanglement

The entanglement after one scenario is $|B_{kk'}^{(1)}|$ where $B_{kk'}^{(1)}$ is the first order correction for the overall travel scenario beta coefficient. In general, if there are n segments of acceleration with different accelerations $h, h', h'', \dots, h^{(n)}$, then

$$|B_{kk'}^{(1)}|_1 = |(\tilde{\beta}_0^{(1)})_{kk'}| |(p+q)h + (p'+q')h' + (p''+q'')h'' + \dots + (p^{(n)}+q^{(n)})h^{(n)}|, \quad (8.5.1)$$

where the p, q 's are phase factors which are complicated combinations of *all* the times within the individual segments and $\tilde{\beta}_0^{(1)}$ is the coefficient to the first order correction to the inertial to accelerated beta. For a long travel scenario it is not possible to write down the phase factors explicitly. It is evident though that there will be combinations of accelerations (and their directions) that will affect the amount of entanglement created.

By using (5.1.15) it is clear that, if one repeats a travel scenario N times, the final entanglement takes the form

$$|B_{kk'}^{(1)}|_N = |(\tilde{\beta}_0^{(1)})_{kk'}| \left| \sum_i (p_i + q_i)h + \sum_i (p'_i + q'_i)h' + \sum_i (p''_i + q''_i)h'' + \dots + \sum_i (p_i^{(n)} + q_i^{(n)})h^{(n)} \right|, \quad (8.5.2)$$

where every $h^{(l)}$ gets N phase factors of the form $\{p_i^{(l)}, q_i^{(l)}\}$, one from each travel scenario in the repetition. On resonance we expect that $\sum_i (p_i^{(n)} + q_i^{(n)}) = N(p^{(n)} + q^{(n)}) \forall i$ and therefore

$$|B_{kk'}^{(1)}|_N = N|B_{kk'}^{(1)}|_1. \quad (8.5.3)$$

We give an explicit example in the next section.

8.6 Travel example: Casimir-like scenario

8.6.1 Casimir-type scenario: same acceleration/deceleration

In this scenario, the Building Block is composed of a segment of uniform acceleration followed immediately by a uniform deceleration of the same magnitude and for the same proper time. The total proper time of one Building Block T is just twice the proper time of the acceleration/deceleration τ , therefore $T = 2\tau$. From (8.4.10) we find then that

$$\tau_n = \frac{n\pi}{\omega_k + \omega_{k'}}, \quad (8.6.1)$$

which is the resonance condition for this particular travel scenario.

Eq. (8.4.10) provides the times for resonance but it does not guarantee that the entanglement does not vanish identically at those times. Therefore one must verify that

$$B_{kk'}^{(1)} \neq 0 \quad (8.6.2)$$

for these times. In fact, $B_{kk'}^{(1)}$ gives the entanglement at the end of the travel [77], therefore if it vanishes there is no entanglement. Let us look at our present case, which we call *Casimir like* scenario.

Then

$$B_{kk'}^{(1)} = |(\beta_0^{(1)})_{kk'}| |g_k^2 - g_k \bar{g}_{k'} + (-1)^{k+k'} g_k \bar{g}_{k'} - (-1)^{k+k'} \bar{g}_{k'}^2| \quad (8.6.3)$$

where $|g_k| = |g_{k'}| = 1$ are the phase factors acquired during a *single* segment of acceleration/deceleration. The factor $(-1)^{k+k'}$ comes by considering leftwards accelerations (deceleration in our case). Therefore, given that $T = 2\tau$, in our specific case:

$$\begin{aligned} g_k &= e^{-i\omega_k \tau} \\ g_{k'} &= e^{-i\omega_{k'} \tau} \\ G_k &= e^{-i\omega_k T} = g_k^2 \\ G_{k'} &= e^{-i\omega_{k'} T} = g_{k'}^2. \end{aligned} \quad (8.6.4)$$

Using these identities, one can verify that (8.6.3) implies that $B_{kk'}^{(1)} = 0$ at the resonance times

$$\tau_n = \frac{2n\pi}{\omega_k + \omega_{k'}} \quad (8.6.5)$$

which means that we expect (non vanishing) entanglement resonances only for the resonance times

$$\tau_n = \frac{(2n+1)\pi}{\omega_k + \omega_{k'}}. \quad (8.6.6)$$

The analytical predictions of this section are demonstrated in Fig. 8.1 where we specialize to massless fields, $k = 1$, $k' = 2$ and resonances are expected at $\tau_1 = \frac{1}{3}\delta$ and $\tau_3 = \delta$. The resonance at $\tau_2 = \frac{2}{3}\delta$ is a null entanglement resonance.

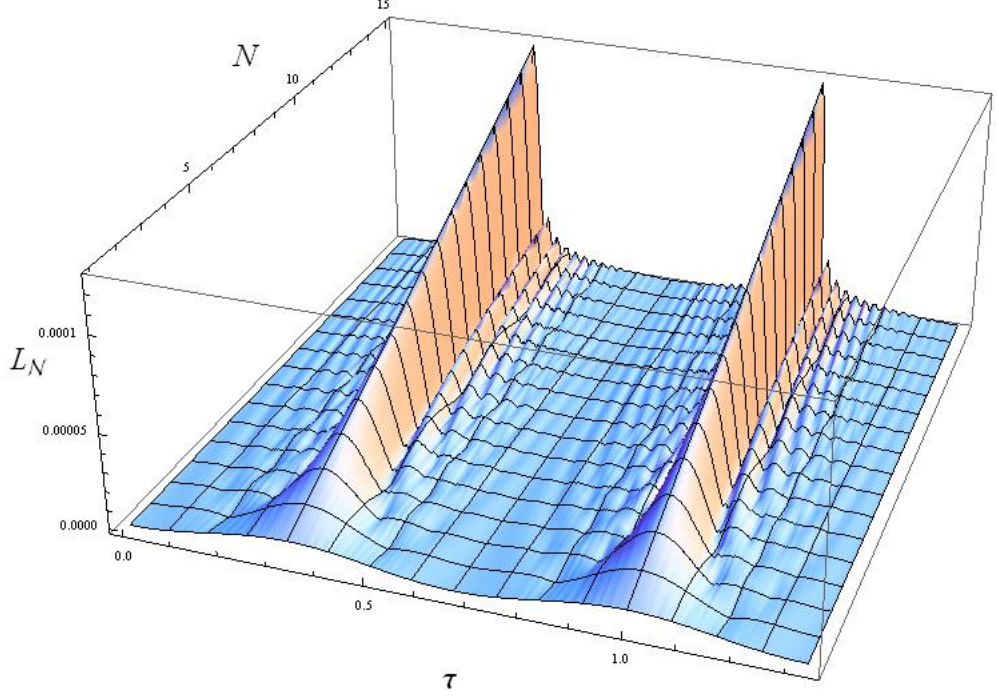


Figure 8.1: The logarithmic negativity L_N is shown as a function of the proper time of acceleration/deceleration τ and the number of repetitions N for $k = 1$, $k' = 2$. Resonances are found as expected at $\tau_1 = \frac{1}{3}\delta$ and $\tau_3 = \delta$. $E_N = 0$ for $\tau_2 = \frac{2}{3}\delta$. We have specialized to massless fields.

8.6.2 Casimir-type scenario: different acceleration/deceleration

We extend the calculations of the subsection 8.6.1 to a Casimir scenario where the acceleration is $h = n\tilde{h}$ and the acceleration/deceleration is $h' = m\tilde{h}$ where $n, m \in \mathbb{N}$. The sign of h' will be taken into account sperately. The entanglement is

$$B_{kk'}^{(1)} = |(\tilde{\beta}_0^{(1)})_{kk'}| |g_k^2 h - g_k \bar{g}_{k'} h + \sigma(k, k') g_k \bar{g}_{k'} h' - \sigma(k, k') \bar{g}_{k'}^2 h'|, \quad (8.6.7)$$

where $\tilde{\beta}_0^{(1)}$ is the coefficient of the first order h or h' and

$$\sigma(k, k') = \begin{cases} 1 & \text{for rightwards accelerations} \\ (-1)^{k+k'} & \text{for leftwards accelerations (deceleration in our notation)} \end{cases}.$$

Therefore, using the values for the accelerations we get

$$B_{kk'}^{(1)} = |(\beta_0^{(1)})_{kk'}| |n g_k^2 - n g_k \bar{g}_{k'} + m \sigma(k, k') g_k \bar{g}_{k'} - m \sigma(k, k') \bar{g}_{k'}^2|. \quad (8.6.8)$$

On resonance we know that $G_k^* - G_{k'} = 0$ and here $g_k^2 = G_k$ and $g_{k'}^2 = G_{k'}$, therefore

$$B_{kk'}^{(1)} = |(\beta_0^{(1)})_{kk'}| |(n - m\sigma(k, k')) - (n - m\sigma(k, k'))\bar{g}_k\bar{g}_{k'}| = |(\beta_0^{(1)})_{kk'}| |n - m\sigma(k, k')| |1 - \bar{g}_k\bar{g}_{k'}|. \quad (8.6.9)$$

Equation (8.6.9) contains all the information we need. If

$$\tau_n = \frac{2n\pi}{\omega_k + \omega_{k'}} \quad (8.6.10)$$

then $g_{k'} = \bar{g}_k$ and the last term in (8.6.9) vanishes as expected because

$$|1 - \bar{g}_k\bar{g}_{k'}| = |g_k - \bar{g}_{k'}|. \quad (8.6.11)$$

If

$$\tau_n = \frac{(2q+1)\pi}{\omega_k + \omega_{k'}} \quad (8.6.12)$$

then $g_{k'} = -\bar{g}_k$ and the last term in (8.6.9) gives $|1 - g_k\bar{g}_{k'}| = |g_k - \bar{g}_{k'}| = 2$. Therefore

$$B_{kk'}^{(1)} = 2|(\beta_0^{(1)})_{kk'}| |n - m\sigma(k, k')|. \quad (8.6.13)$$

We always have to choose oddly separated modes for these scenarios ($|(\beta_0^{(1)})_{kk'}| = 0$ for evenly separated, see (5.1.22)).

Suppose we accelerate towards the right and instead of decelerating, we accelerate again towards the right. Then $\sigma(k, k') = 1$ and

$$B_{kk'}^{(1)} = 2|(\beta_0^{(1)})_{kk'}| |n - m|. \quad (8.6.14)$$

Suppose we accelerate and then decelerate, then $\sigma(k, k') = -1$ and we get

$$B_{kk'}^{(1)} = 2|(\beta_0^{(1)})_{kk'}| |n + m|, \quad (8.6.15)$$

which is what we can verify numerically.

The first of these two cases can be understood as follows: if $n = m$, it means that we accelerate with acceleration h and immediately accelerate again with acceleration $h' = h$. Then we repeat this N times: this is just a Basic Building Block scenario with a very long period of acceleration. Therefore,

$$B_{kk'}^{(1)} = 2|(\beta_0^{(1)})_{kk'}| |n - m| = 0 \quad (8.6.16)$$

and there is no entanglement! This is to be expected: the times for resonance are those for which a BBB has vanishing entanglement, otherwise one could increase the final entanglement at will by accelerating longer.

8.7 Bogoiubov operations

In this Chapter we have analyzed the bipartite entanglement generate between piers of oddly separated modes in a single cavity when the initial state is a coherent state. We have a lose found an additional feature which characterizes the BVT. In this setting they act as a two mode squeezing operation, where the squeezing parameter r is directly related to the correction to the symplectic eigenvalue $\tilde{\nu}^{(1)}$ through

$$r \propto \tilde{\nu}^{(1)} \tag{8.7.1}$$

We can interpret the results of the previous sections as follows: when off resonance, the operations represented by the symplectic matrix S act non-constructively, which does not allow entanglement to be increased. When on resonance, the operations all act constructively and therefore the squeezing is increased by repeating the operation.

8.8 Conclusions

In this chapter we have introduced the TMT, which justifies restricting the BVT to only two oddly separated modes. The BVT are Gaussian transformations and therefore we have chosen to employ initial Gaussian states and CV techniques. When the initial state is the vacuum or a coherent state, one can show that by repeating any travel scenario an arbitrary number of times, one can always find a suitable total time for such scenario to obtain a linear increase of entanglement with the number of repetitions. In addition, genuine two mode squeezing between the two modes is achieved where the squeezing parameter is directly related to the entanglement generated. We have found that there are always resonances when the “frequency” of the repetitions is just an even integer multiple of the sum of the frequencies of the two modes. Such condition is necessary but not sufficient for linear increase of entanglement. The specific form of the B coefficient for the travel scenario adds constraints on the possible times of resonances. As a concrete example we analyze a Casimir-like scenario where a segment of acceleration is immediately followed by a segment of deceleration of same magnitude. We then generalize this specific case to one where the magnitude of acceleration and deceleration need not be the same and the direction can be chosen freely.

Part III

CHAPTER 9

Effects of topology on the nonlocal
correlations within the
Hawking-Unruh radiation

In the previous chapters we have analyzed how the state of motion of observers affects the entanglement initially present in (a family of) maximally entangled states. We have contributed to the understanding of how this resource for QI tasks is affected by relativistic effects. We have also introduced and employed a confined fields in cavities. An open question remains on how entanglement is affected by the curvature of the spacetime. There is wide consensus among the community regarding the structure of the spacetime at small scales not being continuous. In particular, many approaches agree that the topology at small scales might be quantized in some sense.

The standard arena for studies that involve curved spacetimes are black hole spacetimes (See [19, 78]). They have been thoroughly studied in the past four decades and have been extended to different theories of Quantum Gravity.

Previous work in the literature has considered black hole spacetimes where the spatial topology is not trivial. It was argued that there are solutions to Einstein's equations which allow for the spatial topology to be different from \mathbb{R}^3 [79].

In this chapter we analyze charged scalar fields coupled to a (classical) background magnetic or electric field in a $3 + 1$ curved spacetime where the spatial foliation is not topologically equivalent to \mathbb{R}^3 . In particular, we investigate geon spacetimes and the effects, if any, of the presence of non-trivial topology on nonlocal correlations present in relativistic quantum fields.

9.1 Introduction to geons

Given a stationary black hole spacetime with a bifurcate Killing horizon, it may be possible to construct a time-orientable quotient spacetime in which the exterior regions separated by the Killing horizon become identified. In the asymptotically flat case the quotient spacetime is a topological geon in the sense of Sorkin [79], the showcase example being the \mathbb{Z}_2 quotient of Kruskal known as the \mathbb{RP}^3 geon [80–83]. There exist also examples where the quotient spacetime is asymptotically locally flat, asymptotically anti-de Sitter or locally anti-de Sitter [84–87], and we shall understand a topological geon black hole to encompass all these situations, the characteristic property being that the infinity consists of only one component.

Topological geon black holes that arise from a stationary black hole in the manner described above are unlikely to be of interest in astrophysics. They are eternal, in the sense that their exterior region is stationary and the full spacetime contains both a black hole region and a white hole region, and their distant past regions cannot be replaced by a conventional collapsing star without introducing a change of spatial topology. However,

as the spacetime has only one stationary exterior region, the topological geon black holes provide an arena for investigating thermal properties of black holes in an unconventional setting.

To see the issue, consider quantum field theory on Kruskal spacetime [78]. On Kruskal spacetime, there is a distinguished vacuum state known as the Hartle-Hawking(-Israel) vacuum [88–90]. While the Hartle-Hawking vacuum is a pure state, it contains entanglement between the field degrees of freedom that are defined in the opposing exteriors with respect to their respective timelike Killing vectors. Probing the Hartle-Hawking vacuum in one exterior amounts to tracing over degrees of freedom in the causally disconnected exterior, and the outcome of this partial tracing is a thermal density matrix in the Hawking temperature [10]. On the \mathbb{RP}^3 geon, by contrast, a causally disconnected exterior does not exist.

Is there hence thermality in the exterior of the \mathbb{RP}^3 geon, and if so, in what sense?

For a real scalar field on the \mathbb{RP}^3 geon, this issue was analysed in [91]. The Hartle-Hawking vacuum on Kruskal induces a Hartle-Hawking-like vacuum on the geon, and this vacuum does not exhibit thermality when probed by generic operators in the geon’s exterior. However, when the Hartle-Hawking-like vacuum is written as Boulware excitations on the Boulware vacuum [92], the excitations come in correlated pairs, and the expectation value of any operator that is designed to couple to only one member of each pair *is* thermal, in the usual Hawking temperature. In particular, operators with support in the asymptotically distant future (or past) see the Hartle-Hawking-like vacuum as thermal. These properties follow directly from the geometry of quotienting Kruskal into the \mathbb{RP}^3 geon, and they generalise to higher spin [93], to similar quotients for more general geon black holes [87], to geon-like quotients of Rindler and de Sitter spacetimes [91, 94] and also to the context of gauge-gravity correspondence [84, 85] A recent review is given in [95].

When the black hole has a gauge field (such as a background electric or magnetic field), it may be necessary to include charge conjugation in the map with which the gauge bundle of the two-exterior black hole is quotiented into the geon’s gauge bundle. This happens for example for the Maxwell field on the Reissner-Nordström hole, both with electric and magnetic charge [87]; it also happens for generic spherically symmetric Einstein-SU(n) black holes for $n > 2$ [96]. Gauge charges on the geon are then globally defined only up to their overall sign [97], similarly to what is known as Alice strings in the cosmic string context [98–100]. As this sign ambiguity can be fixed within the geon’s exterior, it is unlikely to have interesting consequences for purely classical observations in the geon’s exterior. However, when a quantum field couples to the geon’s gauge field, one

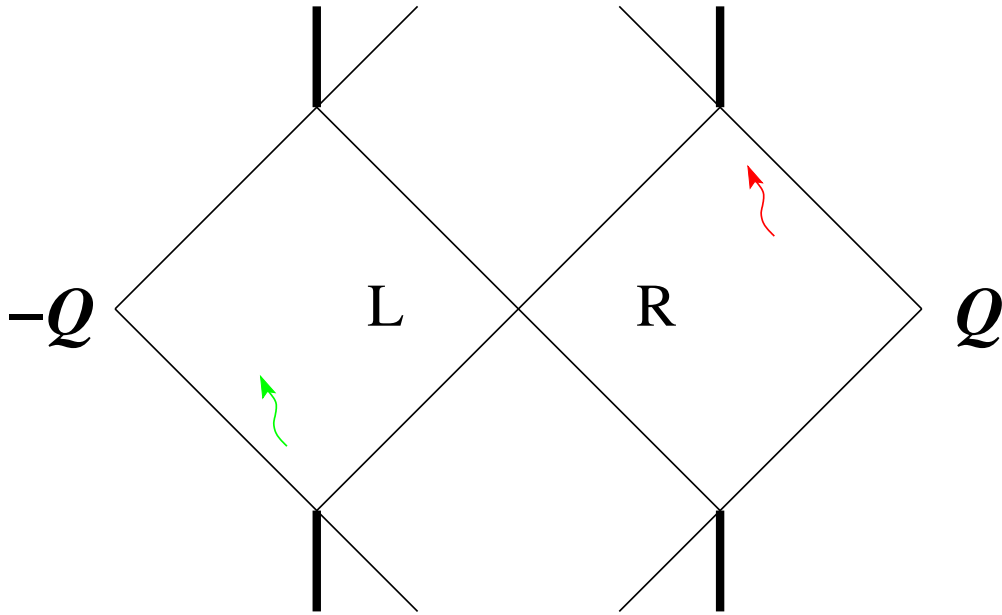


Figure 9.1: Penrose-Carter diagram with two dimensions suppressed of Reissner-Nordström spacetime. The future and past horizons are the $\pi/4$ straight lines. Note the vertical singularity and the inner and outer horizons (the inner horizon is also a Cauchy horizon [19]). Note the correlations contained in the global fields between right and left wedges.

may expect the Hartle-Hawking-like vacuum to contain information about the gauged charge conjugation behind the horizons, in a way that is detectable by observing the vacuum in the geon’s exterior. The purpose of this chapter is to demonstrate that these expectations are correct.

9.1.1 Geons in brief

We briefly introduce the concept of geon using the Reissner-Nordström spacetime example, since this will be considered later on in the Chapter. We will not introduce the details about the spacetime. These can be found in section 9.3.

The simplified Penrose-Carter diagram of the Reissner-Nordström spacetime is depicted in Fig. 9.1 where two dimensions are suppressed and we have highlighted the correlations between fields in the left and right causally disconnected regions. As explained further on, the charge as viewed by observers in the two causally disconnected regions takes opposite values. The spatial foliation of the spacetime can be changed in a nontrivial way by acting with a “mirror” map. This map, unto nontrivial details to maintain the manifold character of the foliation, will be introduced in Section 9.3. The Penrose-Carter diagram of the geon spacetime is depicted in Fig. 9.2 The diagram can

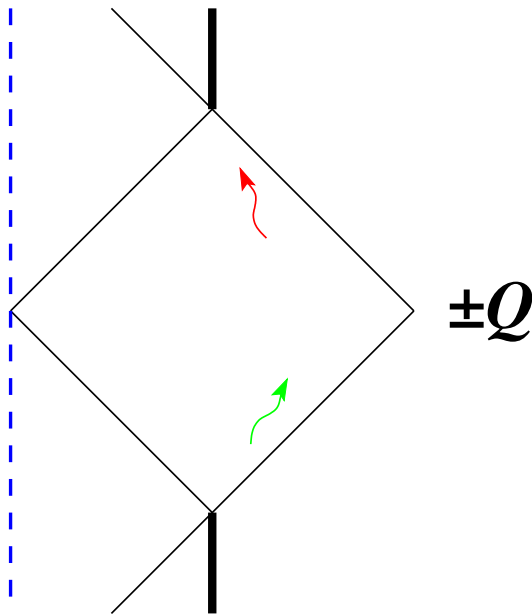


Figure 9.2: Penrose-Carter diagram with two dimensions suppressed for the geon Reissner-Nordström spacetime. The future and past horizons are the $\pi/4$ straight lines. Note the correlations contained in the global fields within the past and future of the *same* (and only!) wedge.

be naively explained as follows: the geon quotient maps every point in Fig. 9.1 on the left of the middle symmetry axis to the corresponding “mirror” point on the right. There is now only one exterior region and therefore the correlations, if any, cannot be between causally disconnected exterior regions. A path that hits the symmetry axis is reflected back continuously (this can be obtained when correctly considering the two suppressed dimensions). The symbol $\pm Q$ is related to the fact that there is no global meaning of charge in this geon Reissner-Nordström spacetime. All details can be found in Section 9.3.

9.2 Scalar field coupled to a $\mathbb{Z}_2 \times U(1)$ Maxwell field

We start by considering a complex scalar field Φ coupled to a prescribed Maxwell field in a (possibly) curved spacetime $(\mathcal{M}, g_{\mu\nu})$. We assume the spacetime to be globally hyperbolic and time-oriented. The action reads [101]

$$S = \int_{\mathcal{M}} [-g^{\mu\nu} (D_\mu \Phi)^* D_\nu \Phi - m^2 \Phi^* \Phi] \sqrt{-g} d^4x, \quad (9.2.1)$$

where the star denotes complex conjugation and $m \geq 0$ is the mass. The gauge-covariant derivative D_μ reads

$$D_\mu := \nabla_\mu - eA_\mu, \quad (9.2.2)$$

where ∇ is the spacetime covariant derivative, A_μ is the Maxwell gauge potential and $e > 0$ is the coupling constant. We use a convention in which A_μ is imaginary.

The field equations can be obtained by (2.2.3) and read

$$(g^{\mu\nu} D_\mu D_\nu - m^2) \phi = 0 , \quad (9.2.3)$$

and the (indefinite because of normalization in Dirac-delta sense) inner product is given by

$$(\phi_1, \phi_2) = i \int_\Sigma \phi_1^*(x) \overleftrightarrow{D}_\mu \phi_2(x) n^\mu d\Sigma , \quad (9.2.4)$$

where Σ is a Cauchy hypersurface, $d\Sigma$ is the induced volume element on Σ and n^μ is the unit normal vector that points to the future, so that $n^\mu v_\mu < 0$ for every timelike future-pointing vector v^μ . When ϕ_1 and ϕ_2 satisfy (9.2.3), the inner product (9.2.4) is independent of the choice of Σ . When $\phi_1 = \phi_2$, the value of the inner product (9.2.4) is interpreted as the charge.

Since the gauge group is $U(1) \simeq SO(2)$, the gauge transformations read

$$(eA_\mu, \phi) \mapsto (eA_\mu + u^{-1} \partial_\mu u, u\phi) , \quad (9.2.5)$$

where u is a $U(1)$ -valued function on (a subset of) \mathcal{M} and we identify $U(1)$ with the set of complex numbers of unit magnitude. These transformations leave the action (9.2.1), the field equation (9.2.3) and the inner product (9.2.4) invariant.

When the gauge group is enlarged to

$$\mathbb{Z}_2 \times U(1) \simeq O(2), \quad (9.2.6)$$

the gauge transformations in the disconnected component read [87, 96, 97]

$$(eA_\mu, \phi) \mapsto (-eA_\mu + u^{-1} \partial_\mu u, u\phi^*) , \quad (9.2.7)$$

where u is again a $U(1)$ -valued function on (a subset of) \mathcal{M} . These transformations leave the action (9.2.1) and the field equation (9.2.3) invariant, but they change the sign of the inner product (9.2.4). The disconnected component of the gauge group makes hence positive charges gauge-equivalent to negative charges. The gauge transformation (9.2.7) indeed reduces to the usual charge conjugation transformation when u is the identity.

The situation of interest for this work is when \mathcal{M} admits a freely-acting involutive isometry J , such that the quotient spacetime

$$\mathcal{M}' := \mathcal{M}/\{\text{Id}, J\} \quad (9.2.8)$$

is globally hyperbolic, and the gauge field configuration satisfies

$$J^*(A) = -A, \quad (9.2.9)$$

where J^* denotes the pull-back by J (for an extensive review on differential geometry see [20]). We wish to define on \mathcal{M}' a charged scalar field that couples to the gauge field.

Recall first that in order to define the gauge field on \mathcal{M}' , it is necessary to use the enlarged gauge group $\mathbb{Z}_2 \times \text{U}(1)$ [87, 96, 97]. We may start from a (not necessarily trivial) principal $\mathbb{Z}_2 \times \text{U}(1)$ bundle P over \mathcal{M} and form its quotient $P' = P/\mathbb{Z}_2$ under a \mathbb{Z}_2 group of bundle automorphisms, where the nontrivial automorphism acts on \mathcal{M} by J and in the fibres by

$$(-\text{Id}_{\mathbb{Z}_2}, \text{Id}_{\text{U}(1)}) \in \mathbb{Z}_2 \times \text{U}(1). \quad (9.2.10)$$

From (9.2.7) and (9.2.9) it is seen that the gauge field configuration is invariant under this map.

If the coupling to the gauge field were not present, we could simply take a scalar field on \mathcal{M} and require it to be invariant under J^* . When the coupling to the gauge field is present, this does not work, since if ϕ solves the field equation (9.2.3) on \mathcal{M} , it follows from (9.2.9) that $J^*\phi$ need not do so; however $(J^*\phi)^*$ does.

We may hence define a scalar field on \mathcal{M}' as a field on \mathcal{M} that satisfies $(J^*\phi)^* = \phi$: the field is invariant under J up to a gauge transformation that lies in the disconnected component of the enlarged gauge group $\mathbb{Z}_2 \times \text{U}(1)$. The gauge group on \mathcal{M}' must hence contain both components of $\mathbb{Z}_2 \times \text{U}(1)$.

9.2.1 Constant background magnetic field: preliminaries

First of all we introduce \mathcal{M}_0 which is a quotient manifold defined as

$$\mathcal{M}_0 := \mathcal{M}/J_0 \quad (9.2.11)$$

where J_0 is defined as follows:

$$J_0 : (t, x, y, z) \mapsto (t, x, y, z + L) \quad (9.2.12)$$

and L is a positive constant. The reason to introduce \mathcal{M}_0 is the following: the geon map for the Reissner-Nordström case is a genuine involution; the maps J_+ and J_- that we will use in this section, defined as

$$J_+ : (t, x, y, z) \mapsto (t, -x, y, z + \frac{L}{2}) \quad (9.2.13a)$$

$$J_- : (t, x, y, z) \mapsto (t, -x, -y, z + \frac{L}{2}) \quad (9.2.13b)$$

are not involutions on \mathcal{M} but are on \mathcal{M}_0 .

We start from the Lagrangian (9.2.1) and wish to look at a charged scalar field coupled to a constant background magnetic field. We choose the field to be in the x direction in

order to model what happens for the geometrical geon. It is suitable to fix a gauge in which

$$\tilde{A} := -iCy\tilde{d}z. \quad (9.2.14)$$

where we use the slide to denote one-forms [20]. We want to address the problem of how does the connection transform under the action of the involution. Take J_+ and pull back the connection under this map. It is easy to check that, given a point $x \in \mathcal{M}_0$

$$\tilde{A}'(x) := J_+^*(\tilde{A})(x) = \tilde{A}(x) \quad (9.2.15)$$

and therefore no issue arises because of the connection.

Consider the involution J_- . Pull back the connection by this map; we obtain

$$\tilde{A}' := J_-^*(\tilde{A}). \quad (9.2.16)$$

If we want to compare the pullback of the connection \tilde{A}' with the connection \tilde{A} itself it is easy to see that

$$\tilde{A}'(x) := J_-^*(\tilde{A})(x) = -\tilde{A}(x), \quad (9.2.17)$$

where $x \in \mathcal{M}$, and therefore we must account for this change of sign if we want to take the geon quotient. We know that there is a gauge freedom allowed in our setting and we will use a gauge transformation to correct for this sign.

To do this, we enlarge the gauge group from $U(1)$ to $O(2)$ as implemented in eq. (9.2.7) and explained in section 9.2 . The joint action of the disconnected component composed with the action of the involution are the map we will use to take the quotient.

9.2.2 Constant background magnetic field - Classical case

We are now in a position to proceed to solve the field equations. We start by solving the field equation on \mathcal{M}_0 of a complex scalar field coupled to the vector potential (9.2.14),

$$(D_\mu D^\mu - m^2)\phi = 0, \quad (9.2.18)$$

which yields an analytic solution in terms of modes

$$U_{n,j,k_x}(x^\mu) = \frac{1}{4\pi\omega_j L} \frac{1}{\sqrt{2^j j! \sqrt{\frac{\pi}{|C|}}}} e^{ik_z^n z} e^{-\frac{1}{2}|C|(y + \frac{k_z^n}{C})^2} H_j\left(\sqrt{|C|}\left(y + \frac{k_z^n}{C}\right)\right) e^{-i\omega_j t} \quad (9.2.19)$$

expressed as functions of Minkowski coordinates, where

$$\omega = \sqrt{2|C|\left(j + \frac{1}{2}\right) + k_x^2 + m^2} \quad (9.2.20)$$

is the time conjugate parameter, k_x is the x coordinate conjugate parameter, which has a continuous spectrum,

$$k_z^{(n)} = \frac{2\pi}{L}n \quad (9.2.21)$$

is the discrete z coordinate Fourier conjugate parameter, $j \in \mathbb{N}$ labels the Hermite polynomials H_j . The explicit derivation of the modes (9.2.19) is not illuminating and cumbersome. We shall not reproduce it here. The normalisation, using equation (9.2.4), does not differ from the usual flat spacetime normalisation since we chose the spatial hypersurfaces to be orthogonal to the ∂_t Killing vector and therefore the time component of the connection vanishes (as can be easily checked by the gauge choice we made). We have

$$(U_{n,j,k_x}, U_{n',j',k'_x}) = \delta_{n,n'} \delta_{j,j'} \delta(k_x - k'_x) \quad (9.2.22)$$

The modes U are found for different values of these quantum numbers and the field can be expanded on a basis formed by these modes.

$$\Phi = \sum_{n \in \mathbb{Z}, j \geq 0} \int_{-\infty}^{+\infty} dk_x [a(n, j, k_x) U_{n,j,k_x}(x^\mu)] \quad (9.2.23)$$

where $a(n, j, k_x)$ are Fourier coefficients that, once we quantize, will become operators. We now will look at the mode solutions to (2.2.16) in Rindler coordinates on the RRW and LLW. We stress that the Rindler time in the two patches increases towards the future and the past respectively.

The field equation, once we Fourier transform the field in z as $\phi = \exp(ik_z^n z) \tilde{\phi}$, reads

$$\left(\frac{k_\eta^2}{\chi^2} + \frac{1}{\chi} \partial_\chi + \partial_\chi^2 + \partial_y^2 - |C|^2 \left(y + \frac{k_z^n}{C} \right)^2 - m^2 \right) \tilde{\phi} = 0 \quad (9.2.24)$$

A solution exists in terms of modified Bessel functions with purely imaginary order K_{ik_η} and Hermite polynomials H_j . A specific solution to the field equation on the right, i.e. a mode is

$$\begin{aligned} R_\pm = & \frac{C_1}{\sqrt{4\pi|k_\eta|L}} \frac{1}{\sqrt{2^j j! \sqrt{\frac{\pi}{|C|}}}} e^{-\frac{1}{2}|C|(y + \frac{k_z^n}{C})^2} H_j \left(\sqrt{|C|} \left(y + \frac{k_z^n}{C} \right) \right) \\ & \times K_{ik_\eta} \left(\sqrt{m^2 + E_j \chi} \right) e^{\mp ik_\eta y} e^{ik_z^n z}, \end{aligned} \quad (9.2.25)$$

where

$$E_j = 2|C|(j + \frac{1}{2}), \quad (9.2.26)$$

the parameter k_η is real, the coefficients $a(j, n, k_\eta)$ are Fourier coefficients and the number C_1 is some normalization constant. The field Φ can then be expanded in terms of (9.2.25) in the same fashion of (9.2.23). Taking equation (9.2.4) where $\langle \tilde{A}, \bar{e}_t \rangle = 0$ we have the

usual inner product of flat spacetime, where we define the constant η hypersurfaces as those on which to perform the integral. Therefore it can be shown that

$$C_1 = \frac{\sqrt{2k_\eta \sinh(\pi k_\eta)}}{\pi} \quad (9.2.27)$$

Fixing the sign of k_η to be positive, we can then rewrite the expansion of the field as

$$\phi = \sum_{j,n} \int_0^{+\infty} dk_\eta [A(j, n, k_\eta)R_+ + (B(j, n, k_\eta))^\dagger R_-] \quad (9.2.28)$$

where all the dependences in the right positive and negative frequency modes R_\pm are dropped for convenience. If ∂_η is the Killing vector in the RRW, then $i\partial_\eta R_\pm = \pm k_\eta R_\pm$. This expansion is defined on the RRW and we can find, in an analogous fashion, a solution of the field equations on the LRW. We define the left positive and negative frequency modes L_\mp to be

$$L_\pm = \frac{1}{\sqrt{4\pi|k_{\eta'}|L}} \frac{1}{\sqrt{2^j j! \sqrt{\frac{\pi}{|C|}}}} e^{-\frac{1}{2}|C|(y + \frac{k_z^n}{C})^2} H_j\left(\sqrt{|C|}\left(y + \frac{k_z^n}{C}\right)\right) K_{ik_{\eta'}}\left(\sqrt{m^2 + E}\chi'\right) e^{\mp ik_{\eta'}\eta'} e^{ik_z^n z} \quad (9.2.29)$$

and they satisfy $i\partial_\eta L_\pm = \pm k_\eta L_\pm$ where now ∂_η is the Killing vector in the LRW.

9.2.3 Constant background magnetic field - Quantum case: \mathcal{M}_0

We will now quantize the field and compute the BVT between the Minkowski type operators and the Rindler type operators. The quantization of the field is straightforward and can be done by promoting the Fourier coefficients, found in the Chapter 2, to operators.

There are four types of Rindler creation and annihilation operators, the ones that live on the RRW and the ones that live on the LRW. In the same way, we expect to find four different types of Minkowski creation and annihilation operators. To find the modes that carry these Minkowski operators, we continue the two modes on the right in both the upper and lower part of the complex t plane. The continuation is simple and, once the normalisation is worked out we have four Minkowski like modes which have the

following form

$$N_1 := \frac{e^{-i\frac{\pi}{2}(j+n)}}{\sqrt{2 \sinh(\pi k_\eta)}} \left[e^{\frac{\pi}{2} k_\eta} R_+ + e^{-\frac{\pi}{2} k_\eta} L_+ \right] \quad (9.2.30a)$$

$$N_2 := \frac{e^{-i\frac{\pi}{2}(j+n)}}{\sqrt{2 \sinh(\pi k_\eta)}} \left[e^{-\frac{\pi}{2} k_\eta} R_- + e^{\frac{\pi}{2} k_\eta} L_- \right] \quad (9.2.30b)$$

$$M_1 := \frac{e^{-i\frac{\pi}{2}(j-n)}}{\sqrt{2 \sinh(\pi k_\eta)}} \left[e^{-\frac{\pi}{2} k_\eta} R_+ + e^{\frac{\pi}{2} k_\eta} L_+ \right] \quad (9.2.30c)$$

$$M_2 := \frac{e^{-i\frac{\pi}{2}(j-n)}}{\sqrt{2 \sinh(\pi k_\eta)}} \left[e^{\frac{\pi}{2} k_\eta} R_- + e^{-\frac{\pi}{2} k_\eta} L_- \right] \quad (9.2.30d)$$

These modes are analytical everywhere, except possibly the horizon: in addition, they share the same vacuum as the M modes. The phases $\exp(-i\frac{\pi}{2}(j \pm n))$ are added in order to simplify expressions that will follow.

The N modes have been obtained by analytical continuation of the R modes to the left in the upper half plane of Minkowski t coordinate, while the M modes by analytical continuation in the lower half plane of Minkowski t coordinate. Therefore, the N modes will be those carrying particles and M modes carrying antiparticles.

We can expand the field as follows: R_\pm and L_\pm have support respectively on the R and on the L. The field Φ can be expanded as

$$\Phi = \int \left(A^M N_1 + B^M N_2 + (C^M)^\dagger M_1 + (D^M)^\dagger M_2 \right) \quad (9.2.31a)$$

$$\Phi = \int \left(a^R R_+ + (b^R)^\dagger L_+ + (c^R)^\dagger R_- + d^R L_- \right) \quad (9.2.31b)$$

where we have dropped all the dependences for the sake of simplicity. They can be easily recovered by looking at the field expansion (9.2.25). The superscripts M and R refer Minkowski and Rindler type operators respectively as usual.

The creation and annihilation operators satisfy the standard commutation relations

$$\left[A^M(n, j, k_\eta), (A^M)^\dagger(n', j', k'_\eta) \right] = \delta_{n, n'} \delta_{j, j'} \delta(k_\eta - k'_\eta) \quad (9.2.32)$$

All other similar commutators yield the same result both for Minkowski and Rindler type of particles. Particle-antiparticle commutators vanish.

We can finally compute the BVT between the different operators. It is particularly simple to find them by reading the coefficients of the R_\pm, L_\pm modes in (9.2.30d) modes.

One finds

$$a^R = \frac{1}{\sqrt{2 \sinh(\pi k_\eta)}} \left[e^{\frac{\pi}{2} k_\eta} A^M + e^{-\frac{\pi}{2} k_\eta} (C^M)^\dagger \right] \quad (9.2.33a)$$

$$(b^R)^\dagger = \frac{1}{\sqrt{2 \sinh(\pi k_\eta)}} \left[e^{-\frac{\pi}{2} k_\eta} A^M + e^{\frac{\pi}{2} k_\eta} (C^M)^\dagger \right] \quad (9.2.33b)$$

$$(c^R)^\dagger = \frac{1}{\sqrt{2 \sinh(\pi k_\eta)}} \left[e^{-\frac{\pi}{2} k_\eta} B^M + e^{\frac{\pi}{2} k_\eta} (D^M)^\dagger \right] \quad (9.2.33c)$$

$$d^R = \frac{1}{\sqrt{2 \sinh(\pi k_\eta)}} \left[e^{\frac{\pi}{2} k_\eta} B^M + e^{-\frac{\pi}{2} k_\eta} (D^M)^\dagger \right] \quad (9.2.33d)$$

It is immediate to check that

$$\langle 0_{\text{Mink}} | (a^R)^\dagger a^R | 0_{\text{Mink}} \rangle \propto \frac{1}{e^{2\pi k_\eta} - 1} \quad (9.2.34)$$

and the same holds for all other Rindler operators. Number expectation values are then thermally distributed (as is well known, since the operators are delta-normalised in the sense of Dirac, there is an infinite constant of proportionality in (9.2.34). This can be taken care of, for example, by smearing off the field).

We now turn our attention to the Rindler particle content of the Minkowski vacuum. We wish to see what type of particles are present.

We start looking at the formally self adjoint operators

$$J := i \sum [(a^R)^\dagger (b^R)^\dagger - a^R b^R] \quad (9.2.35a)$$

$$J' := i \sum [(c^R)^\dagger (d^R)^\dagger - c^R d^R] \quad (9.2.35b)$$

where again the sum is among all the relevant quantum numbers. As in [10, 91] we can show that

$$A^M = e^{-iJ} a^R e^{iJ} \quad (9.2.36a)$$

$$C^M = e^{-iJ} b^R e^{iJ} \quad (9.2.36b)$$

$$B^M = e^{-iJ'} d^R e^{iJ'} \quad (9.2.36c)$$

$$D^M = e^{-iJ'} c^R e^{iJ'} \quad (9.2.36d)$$

Since $[J, J'] = 0$, in general we have that

$$\hat{O}^M = e^{-i(J+J')} \hat{O}^R e^{i(J+J')} \quad (9.2.37)$$

where the two different operators are chosen according to (9.2.36d). \hat{O} stands for any of the operators and the superscript distinguishes between R and M ones. Given (9.2.37) it is trivial to show that

$$|0_M\rangle = e^{-i(J+J')} |0_R\rangle \quad (9.2.38)$$

which in turn implies, after lengthy calculations, that

$$|0_M\rangle = \frac{1}{(\cosh r)^2} \sum_{n,n'}^{+\infty} (\tanh r)^{n+n'} |n_a, n_b, n'_c, n'_d\rangle \quad (9.2.39)$$

where $\tanh r = \exp(-\pi k_\eta)$ while the subscripts to the particle number in the right hand side refer to the corresponding type of operator. Formally

$$|n_a, n_b, n'_c, n'_d\rangle = \frac{((a^R)^\dagger)^{n_a}}{\sqrt{n_a!}} \dots \frac{((d^R)^\dagger)^{n'_d}}{\sqrt{n'_d!}} |0_R\rangle \quad (9.2.40)$$

This completes the characterization of \mathcal{M}

9.2.4 Constant background magnetic field - Quantum case: \mathcal{M}_-

We are ready to do the geon identification: simple properties of the field solutions, together with the action of J_- and Ω , show that the first line of equation (9.2.31) transforms as follows

$$\begin{aligned} \Phi &= \mathcal{F} \left(A^M N_1 + B^M N_2 + (C^M)^\dagger M_1 + (D^M)^\dagger M_2 \right) \xrightarrow{J_- \circ \Omega} \\ \Phi &= \mathcal{F} \left((A^M)^\dagger M_1(-n) + (B^M)^\dagger M_2(-n) + C^M N_1(-n) + D^M M_2(-n) \right). \end{aligned} \quad (9.2.41)$$

The simple transformation (9.2.41) occurs because of our choice of the modes and of the operators.

This suggests that the field expansion which is suitable in order to perform the geon identification is the following:

$$\Phi = \mathcal{F} \left(A^M N_1 + B^M N_2 + (A^M)^\dagger M_1 + (B^M)^\dagger M_2 \right), \quad (9.2.42)$$

which has one problem: there is an overcounting of the modes in the field expansion. The geon identifications identify couples of modes and therefore we need to find a way to expand Φ on a mode basis which is complete and not overcounted. We introduce the operators $\beta_\sigma, \gamma_\sigma$ $\sigma = 0, 1$ and the Hermitian conjugates such that we get

$$\begin{aligned} \Phi &= \mathcal{F}' \left(\beta_0 N_1 + \gamma_1 N_2 + (\beta_1)^\dagger M_1 + (\gamma_0)^\dagger M_2 + (\beta_1)^\dagger N_1(-n) \right. \\ &\quad \left. + (\gamma_0)^\dagger N_2(-n) + \beta_0 M_1(-n) + \gamma_1 M_2(-n) \right). \end{aligned} \quad (9.2.43)$$

The case where $n = 0$ will be discussed further in this section. Whenever there is a dependence on the quantum number n (in the operators and the modes), we suppress it if it is written in the form n , write it otherwise. The superscript prime over the summation symbols stands that we sum only over $n \geq 0$. The main property that it enjoys, as already stated, is to be invariant under the map $J_- \circ \Omega$.

We can now look for the BVT between the RRW modes, which “survive” after the geon identification, and the field in the form (9.2.43). Define first

$$A^M := \begin{cases} \beta_0(n) & n > 0 \\ \beta_1(-n) & n < 0 \end{cases} \quad (9.2.44a)$$

$$B^M := \begin{cases} \gamma_1(n) & n > 0 \\ \gamma_0(-n) & n < 0 \end{cases} \quad (9.2.44b)$$

Then, the BVT transformations read

$$a^R(n) = \frac{1}{\sqrt{2 \sinh(\pi k_\eta)}} \left[e^{\frac{\pi}{2} k_\eta} A^M(n) + e^{-\frac{\pi}{2} k_\eta} (A^M)^\dagger(-n) \right] \quad (9.2.45a)$$

$$(c^R)^\dagger(n) = \frac{1}{\sqrt{2 \sinh(\pi k_\eta)}} \left[e^{-\frac{\pi}{2} k_\eta} B^M(n) + e^{\frac{\pi}{2} k_\eta} (B^M)^\dagger(-n) \right], \quad (9.2.45b)$$

where $n > 0$.

The case in which $n = 0$ needs some extra care. From (9.2.45), it is easy to understand that the operators on the right hand side are not independent but one is the Hermitian conjugate of the other. This means that there will be a different behavior between the R operators with $n \neq 0$ and those with $n = 0$. Notice that even though there are four operators in (9.2.43), they group together into two M operators when one looks at the BVT. This occurs because of the geon identification.

The number expectation value gives exactly the same result as in (9.2.34).

Again, we define two formally self adjoint operators J, J' such that

$$J = i \sum_{m \geq 0} \left[(a^R)^\dagger(-m)(a^R)^\dagger(m) - a^R(-m)a^R(m) \right] \quad (9.2.46a)$$

$$J' = i \sum_{m \geq 0} \left[(c^R)^\dagger(-m)(c^R)^\dagger(m) - c^R(-m)c^R(m) \right]. \quad (9.2.46b)$$

The M vacuum $|0_M\rangle$ can be then expressed in terms of R vacuum $|0_R^{(-)}\rangle$ as follows

$$|0_M\rangle = e^{-i(J+J')} |0_R^{(-)}\rangle. \quad (9.2.47)$$

Explicitly:

$$|0_M\rangle = \prod_{q, q'=1}^{+\infty} \sum_{\mathbf{N}=0}^{+\infty} \frac{(2n-1)!!(2n')!!}{\sqrt{(2n)!(2n')!}} \frac{e^{-\pi k_\eta(n+n'+m+m')}}{(\cosh r)^3} |2n, 2n'\rangle |m\rangle_q |m\rangle_{-q} |m'\rangle_{q'} |m'\rangle_{-q'}, \quad (9.2.48)$$

where, only for notational simplicity, $\mathbf{N} = (n, n', m, m', m, m')$.

The meaning of the kets on the right is understood from the previous results. q is the discrete quantum number that comes from the compactification of the z direction. We notice one important contribution that comes from the $n = 0$ Rindler operators: this

takes the form in the right hand side of (9.2.48) of the part that depends on n and n' . Comparing this part with the one that depends on m, m', q, q' we clearly see a different structure. The calculations are not illuminating - such calculations have been used in [91] - and this issue arises because for $n = 0$ we can see that in both equations (9.2.45) the two operators are not independent. The $n = 0$ case thus gives rise to some extra interesting structure.

9.2.5 Constant background magnetic field - Quantum case: \mathcal{M}_+

One wishes to look also at \mathcal{M}_+ . As already pointed out, there is no problem in taking the quotient of \mathcal{M}_0 because the $U(1)$ gauge group is sufficient since the connection behaves nicely under J_+ :

$$J_+^*(\tilde{A})(x) = \tilde{A}(x) \quad (9.2.49)$$

Taking the quotient is straightforward and the procedure is similar to that of the subsection 9.2.2. Equation (9.2.41) is modified and will take the form

$$\begin{aligned} \Phi &= \int (A^M N_1 + B^M N_2 + (C^M)^\dagger M_1 + (D^M)^\dagger M_2) \xrightarrow{J_-} \\ \Phi &= \int (A^M N_2 + B^M N_1 + (C^M)^\dagger M_2 + (D^M)^\dagger M_1) \end{aligned} \quad (9.2.50)$$

From (9.2.50) we can, following the calculations done on \mathcal{M}_- , write an invariant expansion of the field

$$\Phi = \int (A^M N_1 + A^M N_2 + (C^M)^\dagger M_1 + (C^M)^\dagger M_2), \quad (9.2.51)$$

where we notice that there is no change of the sign of n involved in the modes. The BVT look like

$$a^R = \frac{1}{\sqrt{2 \sinh(\pi k_\eta)}} \left[e^{\frac{\pi}{2} k_\eta} A^M + e^{-\frac{\pi}{2} k_\eta} (C^M)^\dagger \right] \quad (9.2.52a)$$

$$(c^R)^\dagger = \frac{1}{\sqrt{2 \sinh(\pi k_\eta)}} \left[e^{-\frac{\pi}{2} k_\eta} A^M + e^{\frac{\pi}{2} k_\eta} (C^M)^\dagger \right]. \quad (9.2.52b)$$

The R operators have the same thermal distribution (9.2.34) of those in \mathcal{M}_- . What is different is the R particle content of the M vacuum. The same procedure adopted in the subsection 9.2.4 show that

$$|0_M^+\rangle = \frac{1}{\cosh r} \sum_{n=0}^{+\infty} (\tanh r)^n |n_a n_c\rangle, \quad (9.2.53)$$

where we adopt the notation of the previous subsection for the definition of the kets.

9.2.6 Particle correlations and the meaning of charge

Equations (9.2.48) and (9.2.53), together with the following equation

$$|0_M^0\rangle = \frac{1}{\cosh r} \sum_{n,n'=0}^{+\infty} (\tanh r)^{n+n'} |n_A n_B\rangle |n'_C n'_D\rangle, \quad (9.2.54)$$

which can be found in [10, 91], show that different geon identifications affect the particle correlations. While in (9.2.54) there is a particle-antiparticle correlation, as there is in (9.2.53), on \mathcal{M}_- equation (9.2.48) shows that there are particle-particle and antiparticle-antiparticle correlations. Therefore, we can conclude that the presence of a geon quotient does affect the nonlocal correlations present in the Unruh radiation.

At last comment, we are left with the task of understand the meaning of charge in this context. Considering the standard [18] normal ordered charge operator

$$Q := \sum [(a^M)^\dagger a^M + (b^M)^\dagger b^M - (c^M)^\dagger c^M - (d^M)^\dagger d^M], \quad (9.2.55)$$

which is defined in term of R operators on the whole M spacetime, it is easy to check that, once we perform the geon identification

$$Q \equiv 0. \quad (9.2.56)$$

It is important to notice that the charge operator vanishes identically: one can interpret this fact as showing that there is no global notion of charge on this geon spacetime. In this case it is physically meaningless to define a global charge.

9.3 Electrically charged Reissner Nordtrøm spacetime

In this section we proceed to analyse the behavior of a charged scalar field on a curved background coupled to a background electric field. Our aim is to understand how the Unruh radiation is affected by the geon identifications.

Electrically charged Reissner Nordtrøm spacetime - Classical case

We start by considering the Lagrangian (9.2.1) and field equations (9.2.3). Our metric is now, in (t, r, θ, ϕ) coordinates:

$$ds^2 = -F(r)dt^2 + \frac{dr^2}{F(r)} + r^2 d\Omega^2 \quad (9.3.1)$$

where $F(r) := \left(1 - \frac{r_+}{r}\right)\left(1 - \frac{r_-}{r}\right)$ and $r_\pm := M \pm \sqrt{M^2 - Q^2}$. We are in the genuine Black Hole range $0 < |Q| < M$. We fix the gauge to be

$$\tilde{A} = i \frac{Q}{r} \tilde{d}t \quad (9.3.2)$$

where Q is the charge of the black hole as seen from infinity. Since Gauss law holds, it can be shown that, once the global time orientation is given, an observer near \mathcal{I}^+ (the future null infinity) on the right will, say, measure an electric field pointing outwards from the hole; then, an observer at \mathcal{I}^+ on the left will see an electric field pointing inwards. The two observers will therefore disagree on the sign of the charge of the Black Hole. Although this might seem paradoxical, we are reminded that the two observers live in two causally disconnected regions. Therefore, their disagreement cannot be verified.

We proceed to solve (9.2.3) in these new coordinates. One can give an ansatz for the separation of the solution in the following form:

$$\Phi = \sum_{m,l} \int_{-\infty}^{+\infty} d\Omega Y_m^l(\theta, \phi) R(r) e^{\mp i\omega t}, \quad (9.3.3)$$

where $\omega > 0$ is the conjugate variable to the time coordinate.

We can introduce the generalised tortoise coordinate r_* such that

$$\partial_r = \frac{1}{F} \partial_{r_*}. \quad (9.3.4)$$

We express $R(r)$ in terms of a new function $R(r) := \frac{\Psi(r)}{r}$ and we compute the differential equation for Ψ

$$\left[\left(\omega \pm \frac{eQ}{r} \right)^2 + \partial_{r_*}^2 - \frac{1}{r} \frac{\partial F}{\partial r} F + \frac{l(l+1)}{r^2} F - m^2 F \right] \Psi \mathcal{D} \Psi = 0. \quad (9.3.5)$$

We find the usual spherical harmonics $Y_m^l(\theta, \phi)$. Our phase convention for the spherical harmonics is $(Y_m^l(\theta, \phi))^* = (-1)^m Y_{-m}^l(\theta, \phi)$. It is interesting to look at the behavior of the solution (and differential equation) close to the horizon and far from the horizon.

The two asymptotic behaviors of equation (9.3.5) in these regions are:

$$\mathcal{D} \Psi \stackrel{r \gg r_+}{\sim} \left[-\frac{\partial^2}{\partial r_*^2} - (\Omega^2 - m^2) \right] \Psi \quad (9.3.6a)$$

$$\mathcal{D} \Psi \stackrel{r \sim r_+}{\sim} \left[-\frac{\partial^2}{\partial r_*^2} - \left(\Omega \pm \frac{eQ}{r_+} \right)^2 \right] \Psi, \quad (9.3.6b)$$

and Ω is the conjugate variable to the time coordinate in the Fourier expansion. The generalised tortoise coordinate has explicit relation with r

$$r_* = r + \frac{\alpha}{2} \ln \left(\frac{r}{r_+} - 1 \right) - \frac{r_-^2}{r_+^2} \frac{\alpha}{2} \ln \left(\frac{r}{r_-} - 1 \right), \quad (9.3.7)$$

where

$$\alpha := \frac{2r_+^2}{(r_+ - r_-)} = \frac{1}{\kappa} \quad (9.3.8)$$

is the inverse of the surface gravity κ . Notice that $r_* \rightarrow -\infty$ as $r \rightarrow r_+$.

9.3.1 Normalisation

The issue of normalisation brings in some novel features if compared to the flat spacetime normalisation.

Given (9.2.4) suppose one is able, as in the present case, to separate the solutions in the time coordinate

$$\phi(t, x) = \int d\lambda e^{-iEt} \tilde{\phi}_E(x), \quad (9.3.9)$$

where we drop all unimportant labels for the sake of simplicity and λ collects all of the variables of integration. Since $\phi(t, x)$ satisfies the Klein Gordon field equation, it is possible to show that $\tilde{\phi}_E$ satisfy

$$(E - eV)^2 \tilde{\phi}_E(x) = \tilde{\phi}_E(x) - \Delta \tilde{\phi}_E(x) \quad (9.3.10)$$

and Δ is the Laplacian, V is the potential that comes from the connection.

The relation satisfied by modes corresponding to different quantum numbers is

$$\int d\Sigma \bar{\tilde{\phi}}_{E'}(x) (E' + E - 2eV) \tilde{\phi}_E(x) = \epsilon_E \delta(E' - E). \quad (9.3.11)$$

Where it is possible to assume that all ϵ are nonvanishing. The modes are not strictly speaking orthogonal; in turn this relation can be used to determine the normalisation of the modes. $|\epsilon|$ can be absorbed in the definition of the modes but it is not possible to change the sign of the right hand side of (9.3.11).

9.3.2 Low frequencies: $\omega < m$

In the case where $\omega < m$ it is known from [91] that solutions to (9.3.5) vanish exponentially as $r \rightarrow +\infty$. Furthermore, this allows us to check that the near horizon form is a real function. Their behavior is

$$\Psi^\pm(r_*) \sim \cos(k_\pm r_* + \theta_\pm) \quad r_* \rightarrow -\infty \quad (9.3.12a)$$

$$\Psi^\pm(r_*) \sim e^{-\Gamma r_*} \quad r_* \rightarrow +\infty, \quad (9.3.12b)$$

where we have defined

$$\begin{aligned} \Gamma &= \sqrt{m^2 - \omega^2}, \\ k_\pm &:= \omega \pm \frac{2\gamma_Q}{\alpha}, \\ \gamma_Q &:= \frac{eQ\alpha}{2r_+}, \end{aligned} \quad (9.3.13)$$

an the quantity $\frac{eQ}{r_+}$ is the potential at the horizon and θ_\pm is a phase factor uniquely determined by integrating the field equation.

Once the normalization issue is understood then it is easy to check that

$$(\Psi^{\pm'}, \Psi^{\pm}) = \pm 4\pi k_{\pm} \delta_{ll'} \delta_{mm'} \delta(\omega' - \omega) \quad (9.3.14)$$

and we have reintroduced all the quantum numbers in the r.h.s of (9.3.14).

9.3.3 Electrically charged Reissner Nordtrøm spacetime - Quantum Case

In order to quantise the field and then perform the Bogoliubov transformations we first need to analytically continue the modes from the right hand side to the left. We follow section 9.2 both in spirit and in notation.

Following [101], we choose to look for a gauge on the right that is regular across the future horizon. The gauge transformation maps the field Φ into a new field Φ' as follows

$$\Phi' = e^g \Phi \quad (9.3.15)$$

where $g \in \mathcal{L}(U(1)) \simeq i\mathbb{R}$; in particular, as explained in [20], we can write $g = i\Lambda$ where Λ is a function defined on the spacetime (providing us with a local gauge transformation). The gauge choice we make is

$$\Lambda = \frac{eQ\alpha}{2r_+} \left(\ln\left(\frac{r}{r_+} - 1\right) - \ln\left(\frac{r}{r_-} - 1\right) \right). \quad (9.3.16)$$

The coordinates we use are the Ingoing Eddington-Finkelstein (v, r, θ, ϕ) . We then show that

$$e^{i\Lambda} \Psi^{\pm} \sim e^{\pm i\Omega v} \left[f(r) + e^{ik_{\pm}\alpha \ln\left(\frac{r}{r_+} - 1\right)} \times g(r) \right], \quad (9.3.17)$$

where $f(r)$ and $g(r)$ are analytical functions of r . In order to check whether this is a positive or negative frequency we observe that, as pointed out in [101], we need to look at eigenfunctions of the operator $t^{\mu} D_{\mu}$ where \bar{t} is the future pointing normal at \mathcal{H}^+ on the right. It can be shown that it has the form

$$\bar{t} = t^v (1, 0, 0, 0), \quad (9.3.18)$$

where $t^v = T$ is some nonvanishing scaling factor. We also know that the gauge covariant derivative has the form, in the new gauge

$$\tilde{A}^{new} = \tilde{A}^{old} + \tilde{d}\Lambda = \frac{iQ}{r} \tilde{d}v - \frac{iQ}{r\left(1 - \frac{r_-}{r}\right)} \tilde{d}r, \quad (9.3.19)$$

which of course is regular trough \mathcal{H}^+ . Therefore, (the subscript R stands for right),

$$\frac{1}{T} t^{\mu} D_{\mu} (e^{i\Lambda} \Psi^{\pm}) \Big|_R = \mp i\Omega (e^{i\Lambda} \Psi^{\pm}) \Big|_R. \quad (9.3.20)$$

Apart from the scaling factor T , we see that $e^{i\Lambda}\Psi^\pm$ are eigenfunctions of the operator $t^\mu D_\mu$ with eigenvalue $\mp i\Omega$. It is important to notice that these are exactly the same eigenvalues of the solutions to the field equation of a charged scalar field that is not coupled to any background. We conclude that the background does not influence the near horizon definition of positive and negative frequencies. This allows us to use the same arguments that have been used by [8] to continue the modes across the horizon in the relevant half complex global t plane. The exponential on the right hand side of equation (9.3.17) which depends on r is the singular part when we cross the horizon. We can argue that the continuation will result in adding a multiplicative factor to that part of (9.3.17), therefore obtaining a solution of the form

$$e^{i\Lambda}\Psi^\pm|_F \sim e^{\pm i\Omega v} \left[f'(r) + e^{-\alpha k_\pm \pi} e^{ik_\pm \alpha \ln\left(1 - \frac{r}{r_+}\right)} \times g'(r) \right] \Big|_F, \quad (9.3.21)$$

where $f'(r)$ and $g'(r)$ are analytical functions of r . The subscript F stands for Future and means that we must think of being in the future wedge. We wish to continue this mode back to the left wedge. First of all we transform the modes back in (9.3.21) using the gauge Λ . Then we choose a gauge that is regular across $\mathcal{H}^+|_L$. The function Λ' we are looking for is

$$\Lambda' := -\frac{eQ}{r_+} \frac{\alpha}{2} \left(\ln\left(1 - \frac{r}{r_+}\right) - \ln\left(\frac{r}{r_-} - 1\right) \right). \quad (9.3.22)$$

We choose the Outgoing Eddington Finkelstein coordinates (u, r, θ, ϕ) and close to $\mathcal{H}^+|_L$ and once the modes are gauged using this function, they look like

$$e^{i\Lambda}\Psi^\pm|_F \sim e^{\pm i\Omega u} \left[f''(r) + e^{-ik_\pm \alpha \ln\left(1 - \frac{r}{r_+}\right)} \times g''(t) \right] \Big|_F, \quad (9.3.23)$$

where $f''(r)$ and $g''(r)$ are analytical functions of r and we have defined the analogous of the tortoise coordinate in the Future as

$$r_*|_F = r + \frac{\alpha}{2} \ln\left(1 - \frac{r}{r_+}\right) - \frac{r_-^2}{r_+^2} \frac{\alpha}{2} \ln\left(\frac{r}{r_-} - 1\right), \quad (9.3.24)$$

and this has been used to derive the divergent exponential in (9.3.23). We gauge transform the field and the connection as done before and define the operator which determines the positive and negative frequencies on $\mathcal{H}^+|_L$ as $t^\mu D_\mu$ where, again, \bar{t} is the future pointing normal vector to the horizon. It can be easily checked that

$$\frac{1}{T} t^\mu D_\mu (e^{i\Lambda}\Psi^\pm)|_R = \mp i\Omega (e^{i\Lambda}\Psi^\pm)|_F, \quad (9.3.25)$$

where again $\bar{t} = (t^u, 0, 0, 0)$ is the future pointing normal vector and $T = t^u$ is some nonvanishing scaling factor.

We can conclude the following: the modes retain their close to horizon positive and

negative character, allowing us to use simple arguments to continue them across the horizons themselves. We can continue the mode as done before and obtain

$$e^{i\Lambda'} \Psi^\pm \Big|_L \sim e^{\pm i\Omega v} \left[f'''(r) + e^{-\alpha k_\pm \pi} e^{ik_\pm \alpha \ln(\frac{r^\pm}{r} - 1)} \times g'''(r) \right] \Big|_L, \quad (9.3.26)$$

where $f'''(r)$ and $g'''(r)$ are analytical functions of r . We then transform the mode back with the gauge Λ' to have the analogous of the mode on the right hand side. Finally, putting all together, we see that the modes on the right, once continued in the lower half complex plane transform like

$$\Psi^\pm \Big|_R \longrightarrow e^{-\alpha k_\pm \pi} \Psi^\pm \Big|_L. \quad (9.3.27)$$

We define, for convenience,

$$R^\pm := e^{\mp i\Omega t} \Psi_{l\Omega}^\pm Y_{lm} \Big|_R \quad (9.3.28a)$$

$$L^\pm := e^{\mp i\Omega t} \Psi_{l\Omega}^\pm Y_{lm} \Big|_L, \quad (9.3.28b)$$

where, on the right hand side, we have restored the quantum numbers the modes depend on for the sake of completeness. Finally we obtain an explicit solution for the normalised Minkowski like modes

$$N_1 := \frac{e^{\frac{i(l+m)\pi}{2}}}{2\sqrt{\sinh(\pi k_+ \alpha)}} \left[e^{\frac{\alpha\pi}{2} k_+} R^+ + e^{-\frac{\alpha\pi}{2} k_+} L^+ \right] \quad (9.3.29a)$$

$$N_2 := \frac{e^{\frac{i(l+m)\pi}{2}}}{2\sqrt{\sinh(\pi k_- \alpha)}} \left[e^{\frac{\alpha\pi}{2} k_-} R^- + e^{-\frac{\alpha\pi}{2} k_-} L^- \right] \quad (9.3.29b)$$

$$M_1 := \frac{e^{\frac{i(l+m)\pi}{2}}}{2\sqrt{\sinh(\pi k_+ \alpha)}} \left[e^{-\frac{\alpha\pi}{2} k_+} R^+ + e^{\frac{\alpha\pi}{2} k_+} L^+ \right] \quad (9.3.29c)$$

$$M_2 := \frac{e^{\frac{i(l+m)\pi}{2}}}{2\sqrt{\sinh(\pi k_- \alpha)}} \left[e^{-\frac{\alpha\pi}{2} k_-} R^- + e^{\frac{\alpha\pi}{2} k_-} L^- \right]. \quad (9.3.29d)$$

We expand the field in terms of Minkowski like modes and modes that live separately on the right and left side

$$\phi = \int \left(A_1^M N_1 + A_2^M N_2 + (B_1^M)^\dagger M_1 + (B_2^M)^\dagger M_2 \right) \quad (9.3.30a)$$

$$\phi = \int \left(a_1 R^+ + (a_2)^\dagger R^- + (b_1)^\dagger L^+ + b_2 L^- \right). \quad (9.3.30b)$$

We compute the commutators between the operators and again find relations analogue to (9.2.32) where the quantum numbers have to be replaced with m, j, Ω . These relations allow us to compute the Bogoliubov transformations between the different type of

operators

$$(a_1)^\dagger := \frac{1}{2\sqrt{\sinh(\pi k_+ \alpha)}} \left[e^{\frac{\alpha\pi}{2} k_+} (A_1^M)^\dagger + e^{-\frac{\alpha\pi}{2} k_+} B_1^M \right] \quad (9.3.31a)$$

$$b_1 := \frac{1}{2\sqrt{\sinh(\pi k_- \alpha)}} \left[e^{\frac{\alpha\pi}{2} k_-} A_2^M + e^{-\frac{\alpha\pi}{2} k_-} (B_2^M)^\dagger \right] \quad (9.3.31b)$$

$$a_2 := \frac{1}{2\sqrt{\sinh(\pi k_+ \alpha)}} \left[e^{-\frac{\alpha\pi}{2} k_+} (A_1^M)^\dagger + e^{\frac{\alpha\pi}{2} k_+} B_1^M \right] \quad (9.3.31c)$$

$$(b_2)^\dagger := \frac{1}{2\sqrt{\sinh(\pi k_- \alpha)}} \left[e^{-\frac{\alpha\pi}{2} k_-} A_2 + e^{\frac{\alpha\pi}{2} k_-} (B_2^M)^\dagger \right]. \quad (9.3.31d)$$

Computing the usual number expectation value we find, for any of these operators

$$\langle 0_{\mathcal{M}} | o^\dagger o | 0_{\mathcal{M}} \rangle = \frac{1}{4(e^{2\alpha k_\pm \pi} - 1)}, \quad (9.3.32)$$

where o is a generic Rindler operator and the \pm sign depends on the operator. This result agrees with [91].

As done before, we compute how the modes (9.3.29) transform under the geon map. We find that they transform as

$$N_i(m) \longrightarrow M_i(-m) \quad (9.3.33)$$

where $i = 1, 2$; therefore we are able to take the geon identification and find that

$$(a_1)^\dagger := \frac{1}{2\sqrt{\sinh(\pi k_+ \alpha)}} \left[e^{\frac{\alpha\pi}{2} k_+} (A_1^M)^\dagger(m) + e^{-\frac{\alpha\pi}{2} k_+} A_1^M(-m) \right] \quad (9.3.34a)$$

$$a_2 := \frac{1}{2\sqrt{\sinh(\pi k_- \alpha)}} \left[e^{\frac{\alpha\pi}{2} k_-} A_2^M(m) + e^{-\frac{\alpha\pi}{2} k_-} (A_2^M)^\dagger(-m) \right], \quad (9.3.34b)$$

which, again, allows us to see that

$$\langle 0_{\mathcal{M}} | a_i^\dagger a_i | 0_{\mathcal{M}} \rangle = \frac{1}{4(e^{2\alpha k_\pm \pi} - 1)} \quad (9.3.35)$$

where again $i = 1, 2$, the $+$ refers to the type 1 operator while $-$ to the type 2. We have already discussed the $m = 0$ case and the issue here is exactly the same.

9.3.4 High frequencies: $\Omega > m$

We have seen which are the effects on the particle content emitted from a Black Hole of the geon identifications in the case of low frequencies. We now turn our attention to the high frequency case, $\Omega > m$. Following [91] it is possible to show that in this regime, the radial field equation behaves like

$$\mathcal{D}\Psi \stackrel{r \gg r_+}{\sim} \left[\frac{\partial^2}{\partial r_*^2} + \Gamma^2 + \Theta_\pm \frac{\alpha}{2r_*} + \left(1 - \frac{r_-^2}{r_+^2}\right) \Theta_\pm \frac{\ln\left(\frac{2r_*}{\alpha}\right)}{\left(\frac{2r_*}{\alpha}\right)^2} + O\left(\frac{1}{r_*^2}\right) \right] \Psi \quad (9.3.36a)$$

$$\mathcal{D}\Psi \stackrel{r \sim r_+}{\sim} \left[-\frac{\partial^2}{\partial r_*^2} - \left(\Omega \pm \frac{eQ}{r_+}\right)^2 \right] \Psi \quad (9.3.36b)$$

where $\Gamma := \sqrt{\Omega^2 - m^2}$ and

$$\Theta_{\pm} := \frac{2}{\alpha} [(r_+ - r_-)m^2 \pm 2eQ\Omega] \quad (9.3.37)$$

have been defined to simplify the formulas. The asymptotic form of the solutions for $r \gg r_+$ can be shown to take the form

$$\Psi^{\pm} \sim e^{\pm i(\Gamma r_* + \Sigma_{\pm} \ln(\frac{2r_*}{\alpha}))}, \quad (9.3.38)$$

where

$$\Sigma_{\pm} := \frac{\Theta_{\pm}}{2\Gamma}. \quad (9.3.39)$$

Again, since there is a complete formal analogy with calculations in [91], we choose two sets of solutions of the form

$$\overset{\leftarrow}{\Psi}^{\pm} \sim \begin{cases} \overset{\leftarrow}{B}_{\pm} e^{-ik_{\pm} r_*} & r_* \longrightarrow -\infty \\ e^{-i(\Gamma r_* + \Sigma_{\pm} \ln(\frac{2r_*}{\alpha}))} + \overset{\leftarrow}{A}_{\pm} e^{i(\Gamma r_* + \Sigma_{\pm} \ln(\frac{2r_*}{\alpha}))} & r_* \longrightarrow +\infty \end{cases} \quad (9.3.40a)$$

$$\overset{\rightarrow}{\Psi}^{\pm} \sim \begin{cases} e^{ik_{\pm} r_*} + \vec{A}_{\pm} e^{-ik_{\pm} r_*} & r_* \longrightarrow -\infty \\ \vec{B}_{\pm} e^{i(\Gamma r_* + \Sigma_{\pm} \ln(\frac{2r_*}{\alpha}))} & r_* \longrightarrow +\infty \end{cases} \quad (9.3.40b)$$

and the arrows on top stand for “ingoing” and “outgoing”, meaning that we have imposed boundary conditions on these solutions such that the “outgoing” have only an outgoing component at infinity and analogously for the “ingoing” solution.

We can compute the Wronskian of these solutions and, since in this case it is conserved, gain some conditions on the coefficients. One finds that

$$\begin{cases} \Gamma \overset{\leftarrow}{B}_{\pm} = \vec{B}_{\pm} k_{\pm} \\ \Gamma \overset{\leftarrow}{B}_{\pm} (\vec{A}_{\pm})^* = -k_{\pm} \overset{\leftarrow}{A}_{\pm} (\vec{B}_{\pm})^* \\ \Gamma |\overset{\leftarrow}{B}_{\pm}|^2 = k_{\pm} [1 - |\vec{A}_{\pm}|^2] \\ \Gamma [1 - |\overset{\leftarrow}{A}_{\pm}|^2] = k_{\pm} |\vec{B}_{\pm}|^2 \end{cases} \cdot \quad (9.3.41)$$

There are 16 real parameters and 12 real relations that leave us with 4 free parameters which, in principle, are uniquely determined by solving the field equation. There is no interesting insight in repeating these lengthy calculations so we will state the results. We can normalise both the ingoing and outgoing modes, keeping in mind the inner product as defined in [102] and it is possible to show that for

$$e^{\mp i\Omega t} \overset{\leftarrow}{\Psi}^{\pm} \quad (9.3.42)$$

$$e^{\mp i\Omega t} \overset{\rightarrow}{\Psi}^{\pm} \quad (9.3.43)$$

the normalisation constants are

$$\sqrt{2\Gamma \pm \frac{k_{\pm}^2 \mp \Gamma^2}{\Gamma} [1 - |\overset{\leftarrow}{A}_{\pm}|]} \quad (9.3.44)$$

$$\sqrt{\pm 2k_{\pm} \mp \frac{k_{\pm}^2 \mp \Gamma^2}{k_{\pm}} [1 - |\overset{\leftarrow}{A}_{\pm}|]} \quad (9.3.45)$$

respectively. These modes do not transform nicely under our geon map. We will look for a linear combination of the modes, in terms of two pairs of coefficients a_+, b_+ and a_-, b_- in such a way that the field expansion in terms of them is invariant under the geon map. We have two different linear combinations, one for the positive frequencies and one for the negative frequencies. Calculations are tedious and not illuminating, therefore we will briefly explain what are the following steps to take. We would like to normalise these new modes obtained by a linear combination of the old ones. We then define the new modes as

$$R^{\pm} := \left(a_{\pm} e^{\mp i\Omega t} \overset{\rightarrow}{\Psi}^{\pm} + b_{\pm} e^{\mp i\Omega t} \overset{\leftarrow}{\Psi}^{\pm} \right) Y_{lm} \Big|_R, \quad (9.3.46)$$

which are normalised once one does a clever choice of the a and b coefficients using the properties of the Wronskian displayed before. This can be done. Just staring at the definition of R_{\pm} makes one realise that these modes can be continued exactly as those in the low Ω case across the horizons. Formally everything is the same and therefore there are no new mathematical or conceptual issues that arise.

We define the modes

$$N_1 := \frac{(e)^{\frac{i(l+m)\pi}{2}}}{2\sqrt{\sinh(\pi k_+ \alpha)}} \left[e^{\frac{\alpha\pi}{2} k_+} R^+ + e^{-\frac{\alpha\pi}{2} k_+} L^+ \right] \quad (9.3.47a)$$

$$N_2 := \frac{(e)^{\frac{i(l+m)\pi}{2}}}{2\sqrt{\sinh(\pi k_- \alpha)}} \left[e^{\frac{\alpha\pi}{2} k_-} R^- + e^{-\frac{\alpha\pi}{2} k_-} L^- \right] \quad (9.3.47b)$$

$$M_1 := \frac{(e)^{\frac{i(l+m)\pi}{2}}}{2\sqrt{\sinh(\pi k_+ \alpha)}} \left[e^{-\frac{\alpha\pi}{2} k_+} R^+ + e^{\frac{\alpha\pi}{2} k_+} L^+ \right] \quad (9.3.47c)$$

$$M_2 := \frac{(e)^{\frac{i(l+m)\pi}{2}}}{2\sqrt{\sinh(\pi k_- \alpha)}} \left[e^{-\frac{\alpha\pi}{2} k_-} R^- + e^{\frac{\alpha\pi}{2} k_-} L^- \right] \quad (9.3.47d)$$

where it is immediately evident the formal analogy between this case and the the $\Omega < m$ one. We are still left with the unknown coefficients of the linear combinations but we will show how they can be fixed. We check how the modes (9.3.47) transform under the geon map. It can be shown that

$$N_{\sigma}(n) \longrightarrow M_{\sigma}(-n), \quad (9.3.48)$$

where $\sigma = 1, 2$, provided that

$$b_{\pm} = \sqrt{\frac{\Gamma}{k_{\pm}(1 - \overset{\leftarrow}{A}_{\pm})}} \left(a_{\pm}^* - a_{\pm} \overset{\leftarrow}{A}_{\pm} \right). \quad (9.3.49)$$

This fixes b_{\pm} in terms of a_{\pm} leaving us with two real free parameters.

We can once more build a field expansion in term of different modes

$$\phi = \int (A_1^M N_1 + A_2^M N_2 + (B_1^M)^\dagger M_1 + (B_2^M)^\dagger M_2) \quad (9.3.50a)$$

$$\phi = \int (a_1 R^+ + (a_2)^\dagger R^- + (b_1)^\dagger L^+ + b_2 L^-) \quad (9.3.50b)$$

and again there is an exact formal analogy between these relations and (9.3.30). We can conclude that the relations (9.3.32) hold for the operators in the high Ω case as well and (9.3.34) and (9.3.35) too. Therefore, the particle correlations are not affected by Ω being high or low.

There is one more issue that we would like to discuss and that agrees with results well known in literature under the name of superradiant modes: as shown in [103], a necessary condition for the superradiance to occur is that

$$\frac{i}{2\Gamma} W(\Psi^\pm, (\Psi^\pm)^*)|_{\tilde{r}_*} > 0, \quad (9.3.51)$$

where W is the Wronskian defined for two functions f, g as

$$W(f, g) = f'g - fg' \quad (9.3.52)$$

and the point \tilde{r}_* is where some boundary conditions are imposed. Since the Wronskian in our case is constant, it can be calculated either for $r_* \rightarrow \pm\infty$. If we look for superradiance then

$$|\overleftarrow{A}_\pm|^2 > 0, \quad (9.3.53)$$

which in turn, using some of the relations (9.3.41) turns out to be equivalent to $k_\pm < 0$. This implies

$$m < \Omega < \mp \frac{eQ}{r_+} \quad (9.3.54)$$

which perfectly agrees with [19, 101, 103].

9.4 Conclusions

In this chapter we have analyzed charged scalar fields in two different geon spacetimes: flat spacetime where the charged field was coupled to a classical background magnetic field and electrically charged Reissner-Nordström spacetime where the field was coupled to a classical background electric field. We have revised the construction of a geon and have discussed what issues arise when there is a constant classical background magnetic field. In particular, we have found that one needs to enlarge the gauge group to accommodate for transformations within the disconnected component of the enlarged group. These

allow us to define the magnetic geon. We then compute the BVT and show that there is a specific geon configuration for which the standard particle-antiparticle correlations change into particle-particle and antiparticle-antiparticle correlations.

We have also addressed the structure of the nonlocal correlations in the geon version of the electrically charged Reissner-Nordström black hole. We have analyzed the low and high frequency regimes. We find that, as in the previous case, the correlations are affected by the topology of the spatial foliations.

CHAPTER 10

Work in progress and future work

“ Cuando aún era de noche,
cuando aún no había día,
cuando aún no había luz,
se reunieron.
Se convocaron los dioses,
allá en Teotihuacan.”

Codex Matritense

10.1 Work in progress and future work

The results described in this work have been obtained during my PhD studies. I have also initiated and contributed to other projects which are now at different stages of progress. I will briefly describe the projects aims

Slow light - the predictions of the cavities chapters are plagued by the magnitude of the h parameter. Since $h = A\delta/c^2$, already at first order and for reasonable cavities and accelerations, perhaps $\delta = 1\text{cm}$ and $A \sim 1 - 10g$, $h \sim 10^{-16}$. Although one can compute exactly the magnitude of the contribution, it is clear that the effects are very small. Furthermore, in the field of quantum optics, standard laboratory techniques for measuring corrections to entanglement such as tomography, allow for 1 – 5% relative error on the entanglement. These daunting figures seem to indicate that the effects we have found might not be measurable experimentally, at least with current technology.

On the other hand and from a completely different perspective, the Casimir commu- nity has been awaiting experimental demonstration of the dynamical Casimir effect for almost four decades [13].

I have suggested that introducing dispersive media within cavities might allow for “slow light” within and therefore higher values of the h parameters. This simple sug- gestion comes from the observation that $h = A\delta/c^2$ is plagued by a large speed of light in the denominator. If one was able to reproduce the predictions obtained in empty cavities in the case of cavities filled with disperseve media, it might be possible to look for configurations where the new speed of light c_{new} could satisfy $c_{\text{new}} < c$ and perhaps also $c_{\text{new}} \ll c$. I have started investigating such possibilities in collaboration with Dr. Daniele Faccio (Heriot Watt, Edinburgh, UK), Dr. Chris Binns (University of Leices- ter, Leicester, UK), Dr. Sergio Cacciatori (Universita‘ dell’Insurbia, Como, Italy) and colleghi di Sergio e Daniele and Jorma.

Extended detectors in Relativistic Quantum Information - In order to exploit quantum resources, physical devices capable of utilizing entanglement are needed. The standard device considered in literature is the point like Unruh-DeWitt detector which couples locally to global fields [8]. Although it has provided some insight of how to extract entanglement within RQI settings, such detector is a highly idealized device. A more physical implementation is the extended version of the point like Unruh-DeWitt detector, as considered in [104] and further studied in [87]. Such detectors, whether extended or not, couple to the whole spectrum of the field.

In collaborations with Dr. Achim Kempf (University of Waterloo, Canada), Dr. Ivette Fuentes and Dr. Jorma Louko (University of Nottingham, UK), I am currently

investigating extended Unruh-DeWitt detectors when the spatial or frequency distribution is such that one can employ mathematical techniques successfully used in Quantum Gravity to couple the detector to a discrete set of modes. Such approach has the advantage to leave open the opportunity to employ the powerful language of CV to compute detector response, entanglement extraction from fields and so on. We aim at introducing a physical model of detector which could in principle address measurable effects.

Experimental verification of predictions from the cavity travel scenarios - The cavity travel techniques I have described in this work and that have been thoroughly investigated promise to have interesting experimental applications. We envisage that predictions of this work will attract interest from scientists that aim at measuring the effects of relativity on QI tasks. We have become aware that space agencies from Canada and USA are interested in performing space based experiments which involve the use of protocols studied in the area of Quantum Key Distribution. Such agencies have initiated preliminary theoretical interest in expanding on the technological and theoretical understanding of the physics of these settings.

We believe that our results provide the first steps towards designing experiments which can test the effects of relativity on entanglement. Our cavities are local, contain massless bosons and require sizes and acceleration which can be achieved with current technology.

We wish to investigate further our cavity scenarios and provide a concrete and realistic model for quantifying effects of motion on quantum protocols.

Index

- Anticommutator, 87
- Basic Building Block, 63
- Bipartite system, 24
- Bogoliubov identity, 20
- Bogoliubov transformation, 20, 22, 65, 71
- Bogoliubov transformation, bosonic, 22
- Bogoliubov transformation, fermionic, 23
- Bogoliubov Transformations, 19
- Boundary condition, 82, 108
- Building block, 114
- Cauchy surface, 13
- Cavity, 62
- Commutator, CV, 111
- Continuous variable, 110
- Coordinate chart, 12
- Coordinate transformation, 12
- Coordinates, Minkowski, 14
- Coordinates, Rindler, 16, 62, 84
- Covariance matrix, 111
- Degenerate eigenvalues, 70
- Dirac equation, 81, 84
- Dirac-Clifford algebra, 81
- Dirichlet boundary conditions, 62
- Entanglement, 23, 26
- Entanglement, measure of, 26
- Fermionic field, 81
- Field equation, 129
- Field Equations, 11
- Frequency, negative, 20
- Frequency, positive, 20
- Gaussian state, 111
- Gaussian, logarithmic, 42
- Globally hyperbolic, 13, 129
- Hadamard lemma, 88
- Helicity, 82
- Hilbert space, 24
- Inner product, 15, 21, 36, 129
- Inner product, fermionic, 82, 84
- KG equation, 14
- Killing vector, 13, 17, 62, 63
- Least action principle, 11
- Lie derivative, 13
- Logarithmic negativity, 28
- Lorentz transformations, 14
- Manifold, 12
- Metric, 12
- Minkowski spacetime, 14, 16
- Mixedness, 25
- Multipartite system, 24
- Negativity, 27, 39, 51, 113
- Negativity, logarithmic, 116
- Normalization, 19
- Partial trace, 26
- Partial traspose, 70
- Path, 12
- Perturbation theory, 70

INDEX

- Perturbation theory, degenerate, 70, 115
- Perturbative regime, 66
- Phase space variable, 110
- Physical frequency, 50
- Polylogarithm, 72
- Quadrature phase operator, 110
- Resonance condition, 114
- Resonance time, total, 118
- Right/Left handed, 82
- Right/Left movers, 82
- Scalar field, charged, 47, 48
- Scalar field, massive, 15, 62, 76, 100
- Scalar field, massless, 15, 35, 71, 108
- Scalar field, uncharged, 13
- Set of coordinates, 12
- Single Mode Approximation, 38
- Smearing, 41
- Smearing function, 44
- Spacetime, 12
- Spacetime, Minkowski, 62
- Spinor, 81
- State, bipartite, 24
- State, entangled, 25
- State, mixed, 25
- State, partially transposed, 27
- State, pure, 25
- State, separable, 25
- Symplectic eigenvalues, 115
- symplectic form, 110
- Symplectic group, 111
- Symplectic transformation, 111
- Two mode truncation, 108
- Uncertainty relation, 42, 43
- Vector, 12
- Vector field, 12
- Von Neumann Entropy, 27
- Wave packet, 41
- Zero mode, 83

References

- [1] C. H. Bennett, G. Brassard, C. Crépeau, R. Jozsa, A. Peres, and W. K. Wootters. Teleporting an unknown quantum state via dual classical and Einstein-Podolsky-Rosen channels. *Phys. Rev. Lett.*, 70:1895, 1993.
- [2] D. Bouwmeester, J.-W. Pan, K Mattle, M Eibl, H Weinfurter, and A Zeilinger. Experimental quantum teleportation. *Nature*, 390:575, 1997.
- [3] M. Czachor. Einstein-Podolsky-Rosen-bohm experiment with relativistic massive particles. *Phys. Rev. A*, 55:72, 1997.
- [4] A. Peres, P. F. Scudo, and D. R. Terno. Quantum entropy and special relativity. *Phys. Rev. Lett.*, 88:230402, 2002.
- [5] I. Fuentes-Schuller and R. Mann. Alice falls into a black hole. *Phys. Rev. Lett.*, 95:120404, 2005.
- [6] P. M. Alsing, D. McMahon, and G. J. Milburn. Teleportation in a non-inertial frame. *J. Opt. B: Quantum Semiclass. Opt.*, 6:S834, 2004.
- [7] P. M. Alsing, I. Fuentes-Schuller, R. B. Mann, and T. E. Tessier. Entanglement of Dirac fields in noninertial frames. *Phys. Rev. A*, 74:032326, 2006.
- [8] W. G. Unruh. Notes on black hole evaporation. *Phys. Rev. D*, 14:870, 1976.
- [9] A. Fabbri and J. Navarro-Salas. *Modeling Black Hole Evaporation*. Imperial College Press, 2005.
- [10] N. D. Birrell and P. C. W. Davies. *Quantum fields in curved space*. Cambridge University Press, Cambridge, 1984.
- [11] T. G. Downes, I. Fuentes, and T. C. Ralph. Entangling moving cavities in noninertial frames. *Phys. Rev. Lett.*, 106:210502, 2010.
- [12] M. Bordaga, U. Mohideenb, and V. M. Mostepanenko. New developments in the Casimir effect. *Physics Reports*, 353:1, 2001.

REFERENCES

- [13] C. M. Wilson and et.al. Observation of the dynamical Casimir effect in a superconducting circuit. *Nature*, 479:376, 2011.
- [14] J. L. Ball, I. Fuentes-Schuller, and F. P. Schuller. Entanglement in an expanding spacetime. *Phys. Lett. A*, 359:550, 2006.
- [15] D. E. Bruschi, J. Louko, E. Martín-Martínez, A. Dragan, and I. Fuentes. The Unruh effect in quantum information beyond the single-mode approximation. *Phys. Rev. A*, 82:042332, 2010.
- [16] J. Louko. Geon black holes and quantum field theory. *arXiv:1001.0124*. Talk given at the First Mediterranean Conference on Classical and Quantum Gravity, Kolymbari (Crete, Greece), September 2009. Dedicated to Rafael Sorkin.
- [17] P. C. W. Davies. Scalar production in Schwarzschild and Rindler metrics. *J. of Phys. A*, 8:609, 1975.
- [18] M. Srednicki. *Quantum Field Theory*. Cambridge University Press, Cambridge, 2007.
- [19] R. M. Wald. *General Relativity*. University of Chicago Press, Chicago, 1984.
- [20] Y. Choquet-Bruhat and C. M. DeWitt. *Analysis, Manifolds and Physics*. Elsevier, Amsterdam, 1977.
- [21] NIST. *Digital Library of Mathematical Functions*. National Institute of Standards and Technology, 2010.
- [22] R. M. Wald. *Quantum field theory in curved spacetime and black hole thermodynamics*. University of Chicago Press, Chicago, 1994.
- [23] P. W. Shor. *Algorithms for quantum computation: discrete logarithms and factoring*. Foundations of Computer Science, 1994 Proceedings., 35th Annual Symposium on Date of Conference: 20-22 Nov 1994, 1994.
- [24] A. Einstein, B. Podolsky, and N Rosen. Can quantum-mechanical description of physical reality be considered complete? *Phys. Rev.*, 47:777, 1935.
- [25] J. S. Bell. On the Einstein-Poldolsky-Rosen paradox. *Physics*, 1:195, 1964.
- [26] A. Peres. Separability criterion for density matrices. *Phys. Rev. Lett.*, 8:1413, 1996.
- [27] V Vedral and M. B. Plenio. Entanglement measures and purification procedures. *Phys. Rev. A*, 3:1619–1633, 1998.

REFERENCES

- [28] M. Horodecki, P. Horodecki, and R. Horodecki. Mixed-state entanglement and distillation: Is there a “bound” entanglement in nature? *Phys. Rev. Lett.*, 80:5239, 1998.
- [29] G. Vidal and R. F. Werner. Computable measure of entanglement. *Phys. Rev. A*, 65:032314, 2002.
- [30] K. Audenaert, M. B. Plenio, and J. Eisert. Entanglement cost under positive-partial-transpose-preserving operations. *Phys. Rev. Lett.*, 90:027901, 2003.
- [31] K. Audenaert, M. B. Plenio, and J. Eisert. An introduction to entanglement measures. *Quant. Inf. Comput.*, 7:1, 2007.
- [32] D. E. Bruschi, A. Dragan, I. Fuentes, and J. Louko. Particle and antiparticle bosonic entanglement in noninertial frames. *Phys. Rev. D*, 86:025026, 2012.
- [33] D. E. Bruschi, A. Dragan, A. R. Lee, I. Fuentes, and J. Louko. Motion-generated entanglement resonance. *arXiv:1203.0655*, 2012.
- [34] D. E. Bruschi and J. Louko. Charged Unruh effect on geon spacetimes. *arXiv:1003.1297 [gr-qc]*.
- [35] R. M. Gingrich and C. Adami. Quantum entanglement of moving bodies. *Phys. Rev. Lett.*, 89:270402, 2003.
- [36] P. M. Alsing and Milburn G. J. Teleportation with a uniformly accelerated partner. *Phys. Rev. Lett.*, 91:180404, 2003.
- [37] H. Terashima and M. Ueda. Einstein-Podolsky-Rosen correlation in a gravitational field. *Phys. Rev. A*, 69:032113, 2004.
- [38] Y. Shu. Entanglement in relativistic quantum field theory. *Phys. Rev. D*, 70:105001, 2004.
- [39] G. Adesso, I. Fuentes-Schuller, and M. Ericsson. Continuous-variable entanglement sharing in noninertial frames. *Phys. Rev. A*, 76:062112, 2007.
- [40] K. Brádler. Eavesdropping of quantum communication from a noninertial frame. *Phys. Rev. A*, 75:022311, 2007.
- [41] Y. Ling, S. He, W. Qiu, and H. Zhang. Quantum entanglement of electromagnetic field in non-inertial reference frames. *J. of Phys. A*, 40:9025, 2007.
- [42] D. Ahn, Y Moon, R. Mann, and I. Fuentes-Schuller. The black hole final state for the Dirac fields in Schwarzschild spacetime. *JHEP*, 06:062, 2008.

REFERENCES

- [43] Q. Pan and J. Jing. Hawking radiation, entanglement, and teleportation in the background of an asymptotically flat static black hole. *Phys. Rev. D*, 78:065015, 2008.
- [44] J. Doukas and L. C. L. Hollenberg. Loss of spin entanglement for accelerated electrons in electric and magnetic fields. *Phys. Rev. A*, 79:052109, 2009.
- [45] G. Steeg and N. C. Menicucci. Entangling power of an expanding universe. *Phys. Rev. D*, 79:044027, 2009.
- [46] J. León and E. Martín-Martínez. Spin and occupation number entanglement of Dirac fields for noninertial observers. *Phys. Rev. A*, 80:012314, 2009.
- [47] G. Adesso and I. Fuentes-Schuller. Correlation loss and multipartite entanglement across a black hole horizons. *Quant. Inf. Comput.*, 9:0657, 2009.
- [48] N. Friis, P. Köhler, E. Martín-Martínez, and R. A. Bertlmann. Residual entanglement of accelerated fermions is not nonlocal. *Phys. Rev. A*, 84:062111, 2011.
- [49] E. Martín-Martínez and J. León. Quantum correlations through event horizons: Fermionic versus bosonic entanglement. *Phys. Rev. A*, 81:032320, 2010.
- [50] E. Martín-Martínez and J. León. Population bound effects on bosonic correlations in noninertial frames. *Phys. Rev. A*, 81:052305, 2010.
- [51] M. Montero and E. Martín-Martínez. The entangling side of the Unruh-Hawking effect. *JHEP*, 1107:006, 2011.
- [52] P. Villoresi, T. Jennewein, F. Tamburini, M. Aspelmeyer, Bonato, R. Ursin, C. Pernechele, V. Luceri, G. Bianco, A. Zeilinger, and C. Barbieri. Experimental verification of the feasibility of a quantum channel between space and earth. *New J. Phys.*, 10:033038, 2008.
- [53] C. Bonato, A. Tomaello, V. D. Deppo, G. Naletto, and P. Villoresi. Feasibility of satellite quantum key distribution. *New J. Phys.*, 11:045017, 2009.
- [54] S. Schlicht. Considerations on the Unruh effect: Causality and regularization. *Class. Quant. Grav.*, 21:4647, 2004.
- [55] P. Langlois. Causal particle detectors and topology. *Annals Phys.*, 321:2027, 2005.
- [56] A. Rauschenbeutel, P. Bertet, S. Osnaghi, G. Nogues, M. Brune, J.M. Raimond, and S. Haroche. Controlled entanglement of two field modes in a cavity quantum electrodynamics experiment. *Phys. Rev. A*, 64:050301, 2001.

REFERENCES

- [57] D. E. Browne, M. B. Plenio, and S. F. Huelga. Robust creation of entanglement between ions in spatially separate cavities. *Phys. Rev. Lett.*, 91:067901, 2003.
- [58] D. E. Bruschi, J. Louko, and I. Fuentes. Voyage to alpha centauri: Entanglement degradation of cavity modes due to motion. *Phys. Rev. D*, 85:061701(R), 2012.
- [59] T. M. Dunster. Bessel functions of purely imaginary order, with an application to second-order linear differential equations having a large parameter. *SIAM J. Math. Anal.*, 21:995, 1990.
- [60] E. Martín-Martínez and I. Fuentes. Redistribution of particle and antiparticle entanglement in noninertial frames. *Phys. Rev. A*, 83:052306, 2011.
- [61] E. Martín-Martínez. Relativistic quantum information: developments in quantum information in general relativistic scenarios. *arXiv:1106.0280 [quant-ph]*, PhD Thesis, 2011.
- [62] J. F. Clauser, M. A. Horne, A. Shimony, and R. A. Holt. Proposed experiment to test local hidden-variable theories. *Phys. Rev. Lett.*, 23:880, 1969.
- [63] R. Horodecki, P. Horodecki, and M. Horodecki. Violating Bell inequality by mixed spin-1/2 states: necessary and sufficient condition. *Phys. Lett. A*, 200:340, 1995.
- [64] M. Reed and M. Simon. *Methods of Modern Mathematical Physics Vol. 2*. Academic Press, 1975.
- [65] G. Bonneau, J. Faraut, and G. Valent. Self-adjoint extensions of operators and the teaching of quantum mechanics. *Am. J. Phys*, 69:322, 2001.
- [66] D. McMahon, P. M. Alsing, and P. Embid. The Dirac equation in Rindler space: A pedagogical introduction. *arXiv:gr-qc/0601010v2*, 2006.
- [67] M. Montero and E. Martín-Martínez. Fermionic entanglement ambiguity in non-inertial frames. *Phys. Rev. A*, 83:062323, 2011.
- [68] A. Smith and R. B. Mann. Persistence of tripartite nonlocality for non-inertial observers. *arXiv:1107.4633v1 [quant-ph]*, 2011.
- [69] N. Friis, D. E. Bruschi, J. Louko, and I. Fuentes. Motion generates entanglement. *arXiv:1201.0549*, 2012.
- [70] V. V. Dodonov. Current status of the dynamical Casimir effect. *Physica Scripta*, 82:038105, 2010.

REFERENCES

- [71] V. V. Dodonov, A. B. Klimov, and V. I. Man'ko. Generation of squeezed states in a resonator with a moving wall. *Phys. Lett. A*, 149:225, 1990.
- [72] N. Friis, A. R. Lee, D. E. Bruschi, and J. Louko. Kinematic entanglement degradation of fermionic cavity modes. *Phys. Rev. D*, 85:025012, 2012.
- [73] G Adesso. *Entanglement of Gaussian states*. arXiv:quant-ph/0702069, 2007. Ph.D Thesis.
- [74] S. L. Braunstein and P. van Loock. Quantum information with continuous variables. *Rev. Mod. Phys.*, 77:513, 2005.
- [75] J. Laurat, G. Keller, J. A. Oliveira-Huguenin, C. Fabre, T. Coudreau, A. Serafini, G. Adesso, and F. Illuminati. Entanglement of two-mode gaussian states: characterization and experimental production and manipulation. *J. Optics B*, 7:S577, 2005.
- [76] R. Simon. Peres-horodecki separability criterion for continuous variable systems. *Phys. Rev. Lett*, 84:2726-2729, 2000.
- [77] N Friis and I. Fuentes. Entanglement generation in relativistic quantum fields. *arXiv:1204.0617*, 2012.
- [78] C. W. Misner, K. S. Thorne, and J. A. Wheeler. *Gravitation*. W. H. Freeman, 1973.
- [79] R. D. Sorkin. *Introduction to topological geons*. Plenum Press, New York, 1986.
- [80] C. W. Misner and J. A. Wheeler. Classical physics as geometry: Gravitation, electromagnetism, unquantized charge, and mass as properties of curved empty space. *Annals Phys.*, 525, 1957.
- [81] D. Giulini. 3-manifolds in canonical quantum gravity. *Ph.D. Thesis*, 1990.
- [82] D. Giulini. *Two-body interaction energies in classical general relativity*. World Scientific, Singapore, 1992.
- [83] J. L. Friedman, JK. Schleich, and D. M. Witt. Topological censorship. *Phys. Rev. Lett.*, 1486, 1993.
- [84] J. Louko and D. Marolf. Single-exterior black holes and the ads-cft conjecture. *Phys. Rev. D*, 59:066002, 1999.
- [85] J. Louko, D. Marolf, and S. F. Ross. On geodesic propagators and black hole holography. *Phys. Rev. D*, 62:044041, 2000.

REFERENCES

- [86] J. M. Maldacena. Eternal black holes in anti-de-Sitter. *JHEP*, 0304:021, 2003.
- [87] J. Louko, R. B. Mann, and D. Marolf. Geons with spin and charge. *Class. Quant. Grav.*, 22:1451, 2005.
- [88] J. B. Hartle and S. W. Hawking. Path integral derivation of black hole radiance. *Phys. Rev. D*, 13:2188, 1976.
- [89] W. Israel. Thermo field dynamics of black holes. *Phys. Lett. A*, 57:107, 1976.
- [90] B. S. Kay and R. M. Wald. Theorems on the uniqueness and thermal properties of stationary, nonsingular, quasifree states on space-times with a bifurcate Killing horizon. *Phys. Rept.*, 207:49, 1991.
- [91] J. Louko and D. Marolf. Inextendible Schwarzschild black hole with a single exterior: How thermal is the Hawking radiation? *Phys. Rev. D*, 58:024007, 1998.
- [92] D. G. Boulware. Quantum field theory in Schwarzschild and Rindler spaces. *Phys. Rev. D*, 11:1404, 1975.
- [93] P. Langlois. Hawking radiation for Dirac spinors on the RP^3 geon. *Phys. Rev. D*, 70:104008, 2004.
- [94] J. Louko and K. Scleich. The exponential law: Monopole detectors, Bogoliubov transformations, and the thermal nature of the Euclidean vacuum in RP^3 de Sitter spacetime. *Class. Quant. Grav.*, 16:2005, 1999.
- [95] J. Louko. Geon black holes and quantum field theory. *J. Phys.: Conf. Ser.*, 222:012038, 2010.
- [96] G. T. Kottanattu and J. Louko. Topological geon black holes in Einstein-Yang-Mills theory. *Commun. Math. Phys.*, 303:127–148, 2011.
- [97] J. E. Kiskis. Disconnected gauge groups and the global violation of charge conservation. *Phys. Rev. D*, 17:3196, 1978.
- [98] A. S. Schwarz. Field theories with no local conservation of the electric charge. *Nucl. Phys. B*, 208:141, 1982.
- [99] J. Preskill and L. M. Krauss. Local discrete symmetry and quantum mechanical hair. *Nucl. Phys. B*, 341:50, 1990.
- [100] M. G. Alford, K. Benson, S. R. Coleman, March-Russell J., and F. Wilczek. Zero modes of nonabelian vortices. *Nucl. Phys. B*, 349:414, 1991.

REFERENCES

- [101] G. W. Gibbons. Vacuum polarization and the spontaneous loss of charge by black holes. *Commun. Math. Phys.*, 44:245, 1975.
- [102] H. Snyder and J. Weinberg. Stationary states of scalar and vector fields. *Phys. Rev.*, 57:307, 1940.
- [103] M. Richartz, S. Weinfurtner, Penner A. J., and W. G. Unruh. General universal superradiant scattering. *Phys. Rev. D.*, 80:124016, 2009.
- [104] S. Takagi. Vacuum noise and stress induced by uniform acceleration. *Prog. Theor. Phys. Suppl.*, 88:1, 1986.